

# Ambient Air Quality Assessment of Twelve Inhabited Areas in the State of Kuwait between Years 2011-2014

Ayed A. Al-Fadhli

**Abstract**—Environmental awareness is of growing concern in the state of Kuwait, especially after the recognition of Kuwait Environment Public Authority (KUEPA) as a separate entity with legal power back in year 2001. In this relation, the outdoor air quality data collected over the period of five years (2011-2014) were analyzed for twelve residential areas in the state of Kuwait which cover most of the country living territories. Data points were collected in two different time spans; monthly average data points and annual mean averages which were used to calculate the Year Average Common Air Quality Index (YACAQI) city background sites for the following pollutants: SO<sub>2</sub>, NO<sub>2</sub>, PM10 & Benzene in order to compare Kuwait outdoor air quality in compare to the European norms using the air quality index (AQI) in a unit-less to identify how polluted the air was and deviation severity. The results indicate that the YACAQI for NO<sub>2</sub> and PM10 are above the European standard to all the studied area, where the as for SO<sub>2</sub> level were found to be below YACAQI except for three locations which are Al-Shuaiba industrial area, Al-Fehheel & Al-Salam residential areas.

**Index Terms**—KUEPA, YACAQI, AQI, SO<sub>2</sub>, NO<sub>2</sub>, PM10, Benzene.

## I. INTRODUCTION

Many Gulf Council Countries (GCC) suffer from air pollution health effects especially when it comes to respiratory system chronic diseases and cancers associated with such airborne pollutants [1]. Kuwait is not an exception, being a petroleum industry oriented country. Many pollution sources are linked with the downstream/upstream industry in the state but yet still little action is taken by the concerned parties. One way of monitoring such pollution levels is what has become a standard approach of Air Quality Indices (AQI) calculation. Each Air Quality Index is a standardized indicator of the air quality in a given location. It measures mainly ground-level ozone and particulates but may also include Sulphur dioxide, and nitrogen dioxide. Various agencies around the world measure such indices, though definitions may vary between places. In the US, EPA calculates the AQI for five major air pollutants regulated by the Clean Air Act: ground-level ozone, particle pollution (also known as particulate matter), carbon monoxide, sulfur dioxide, and nitrogen dioxide. For each of these pollutants, EPA has established national air quality standards to protect public health. Ground-level ozone and airborne particles are the two pollutants that pose the greatest threat to human health in US.

Many scientists have devoted their work towards air pollution monitoring and standardizing rules and regulations governing cities around the world. This could be determined by literature available regarding the matter. An air quality monitoring methodology was presented by Landulfo *et al.* [2], by employing an elastic backscattering Lidar, sun photometer data, air quality indexing and meteorological data in the city of São Paulo, Brazil, a typical Urban Area. This procedure was made aiming to gather information from different optical atmospheric techniques and add this information to the air quality data provided regularly by the environmental agencies in the city. The parameters obtained by the Lidar system, such as planetary boundary layer height, aerosol optical thickness and aerosol extinction and backscattering aerosol coefficients are correlated with air quality indexes/reports provided by state environmental control agencies in order to extend the database information concerning pollution assessment and abate policies.

In India [3], the measured 24 hour average criteria pollutants such as sulfur dioxide, oxides of nitrogen, respirable suspended particulate matter and suspended particulate matter for the period from 1997 to 2005 at three air quality monitoring stations were used for the development of AQIs. The results indicated that the air pollution at all the three air quality monitoring stations can be characterized as 'good' and 'moderate' for SO<sub>2</sub> and NO<sub>x</sub> concentrations for all days from 1997 to 2004. The Pollution Standards Index (PSI) was initially established in response to a dramatic increase in the number of people suffering respiratory irritation due to the deteriorating air quality.

The PSI was subsequently revised and implemented by the USEPA in 1999, and became known as the (AQI) that includes data relating to particle suspension, PM<sub>2.5</sub>, and a selective options of either 8-hour or 1-hour ozone concentration during increased O<sub>3</sub> periods. This was discussed in the publication of Cheng *et al.* [4]. An aggregate AQI based on the combined effects of five criteria pollutants (CO, SO<sub>2</sub>, NO<sub>2</sub>, O<sub>3</sub> and PM10) taking into account the European standards was developed previously [5]. An evaluation was carried out for each monitoring station and for the whole area of Athens, Greece. A comparison was made with a modified version of Environmental Protection Agency/USA (USEPA) maximum value AQI model adjusted for European conditions. Hourly data of air pollutants from 4 monitoring stations, available during 1983–1999, were analyzed for the development of the proposed index. The objective of this study is to compare the Kuwait outdoor air quality in compare to the European norms using the air quality index (AQI) by calculating the Year Average Common Air Quality Index (YACAQI) city background sites

Manuscript received July 10, 2017; revised September 19, 2017.

Ayed A. Al-Fadhli is with Kuwait Petroleum Corporation, P. O. Box 26565, 13126, Safat, Kuwait (e-mail: ayf@kpc.com.kw).

for the following pollutants: SO<sub>2</sub>, NO<sub>2</sub>, PM10 & Benzene.

## II. INVESTIGATED AREA DESCRIPTION

The state of Kuwait is divided into six provinces are known as Kuwait Governorates which are namely as Al-Asimah ( $\approx 200 \text{ kg}^2$ ), Al-Ahmadi ( $\approx 5,120 \text{ kg}^2$ ), Al-Farwaniyah ( $\approx 190 \text{ kg}^2$ ), Al-Jahrah ( $\approx 11,230 \text{ kg}^2$ ), Hawalli ( $\approx 80 \text{ kg}^2$ ) and Mubarak Al-Kabir ( $\approx 100 \text{ kg}^2$ ). The population of each governorates are indicated as per the following table (Table I):

TABLE I: KUWAIT TOTAL POPULATION BY GOVERNORATES AS OF JUNE 2016 [6]

Governorates of Kuwait	No. of Residents
Al-Asimah	552,237
Al-Ahmadi	909,812
Al-Farwaniyah	1,155,877
Al-Jahrah	531,498
Hawalli	928,783
Mubarak Al-Kabir	246,877
Unknown	5,245
Total	4,330,308

The study consider a twelve residential areas in the state of Kuwait which cover most of the country living territories are indicated in below table along with number of residents of each area as publish by the Public Authority of Civil information PACI on June 2016 (Table II). All of the areas are inhibited expect Al-Mutla area as it is currently under planning stage. However, it is used as desert camping area in winter season between the months of November to March.

TABLE II: NO. OF RESIDENTS FOR THE STUDIED AREAS AS OF JUNE 2016 [6]

Area	No. of Residents
Al-Mansoria	9,260
Al-Qurain	32,233
Al-Reqa	52,126
Al-Jahra	65,186
Ali Al-Salem	54,253
Al-Mutla	No
Al-Rumeithiya	60,211
Al-Feheheel	110,110
Al-Shuaiba	873
Saad Al-Abdullah	94,413
Al-Shuwaikh	5,667
Al-Salaam	25,479

## III. DATA SOURCE

The data used in this study were secured form the Kuwait Environment Public Authority (KUEPA) where they have stationary stations in all and every studied areas and most of the stations is operated with a number of air sampling devices and analyzers with a tolerance of 1%. Air probe was approximately 15 m above sea level. All data were stored and manipulated with a special computer software. Pollutants collected by the station included the following: CH<sub>4</sub> (ppm), n-MHC (ppm), CO (ppm), CO<sub>2</sub> (ppm), NO (ppb), NO<sub>2</sub> (ppb), NO<sub>x</sub> (ppb), VOCs (ppb), mp-Xylenes (ppb), NH<sub>3</sub> (ppb), H<sub>2</sub>S (ppb) and O<sub>3</sub> (ppb). Metrological conditions were collected via a fixed weathering station recording the following: wind speed (ms-1) and direction (0), relative humidity (%) and ambient temperature (0C).

## IV. METHODOLOGY

An air quality index (AQI) is a unit-less number used by government agencies to communicate to the public how polluted the air currently is or how polluted it is forecast to become. As the AQI increases, an increasingly large percentage of the population is likely to experience increasingly severe adverse health effects. Different countries have their own air quality indices, corresponding to different national air quality standards. Some of these are the Air Quality Health Index (Canada), the Air Pollution Index (Malaysia), and the Pollutant Standards Index (Singapore).

In this relation, The European Union has taken many initiatives to support their local and regional authorities in actions to mitigate air pollution and climate change and to provide updated and comparable information to their citizens. Accordingly, EU funded a project called "CITEAIR-II" project (2004-2007) [7] which among other things developed and implemented air quality indices on the European level. This project leads to present the air quality situation in European cities in a comparable and easily understandable way, all detailed measurements are transformed into a single relative figure: the Common Air Quality Index (or CAQI). Three different indices have been developed to enable the comparison of three different time scale:

- An hourly index: describes the air quality today, based on hourly values and updated every hours.
- A daily index: Stands for the general air quality situation of yesterday, based on daily values and updated once a day.
- An annual index: Which represents the city's general air quality conditions throughout the year and compare to European air quality norms. This index is based on the pollutants year average compare to annual limit values, and updated once a year.

The common annual air quality index provides a general overview of the air quality situation in a given city all the year through and regarding to the European norms. The annual index is aimed at better taking into account long term exposure to air pollution based on distance to the target set by the EU annual norms, those norms being linked most of the time to recommendations and health protection set up by World Health Organization.

The Year Average Common Air Quality Index (YAAQI) can be calculated for both background and traffic conditions but its principle of calculation is different from the hourly and daily indices. It is presented as a distance to a target index, this target being derived from the EU directives (annual air quality standards and objectives):

- If the index is higher than 1: for one or more pollutants the limit values are not met.
- If the index is below 1: on average the limit values are met.

In this paper we will ably the third scale to calculate YACAQI city background of the selected sites, in order to understand what local air quality means to health in those areas in compare to EU major cities. The sub-indices are calculated as shown in Table III and as explained in Elshout and Léger [8].

TABLE III: CALCULATION SCHEME FOR THE YEAR AVERAGE INDEX

Pollutant	Target value / limit value	Calculation
NO <sub>2</sub>	Year average is 40 µg/m <sup>3</sup>	Year average / 40
PM10	average / 40 , Year average is 40 µg/m <sup>3</sup>	Year average / 40
SO <sub>2</sub>	Year average is 20 µg/m <sup>3</sup>	Year average / 20
Benzene	Year average is 5 µg/m <sup>3</sup>	Year average / 5

## V. RESULT AND DISCUSSION

Only two areas out of twelve studied areas in Kuwait is aligned with the air quality for the European level in term of Nitrogen Dioxide (NO<sub>2</sub>) which area Al-Shuiaba and Al-Mutlaa areas, that can be justified as both areas are consider a low in population knowing the fact that the main source of automobile transportation activities, knowing Nitrogen is released during fuel combustion as it combines with oxygen atoms to create nitric oxide (NO). This further combines with oxygen to create nitrogen dioxide (NO<sub>2</sub>). Nitric oxide is not considered to be hazardous to health at typical ambient concentrations, but nitrogen dioxide can be. Nitrogen dioxide and nitric oxide are referred to together as oxides of nitrogen (NO<sub>x</sub>). NO<sub>x</sub> gases react to form smog and acid rain as well as being central to the formation of fine particles (PM) and ground level ozone, both of which are associated with adverse health effects.

Al-Qurain, Al-Feheheel and Al-Salam have the highest index among the studied areas (Table IV) as they are close to the main country highways connecting the center to border areas of the country. Moreover, those highways used by almost of Kuwait residences on daily base travelling to center in the motoring for the work and business and back to home on the evening.

TABLE IV: ANNUAL NO<sub>2</sub> INDEX BY AREA (2011-2014)

Year/Area	2011	2012	2013	2014
Al-Mansoria	1.7	2.3	2.1	1.3
Al-Qurain	2.4	2.3	2.8	2.1
Al-Reqa	2.1	1.2	1.9	N/A
Al-Jahra	1.0	1.2	1.0	1.2
Ali Al-Salem	1.6	2.0	2.2	2.4
Al-Mutla	0.9	0.9	1.2	1.0
Al-Rumeithiya	2.1	2.3	1.5	1.5
Al-Feheheel	2.1	3.1	3.9	2.6
Al-Shuaiba	1.0	0.5	N/A	N/A
Saad Al-Abdullah	1.5	2.0	1.5	1.5
Al-Shuwaikh	1.7	1.7	1.6	1.5
Al-Salaam	3.6	2.9	2.7	1.4

TABLE V: ANNUAL SO<sub>2</sub> INDEX BY AREA (2011-2014)

Year/Area	2011	2012	2013	2014
Al-Mansoria	0.6	0.6	0.8	0.7
Al-Qurain	0.5	0.7	0.7	0.8
Al-Reqa	0.7	1.2	0.7	N/A
Al-Jahra	0.8	0.7	0.7	0.8
Ali Al-Salem	0.9	0.8	1.3	1.4
Al-Mutla	0.6	0.4	0.5	0.8
Al-Rumeithiya	0.7	0.7	0.8	1.4
Al-Feheheel	1.0	1.9	4.2	3.4
Al-Shuaiba	1.8	1.3	N/A	N/A
Saad Al-Abdullah	0.9	1.2	1.4	1.2
Al-Shuwaikh	1.1	1.0	1.1	0.9
Al-Salaam	2.3	1.6	2.4	1.7

Sulfur dioxide (SO<sub>2</sub>) belongs to the family of sulfur oxide (SO<sub>x</sub>) gases. These gases are formed when fuel containing sulfur (mainly Crude oil) is burned (e.g., for electricity

generation). In the state of Kuwait, the Ministry of Electricity and Water is using Crude Oil and/or Fuel oil production with the sulfur content is 2.6% S and 4% S respectively. This study indicate the levels of the SO<sub>2</sub> in all areas are below or slightly higher that the EU standard expect for Al-Feheheel area (Table V) which is located near to heavy industrial area in the country such three refineries with capacity of around 927 KBPD and related petrochemical industry.

The results for Benzene index for Al-Jahra, Al-Shuiba and Saad Al-Abdullah (Table VI) are below the unit index over the four year study, where the other areas are swing slightly above or on the threshold limits.

TABLE VI: ANNUAL BENZENE INDEX BY STATION (2011-2014)

Year/Area	2011	2012	2013	2014
Al-Jahra	0.8	0.5	0.4	0.3
Ali Al-Salem	0.6	1.3	1.5	1.4
Al-Feheheel	0.5	1.1	0.8	0.9
Al-Shuaiba	0.3	0.3	N/A	N/A
Saad Al-Abdullah	0.6	0.8	0.7	0.6
Al-Shuwaikh	1.4	1.1	1.1	0.9
Al-Salaam	0.8	0.9	1.1	0.8

The annual PM10 index was too high in compare to EU standard which reach three to eight times higher (Table VII) that was expected in view of the fact that Kuwait in specific and Middle East countries in general having a very large desert areas and sand storms consider a norm situation. However, it was useful to scale the studied areas in the EU benchmark.

TABLE VII: ANNUAL PM10 INDEX BY AREA (2011-2014)

Year/Area	2011	2012	2013	2014
Al-Mansoria	1.8	8.2	5.7	4.0
Al-Reqa	5.5	6.7	4.8	N/A
Al-Jahra	4.3	5.0	6.0	2.9
Ali Al-Salem	8.3	9.1	6.3	4.3
Al-Mutla	8.7	5.8	4.2	3.2
Al-Rumeithiya	5.2	8.0	7.2	3.8
Al-Feheheel	3.4	4.4	4.0	2.7
Al-Shuaiba	1.8	1.1	N/A	N/A
Saad Al-Abdullah	6.1	7.0	4.1	2.8
Al-Shuwaikh	5.0	5.3	4.4	3.4
Al-Salaam	3.6	5.9	4.2	3.8

## VI. CONCLUSION

The study has provided a preliminary assessment of the air quality assessment of twelve residential areas in the state of Kuwait based Year Average Common Air Quality Index (YACAQI) city background sites, for the study it was found that the levels particulate matter is an important issue in the state of Kuwait and proper mitigation protocols must be applied. In general, there is a need to be closely monitored the NO<sub>x</sub> emission in the state of Kuwait, which is quite a serious issue linked to vehicle emission and traffic congestion. Traffic movement is also a main possible emission source of benzene and other VOC pollutants.

With a population of over three million and a vehicle fleet of more than one million and both growing rapidly, Kuwait City is experiencing increasing volumes of traffic, greater trip frequency and increasing trip length [9]. Thus the outdoor air quality is becoming a major air pollution issue and concern, for the people living in Kuwait City

A vast chance of initiatives can be applied to reduce the air

pollutants from transportations sources such as increase the awareness to for using the public transportation means (e.g. Buses, shuttles etc..) and/or imposing gradually the electric cars are on the road, which is currently under development stage and having a promise future to become vehicles of best choice for urban transportation. Tesla is the best known electric car company that is addressing the need for local battery manufacturing and is building charging stations that are essential for long distance travel in their cars.

In general, there is a high variance of the data due to the difference between the sources of each pollutant, and different activities that may lead to the increase of pollutant in the studied areas. Some extra factors (i.e. metrological factors) and phenomena needs further study and further investigation.

#### REFERENCES

- [1] S. M. Al-Salem and W. S. Bouhamrah, "Ambient concentrations of benzene and other VOCs at typical industrial sites in Kuwait and their cancer risk assessment," *Res. J. Chem. Environ.*, vol. 10, no. 3, pp. 42–46, 2006.
- [2] E. Landulfo, C. A. Matos, A. S Torres, P. Sawamura, and S. T. Uehara, "Air quality assessment using a multi-instrument approach and air quality indexing in an urban area," *Atm. Res.*, vol. 85, no. 1, pp. 98–111, 2007.
- [3] S. M. S. Nagendra, K. Venugopal, and S. L. Jones, "Assessment of air quality near traffic intersections in Bangalore city using air quality indices," *Trans Res. Part D: Transport and Environment*, vol. 12, no. 3, pp. 167–176, 2007.
- [4] W. L. Cheng, Y. S. Chen, J. Zhang, T. J. Lyons, J. L. Pai, and S. H. Chang, "Comparison of the revised air quality index with the PSI and AQI indices," *Sci. Total Environ.*, vol. 382, no. 2-3, pp. 191–198, 2007.
- [5] G. Kyrkilis, A. Chaloulakou, and P. A. Kassomenos, "Development of an aggregate air quality index for an urban Mediterranean agglomeration: Relation to potential health effects," *Environ. Int.*, vol. 33, no. 5, pp. 670–676, 2007.
- [6] The public authority for civil information, PACI. [Online]. Available: <https://www.paci.gov.kw/Default.aspx>
- [7] CAQI air quality index comparing urban air quality across borders. (2012). [Online]. Available: [www.airqualitynow.eu/download/CITEAIR-Comparing\\_Urban\\_Air\\_Quality\\_across\\_Borders.pdf](http://www.airqualitynow.eu/download/CITEAIR-Comparing_Urban_Air_Quality_across_Borders.pdf)
- [8] E. Sef Van Den and K. Léger, "Comparing urban air quality across borders. A review of existing air quality indices and the proposal of a common alternative," *DCMR*, Schiedam, 2007.
- [9] N. Al-Mutairi and P. Koushki, "Potential contribution of traffic to air pollution in the state of kuwait," *American Journal of Environmental Sciences*, vol. 5, pp. 218-222, 2009.



**Ayed Al-Fadhli** graduated from Kuwait University, College of Engineering and Petroleum, holding a BSc degree in 2005 and an MSc degree in 2007 in chemical engineering and an MSc degree in 2012 in environmental science, where he started his career in 2004 as a planning and economical studies analyst and as a planning marketing at KPC International Marketing.

Eng. Al-Fadhli is a volunteer researcher specializes in environmental aspects, and a particular research interest of him includes the air pollution and life cycle assessment (LCA). He has authored/co-authored a number of refereed journal and conference papers.



# **Energy and Petroleum Engineering**



# Glycerol Esterification with Acetic Acid by Reactive Distillation Using Hexane as an Entrainer

Tatiane F. C. Souza, Newton L. Ferreira, Maristhela Marin, and Roberto Guardani

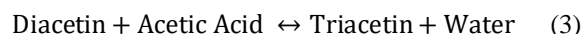
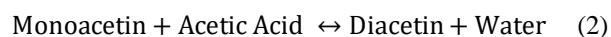
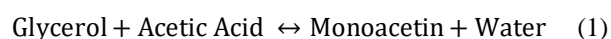
**Abstract**—A process design study was carried out, aimed at the design of a triacetin production process from glycerol, as a way to increase the feasibility of biodiesel production. Glycerol esterification with acetic acid involves three consecutive reversible acetylation reactions and in each step, water is produced, resulting in limited conversion and low selectivity [1]. One way to increase the triacetin selectivity is to continuously remove water from the reaction medium, in order to shift the equilibrium. The proposed process is based on the reaction system described by Galan *et al.* [2], consisting of the esterification of glycerol using excess acetic acid as catalyst. In the first step of the present study an evaluation of the kinetic parameters was carried out, based on published experimental data [2]. The reaction conditions were then evaluated in terms of glycerol conversion and selectivity for different reaction times and temperatures. Based on the results, the process was simulated in a reactive distillation column, and different configurations were studied by using the Aspen Plus® simulator. In the separation units the NRTL-HOC equilibrium model with binary interaction parameters proposed by Hung *et al.* [3] was adopted. Water removal from the top stream of the column was increased by feeding hexane as an entrainer in the reactive distillation column. Hexane is recovered in a separate unit and recycled to the process. The conceptual process specifications of an optimized industrial plant configuration were estimated for minimum specific energy consumption for production of 99.9 % molar purity triacetin with complete glycerol conversion.

**Index Terms**—Glycerol esterification, triacetin, reactive distillation, simulation.

## I. INTRODUCTION

Glycerol is a by-product from the esterification of vegetable oils and fats, and is generated at a ratio of ca. 0.1 kg per kg of biodiesel produced. In recent years, mainly due to biodiesel production, the available quantity of glycerol in the market is increasing significantly, and many processes that use glycerol are being studied and developed. Triacetin production through the esterification of glycerol with acetic acid is one of the possible routes to transform glycerol into valuable products, since triacetin has a market possibility as plasticizer and fuel additive. It has been reported that adding triacetin to the biodiesel can reduce CO emissions [4] and improve the biodiesel flowability under low temperatures. Glycerol esterification with acetic acid is composed of three consecutive equilibrium reactions, and is carried out in the

presence of an acidic catalyst. In each acetylation step water is produced.



The presence of water limits glycerol conversion and triacetin selectivity, and this has motivated studies aimed at identifying favorable conditions for this reaction system, in terms of temperature, acetic acid/glycerol ratio, pressure and catalyst concentration. In order to reduce the impact of the water formation, Liao *et al.* studied the use of acetic anhydride instead of acetic acid, concluding that thermodynamically the triacetin production with this reagent is more favorable than with acetic acid [5]. However, acetic anhydride is relatively expensive, and its use can make the production process unfeasible in economic terms. Gonçalves *et al.* analyzed the catalysis performance of different catalysts, such as ion-exchange resins (Amberlyst-15, K-10, HZSM-5 and HUSY) and niobic acid. The study showed that the Amberlyst-15 resin was the one that presented the highest glycerol conversion (97 %) [6].

There are not many published studies on the kinetics of the reaction system. Mufrodi *et al.* studied the batch triacetin production catalyzed by sulfuric acid and obtained 77.84 % triacetin selectivity [7]. The kinetic parameters, based on the Arrhenius model, were obtained for the six reactions (direct and reverse reactions of each acetylation step). Following this same model, Galan *et al.* studied the reaction kinetics for the esterification of glycerol with excess of acetic acid as catalyst, as a way to shift the equilibrium to the products [2].

Hung *et al.* designed a reactive distillation (RD) column to produce triacetin from glycerol, and in order to increase the water removal at the top of the RD column, isobutyl acetate and ethylene dichloride were used as entrainers. The effect of the entrainer was evaluated for both processes. The authors concluded that the process using entrainer can reduce the total annual production cost by more than 34 % [3].

In the present study, the kinetic parameters obtained by Galan *et al.* [2] for reactions 1 to 3 were evaluated and then used in the simulation of an industrial process based on reactive distillation. However, in this case hexane was adopted as entrainer to promote water removal at the top of the column. In the separation units the NRTL-HOC equilibrium model with binary interaction parameters proposed by Hung *et al.* [3] was adopted. The process conditions that lead to high glycerol conversion and high purity triacetin were studied by means of simulations for

Manuscript received August 30, 2017; revised November 20, 2017.

Tatiane Fernandes, Caetano Souza, and Roberto Guardani are with Escola Politécnica da Universidade de São Paulo, Brazil (e-mail: tatianefcsouza@gmail.com, guardani@usp.br).

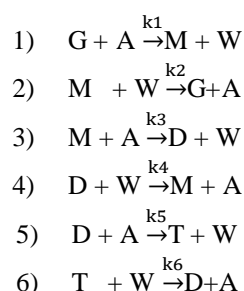
Newton Libanio Ferreira and Maristhela Marin are with Centro Universitário FEL, Brazil (e-mail: newton.libanio@uol.com.br, marimari@fei.edu.br).

different process configurations, in order to identify the optimal conditions in terms of minimum energy consumption. Finally, a triacetin production unit that uses glycerol produced in a typical biodiesel plant was proposed.

All simulations and parameter fitting studies were performed in Scilab and Aspen Plus simulation platforms.

## II. REACTION KINETICS

Considering a batch pressurized reactor, Galan *et al* [2] carried out experimentally the reaction of glycerol with excess acetic acid (proportion 1:12, i.e., four times in excess) at two temperatures, namely 120 °C and 160 °C, under ca. 10 bar pressure, in order to prevent acetic acid evaporation during the reaction and thus decrease glycerol conversion. The three consecutive equilibrium reactions can be represented as six direct reactions, as follows:



The symbols are G: glycerol; A: acetic acid; M: monoacetin; D: diacetin; T: triacetin and W: water.

The second order reaction rates are represented as:

$$\begin{aligned}
 r'_1 &= k_1 \cdot C_A \cdot C_G \\
 r'_2 &= k_2 \cdot C_M \cdot C_W \\
 r'_3 &= k_3 \cdot C_M \cdot C_A \\
 r'_4 &= k_4 \cdot C_D \cdot C_W \\
 r'_5 &= k_5 \cdot C_D \cdot C_A \\
 r'_6 &= k_6 \cdot C_T \cdot C_W
 \end{aligned}$$

With the kinetic constants for reaction *i* expressed according to the Arrhenius model:

$$k_i = A_i \cdot e^{\frac{-E_i}{R \cdot T}}$$

where  $A_i$  is the pre-exponential factor and  $E_i$  is the activation energy for each reaction.

The experimental values of these constants were fitted from the experimental data at each temperature, and are shown in Table I.

TABLE I: ADJUSTED KINETIC PARAMETERS [L/MOL.S] OBTAINED BY GALAN *ET AL.* [2]

Temperature	120 °C	160 °C
$k_1$	2,38E-04	2,56E-04
$k_2$	1,20E-01	7,62E-02
$k_3$	6,30E-04	5,30E-04
$k_4$	3,14E-03	8,78E-03
$k_5$	1,09E-04	1,96E-04
$k_6$	2,59E-03	4,76E-03

For two temperatures, the system of equations is determined, and thus the two parameters are directly obtained for each rate constant, as shown in Table II.

These constants were evaluated by simulating a batch reactor under similar conditions to those adopted by Galan *et al.* [2]. i.e., by feeding 22 mL glycerol and 208 mL acetic acid to the reactor, and 8 hours of reaction time. The system equilibrium was achieved after around 15 minutes of reaction at 120 °C, and around 10 minutes at 160 °C. The concentration of the species during the reaction time is shown in Figs. 1 and 2, for 120 °C and 160 °C, respectively.

TABLE II: ARRHENIUS PARAMETERS FOR THE REACTION SYSTEM

	$A_i$ (L/mol.s)	$E_i$ (cal/mol)
Reaction 1	5,24E-04	6,17E+02
Reaction 2	8,56E-04	-3,86E+03
Reaction 3	9,69E-05	-1,46E+03
Reaction 4	2,16E+02	8,70E+03
Reaction 5	6,26E-02	4,96E+03
Reaction 6	1,86	5,14E+03

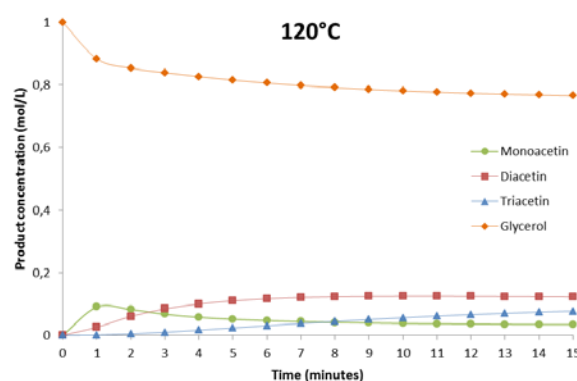


Fig. 1. Species concentration over reaction time for the simulated reactor at 120 °C, considering the Arrhenius parameters obtained by Galan *et al.*[2].

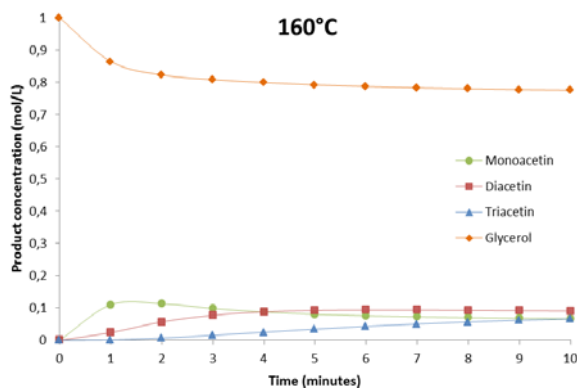


Fig. 2. Species concentration over reaction time for the simulated reactor at 160 °C, considering the Arrhenius parameters obtained by Galan *et al.*[2].

As shown in the plots, the maximum glycerol conversion was ca. 25 % for both temperatures, and, although the product distribution is different, conversion to triacetin remained low in both cases. This is a clear evidence of the effect of the presence of water in the system, indicating the need for water removal, which can be accomplished by reactive distillation, as suggested by Galan *et al* [2].

## III. PROCESS DESIGN

### A. Methods

The design of the triacetin production process was based on the following criteria:

- 1) the adopted triacetin plant capacity is based on a

typical biodiesel production facility in Brazil, with an average installed capacity to produce ca. 400 m<sup>3</sup> of biodiesel per day [8], and around 1500 kg/h of glycerol (17 kmol/h approximately); this is the adopted glycerol flowrate in the feed stream;

- 2) The product stream contains minimum 99 % of triacetin (molar base);
- 3) Among the components involved in the process, monoacetin and diacetin are not present in the properties databank of the simulator. Thus, the parameters for the equilibrium correlations were estimated by the simulator from the molecular structures of these two species, which were fed to the software. Due to their molecular structures, the most favorable isomers to form during the reactions are 1-monoacetin and 1,3-diacetin [9], and thus these isomers were adopted to represent the monoacetin and diacetin in the simulations;
- 4) the NRTL-HOC thermodynamic model was adopted, because it can well represent aqueous electrolyte systems, and in addition, the Hayden-O'Connell model provides an adequate representation of the vapor phase behavior, since during the reaction gaseous species are generated, mainly due to acetic acid evaporation; the binary interaction parameters were the same ones adopted by Hung *et al.* [3];
- 5) The reaction rates were modeled according to the previously described kinetic model, with the kinetic parameters shown in Table II. As in the study by Galan *et al.* [2], four times molar excess of acetic acid was adopted, so that 1 mol of glycerol to 12 mol of acetic acid was fed to the reactive distillation column.
- 6) The two reagent streams are assumed to contain 5 % of water as impurity (mol base), as adopted by Hung *et al.* [3]. The specifications of these streams are listed in Table III.
- 7) Hexane was used as a water entrainer in the column, due to its low solubility in water, which can improve its separation and recovery, and also because hexane forms an azeotrope with water at a moderate temperature (49.2 °C), which can facilitate water entrainment.

The next section describes the design of the process.

### B. Proposed Triacetin Production Process

The processing units and streams of the proposed triacetin production process are represented by the flowsheet shown in Fig. 3. The process consists of recycle circuits for hexane (entrainer) and for the excess acetic acid, as well as for the bottom stream from the reactive distillation column, as a way to convert all the glycerol and reaction intermediates, and to produce a product stream with more than 99 % triacetin. The main unit operations are:

C1 – Reactive distillation column, in which the reactions take place, and water is removed by hexane in the top stream.

C2 – Acetic acid removal column, in which the excess acetic acid is removed in the top stream, and glycerol, monoacetin and diacetin are recovered in the bottom stream. This bottom stream is mixed with the bottom stream from column C3 and returned to the reactive column. Triacetin is removed in stream 7, as an intermediate exit stream from

column C2, specified according to the temperature profile along the column.

C3 – Triacetin purification column, in which the remaining glycerol, diacetin and monoacetin are removed in the bottom stream, which is returned to the reactive distillation column. The product stream 10 from the top of column C3 contains more than 99 % molar fraction of triacetin.

H1 – Condenser of the reactive distillation column: The condenser of this column cannot be directly connected to the reactive column, since it is necessary to separate the hexane from the top stream, which it takes place at the decanter.

D1 – Decanter: The condensed top stream from the reactive distillation column is decanted to separate hexane from the solution of acetic acid in water.

M1 – Hexane mixer: The hexane stream recovered at the decanter is mixed with the hexane make-up stream forming the feed stream to the reactive distillation column.

M2 – Heavy components mixer: The bottom streams from columns C2 and C3, consisting mainly of glycerol, diacetin and monoacetin, are mixed and fed to the reactive distillation column.

M3 – Mixer of recovered acetic acid: The top stream from column C2 and the bottom stream from the decanter D1, which are rich in acetic acid, are mixed and sent to an acetic acid recovery unit, outside the limits of the triacetin production unit.

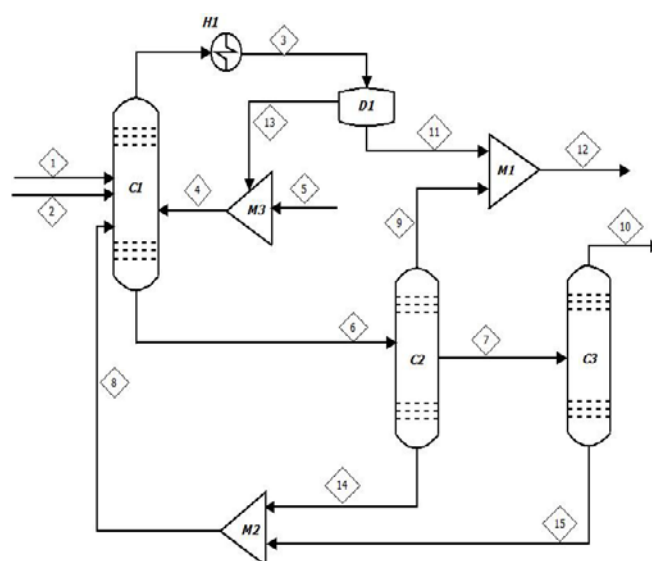


Fig. 3. Proposed flowsheet for the triacetin production process with hexane as an entrainer.

TABLE III: PROCESS FEED STREAMS

		1	2
Mole Flow (kmol/h)	Acetic acid	0	193,8
	Glycerol	16,15	0
	Water	0,85	10,2
Total Flow (kmol/h)		17	204
Total Flow (kg/hr)		1502,6	11821,9
Temperature (°C)		80	80
Pressure (bar)		1	1
State		Liquid	Liquid

The streams numbered “1” and “2” in Fig. 3 are the feed of glycerol and acetic acid respectively. Stream “5” is the hexane make-up required to replace hexane losses in the hexane cycle. Stream “8” is the bottom recovery from

columns C2 and C3, and is mainly composed of heavy components (glycerol, diacetin and monoacetin). This stream is returned to the reactive distillation column (C1) to continue the reaction to triacetin.

The operation conditions and main characteristics of the streams are discussed in the next section.

### C. Results and Discussion

The reactive distillation column C1 is divided in two sections: reaction zone and separation zone. The reaction zone is composed of the bottom part of the column and is where the reaction takes place. The separation zone is in the top part of the column, where water is removed, with hexane as entrainer. The configuration of column C1 was designed in order to maximize the water removal at the top and glycerol conversion. The pressure in the column affects the gas-liquid equilibrium composition and temperature, and thus affects the maximum attainable glycerol conversion and triacetin selectivity at the bottom part, as shown in Fig. 4. Based on this behavior, the pressure in column C1 was set to 1 bar. Under this pressure water forms an azeotrope with hexane at 49.02 °C, with molar composition of 0.33 water and 0.67 hexane. Although the water content is low at the azeotropic composition when compared to other common entrainers, such as isobutyl acetate and ethylene dichloride, hexane has the advantage of lower cost, and the water removal rate from the column is adequate to reach the conversion requirements.

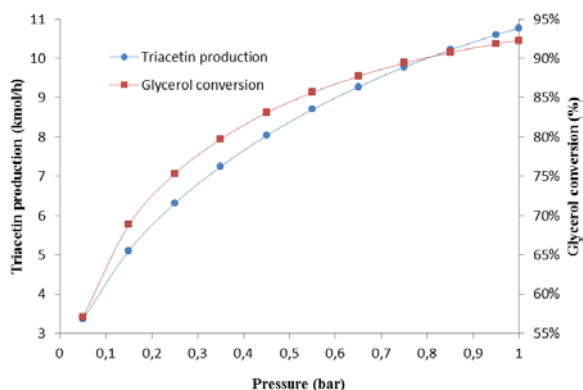


Fig. 4. Effect of C1 pressure on the triacetin production and glycerol conversion at the column.

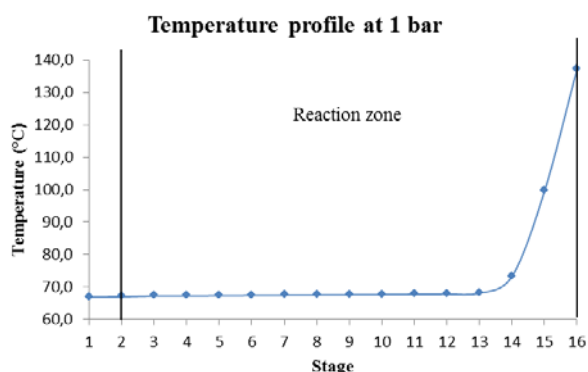


Fig. 5. Temperature profile of the reactive distillation column (C1).

A study was carried out in order to select a favorable reboiler duty, by varying the mass flow ratio of the bottom to feed streams. This resulted in a column with 16 stages, in which the 16<sup>th</sup> stage consists of the reboiler. The condenser is a separate unit, since it is necessary to separate hexane from the water-acetic acid solution in a decanter prior to its return

to the column. The feed streams (streams 1 and 2) are fed at stage 2, and the hexane reflux (stream 4) is fed at stage 1. The reaction zone is distributed over stages 2 to 16, and the recover process stream (stream 8) is fed at stage 2, the same stage as the feed streams.

Fig. 5 shows the temperature profile in column C1. There is an increase of the temperature in the reaction zone, mainly at stage 16, where the residence time is larger. This increase of the temperature is due to the exothermic reaction of glycerol to acetic acid [10], which favors the formation of the hexane-water stream.

The top stream is condensed and decanted. The outlet temperature of the condenser and at the decanter were studied in order to maximize the separation of water from hexane. Lower temperatures favor the water removal (Fig. 6). Based on these results, the temperature of the outlet stream from the condenser (stream 3) was set to 5 °C at 1 bar. The heat removal from the condenser is estimated at ca. 18.5 MW.

### Water removal at the decanter

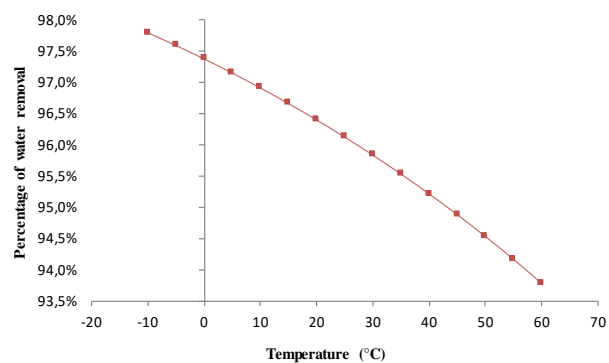


Fig. 6. Effect of temperature on the percentage of water removal at the decanter (1 bar).

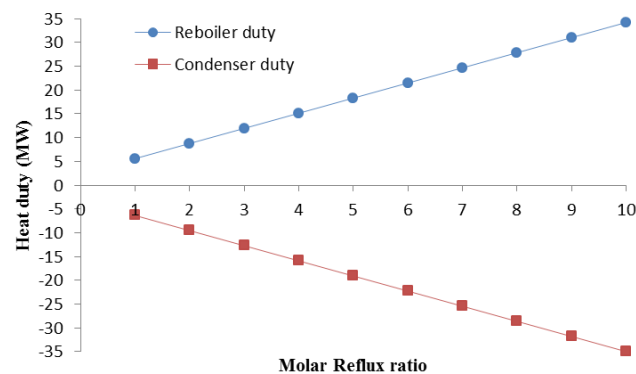


Fig. 7. Effect of molar reflux ratio on the condenser and reboiler heat duties in column C2.

Stream 3, which contains mainly hexane, is decanted, mixed to the hexane make-up stream and fed to column C1. The flowrate of the make-up stream is relatively small (20.5 kg/h), and replaces hexane losses in the decanter and at the bottom stream from C1.

The column C1 reboiler operates at 137.2 °C and its heat duty is ca. 18 MW. The bottom stream is fed in the second column (C2) to remove the excess acetic acid.

In column C2 the excess acetic acid is removed. This excess in the process feed stream is necessary, since, as described previously, acetic acid is a reagent and a catalyst, too. Triacetin is not the heaviest component of the system, so it has to be withdrawn at an intermediate stage of the column,

and glycerol, monoacetin and diacetin, heavier components, are recovered at the bottom of column C2. This column was designed in order to remove all the acetic acid excess at the top. The favorable conditions were estimated by simulating the column behavior for different distillate flowrates and reflux ratios, and intermediate product flowrates, which are directly related to the condenser and reboiler heat duties (Fig. 7). Lower pressures favor the acetic acid removal, since it reduces the amount of acetic acid in the product and the triacetin loss at the top (Fig. 8).

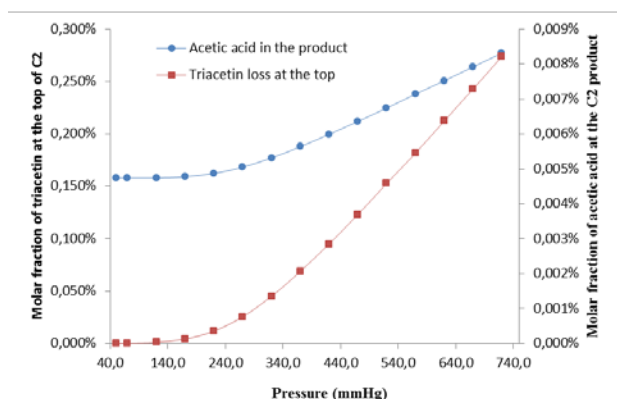


Fig. 8. Effect of pressure on the molar fraction of triacetin at the C2 top stream and molar fraction of acetic acid at the product stream from C2.

The optimal design, represented by minimum energy consumption and high product purity, resulted in a column with 15 stages, where the first stage is the condenser and the 15<sup>th</sup> stage is the reboiler. The column pressure was set to 50 mmHg (0.07 bar) in order to favor the triacetin purity (Fig. 8). The feed enters at stage 3, and the intermediate product is withdrawn at stage 5 (Fig. 9).

#### Temperature profile at 0,07 bar (50mmHg)

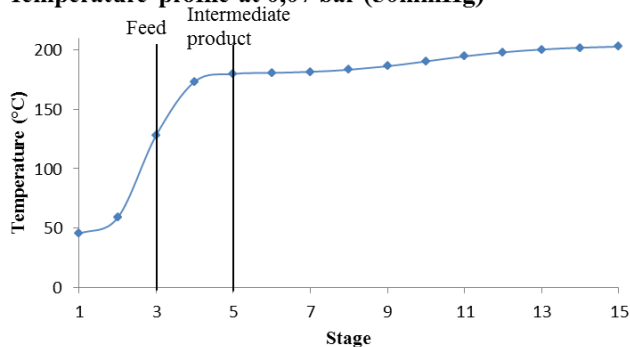


Fig. 9. Temperature profile of the acetic acid removal column (C2).

#### Composition profile: Liquid Phase

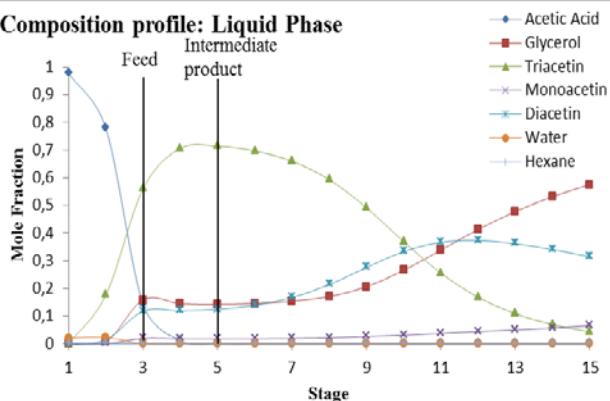


Fig. 10. Molar liquid composition profile at column C2.

The molar compositions of the vapor and liquid phases in the acetic acid removal column C2 are shown in Figs. 10 and 11). The triacetin mole fraction profile was the adopted criteria to specify the stage in which the intermediate stream 7 is placed. This stream (stream 7 in Fig. 3) has 72 % molar fraction of triacetin, and the remaining components are mainly diacetin and glycerol. This stream is fed to column C3, where the remaining heavier compounds are removed in order to attend the required product specifications. The top stream from column C2 is rich in acetic acid, and is sent to the recovery unit. The bottom stream is rich in diacetin and glycerol. This stream is mixed with the bottom stream from column C3 and returned to the reactive distillation column (C1).

#### Composition profile: Vapor Phase

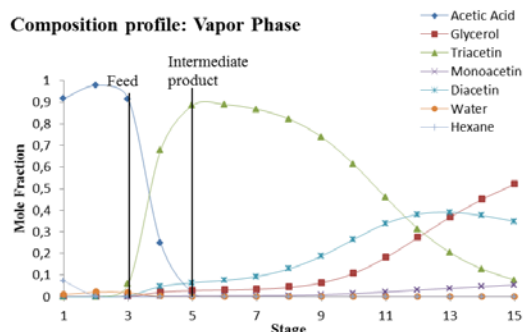


Fig. 11. Molar vapor composition profile at column C2.

The optimal reflux ratio in column C2 is 1, the condenser removal duty is 1547.5 kW, and the reboiler duty is 1430 kW.

The triacetin purification column (C3) was designed in a way to guarantee that the top stream attends the triacetin purity level (more than 99 % molar). The column pressure, distillate flowrate and reflux ratio, which are directly related to condenser and reboiler heat duties, were optimized in order to attend the required specifications (Fig. 12).

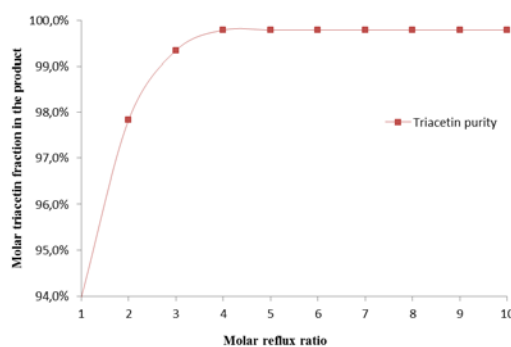


Fig. 12. Effect of the molar reflux ratio on the molar triacetin fraction in the product (purity).

#### Temperature profile at 0,07 bar (50mmHg)

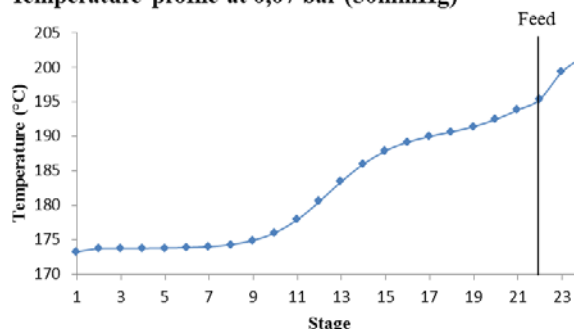


Fig. 13. Temperature profile of triacetin purification column (C3).

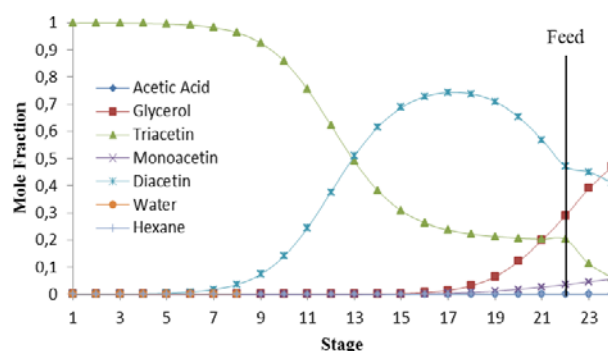
**Composition profile: Liquid Phase**


Fig. 14. Molar liquid composition profile at column C3.

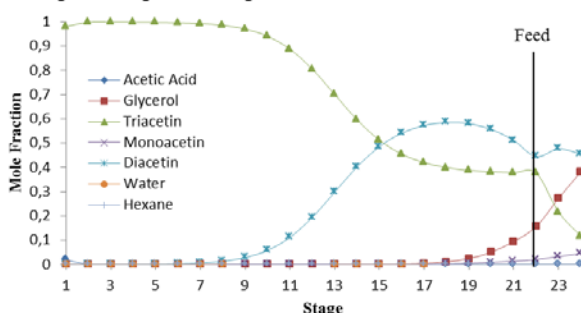
**Composition profile: Vapor Phase**


Fig. 15. Vapor liquid composition profile at column C3.

As a result, column C3 has 24 stages: the first stage is the condenser and the 24<sup>th</sup> stage is the reboiler. The feed stream (stream 7) is fed at the 22<sup>nd</sup> stage. The column pressure was set to 50 mmHg (0.07 bar), and the reboiler operates at 201.6 °C (Fig.13).

Fig. 14 and Fig. 15 show the molar fraction of the

components in the liquid and vapor phases, respectively, in column C3. The top stream contains triacetin within the required specifications, while the bottom stream is rich in diacetin and glycerol. This stream is mixed with the bottom stream from C2 (stream 8, Fig. 3) and is returned to the reactive distillation column. The optimal reflux ratio in column C3 is 4, the condenser removal duty is 1478.4 kW and the reboiler duty 1478.5 kW.

The main characteristics of the product obtained at the top of column C3 are shown in Table IV.

TABLE IV: PROCESS PRODUCT STREAM (STREAM 10)

	Molar Flowrate (kmol/h)	Mole Fraction
Acetic acid	0.017	0.001
Glycerol	1.8E-12	10.9ppb
Triacetin	16.15	0.999
Monoacetin	7.8E-11	4.8ppb
Diacetin	2.03E-3	126ppm
Water	8.4E-6	0.52ppm
Hexane	2.5E-12	15.7ppb
Mass Flow (kg/hr)	3523.5	
Temperature (°C)	173.2	
State	Liquid	

The hexane mass flowrate circulating in the reactive distillation column C1 is 126.7 t/h. This flowrate is considerably larger than that for other entrainers, such as isobutyl acetate or ethylene dichloride. However, hexane is less expensive and requires less energy and smaller equipments to separate it from the other components.

The main characteristics of all streams represented in Fig. 3 are listed in Table V.

TABLE V: MAIN CHARACTERISTICS OF PROCESS STREAMS (OPTIMAL CONFIGURATION)

	1	2	3	4	5	6	7	8	9	10	11	12	13	14	15
Molar Fraction															
Acetic acid	0	0.95	0.049	0.021	0	0.69	0.0007	0	0.98	0.001	0.44	0.71	0.021	trace	0.002ppm
Glycerol	0.95	0	10.4ppm	360ppb	0	0.1	0.14	0.55	0.28ppm	10.9ppb	1.6ppm	95ppm	360ppb	0.58	0.47
Triacetin	0	0	0.002ppm	107ppb	0	0.12	0.72	0.048	60ppm	0.999	302ppm	0.3ppm	107ppb	0.04	0.06
Monoacetin	0	0	0.003ppm	10ppb	0	0.012	0.017	0.063	926ppm	4.8ppb	403ppm	663ppm	10ppb	0.066	0.06
Diacetin	0	0	0.04ppm	317ppb	0	0.063	0.12	0.34	2.6ppm	126ppm	64ppm	1.6ppm	317ppb	0.32	0.41
Water	0.05	0.05	0.037	0.001	0	0.015	0.4ppm	0	0.02	0.52ppm	0.56	0.29	0.0012	trace	trace
Hexane	0	0	0.91	0.977	1	0.0009	0.1ppb	0	0.001	15.7ppb	0.001	0.002	0.98	trace	trace
Molar Flow (kmol/h)	17	204	1606.8	1503.8	0.24	144.6	23.2	26.65	101.8	16.2	103.3	205.1	1503.6	19.6	7.0
Mass Flow (kg/h)	1502.6	11821.9	132400	128627	20.54	13002.1	4484.8	3450.2	6028.5	3523.5	3793.2	9821.6	3145	32.6	961.3
Temperature (°C)	80	80	5	5	45	137.2	179.9	202.6	45.1	173.2	5	29.3	5	203	201.6
Pressure (bar)	1	1	1	1	1	1	0.07	1	0.07	0.07	1	1	1	0.07	0.07
State	Liquid	Liquid	Liquid	Liquid	Liquid	Liquid	Liquid	Liquid	Liquid	Liquid	Liquid	Liquid	Liquid	Liquid	Liquid

**IV. CONCLUSIONS**

In this paper, the design of an industrial triacetin production unit from glycerol was investigated, as a way to increase the feasibility of biodiesel production. First, the kinetic parameters obtained by Galan *et al.* [2] were analyzed and applied to a reactive distillation column. By means of planned simulations, the structure of the reaction and

separation units was defined, and the specifications for the processing units and process streams were selected. The operational conditions of the columns were studied in order to accomplish the product requirements and minimize the energy consumption. The proposed configuration is able to completely convert glycerol to triacetin with high level of purity (99.9 %). The amount of heat removed from the condensers of the entire process corresponds to 21.9 MJ/kg of product, and the amount of heat required at the reboilers is

21.4 MJ/kg of product.

The information provided in this paper can be adopted as a basis for specific feasibility studies at a conceptual process design level.

#### REFERENCES

- [1] N. Bremus, G. Dieckelmann, L. Jeromin, W. Rupilius, H. Schutt, and H. K. auf Aktien, "Process for the continuous production of triacetin," U.S. Patent 4381407, 1981.
- [2] M.-I. Galan, J. Bonet, R. Sire, J.-M. Reneuauame, and A. E. Plesu, "From residual to useful oil: Revalorization of glycerin from the biodiesel synthesis," *Bioresource Technology*, vol. 100, pp. 3775-3778, 2009.
- [3] S. K. Hung, C. C. Lee, H. Y. Lee, C. L. Lee, and I. L. Chien, "Improved design and control of triacetin reactive distillation process for the utilization of glycerol," *Industrial & Engineering Chemistry Research*, vol. 53, pp. 11989-12002, 2014.
- [4] C. V. Lacerda, M. J. Carvalho, A. R. Ratton, I. P. Soares, and L. E. Borges, "Synthesis of triacetin and evaluation on motor," *J. Braz. Chem. Soc.*, vol. 26, no. 8, pp. 1625-1631, 2015.
- [5] X. Liao, Y. Zhu, S.-G. Wang, and Y. Li, "Producing triacetyl glycerol with glycerol by two steps: Esterification and acetylation," *Fuel Processing Technology*, vol. 90, pp. 988-993, 2009.
- [6] V. L. Gonçalves, B. P. Pinto, J. C. Silva, and C. J. Mota, "Acetylation of glycerol catalyzed by different solid acids," *Science Direct - Catalysis Today*, vol. 133-135, pp. 673-677, 2008.
- [7] Z. Mufrodi, S. Rochmadi, and A. Budiman, "Chemical kinetics for synthesis of triacetin from biodiesel byproduct," *International Journal of Chemistry*, vol. 4, pp. 101-107, 2012.
- [8] Ministério de Minas e Energia Brasileiro, "Boletim Mensal dos Biocombustíveis," *Monthly Bulletin of Biofuels*, Edition nº106, Dec. 2016.

- [9] X. Liao, Y. Zhu, S.-G. Wang, H. Chen, and Y. Li, "Theoretical elucidation of acetylating glycerol with acetic acid and acetic anhydride," *Appl. Catal. B.*, vol. 94, pp. 64-70, 2010.
- [10] P. Atkins and J. Paula, *Atkins' Physical Chemistry*, New York, Oxford University Press, 2006, pp. 200-234.



**Tatiane Fernandes Caetano Souza** earned her chemical engineering degree in 2013 from Escola Politécnica da Universidade de São Paulo (EPUSP), Brazil, and her industrial/generalist engineering degree in 2014 from Ecole Centrale de Lille, France. Presently she is pursuing a master degree in the field of chemical engineering with emphasis on process engineering design and simulation in the Chemical Engineering Department at Escola Politécnica da Universidade de São Paulo (EPUSP). She has 4 years' experience on working as a process engineer for a project engineering company from Brazil, Promon Engenharia.



**Roberto Guardani** is chemical engineer, professor at the Chemical Engineering Department, University of São Paulo, carries out research in the area of process systems engineering, involving: Mathematical modeling, simulation and optimization; multivariate statistical modeling, applied mainly in the following subjects: Industrial effluents treatment; atmospheric emissions; processes involving particles, with emphasis on fluidization, crystallization, multiphase flow; development of in-process measurement techniques.

# Experimental Investigation of Injection Pressure Effect on the Natural Gas Storage in Aquifers

E. Kazemi Tooseh, A. Jafari, and A. Teymouri

**Abstract**—Storing natural gas in underground reservoirs is a key element in the gas supply market. Depleted oil and gas reservoirs, salt caverns and aquifers are major candidates for natural gas storage, and between them aquifers have a high potential for effective balancing of a variable demand market. Aquifers are underground water bearing formations which may extend over distances of several miles, and in the absence of depleted reservoirs, saline aquifers are a proper option for underground gas storage. Because of water and gas movements in the reservoir, it is worth to know about the flow behavior across the porous medium. The behavior of natural gas in contact with brine has not been considered widely in the literature, and the effect of injection pressure on the process has not been studied experimentally before. Therefore, for the first time in this research the natural gas storage capacity at different pressures were calculated and gas and water flow behavior under high injection pressures in a low permeability rock is investigated by experimental tests.

Natural gas flooding experiments were performed using a core flood set up at constant temperature 46 °C, and in each test the low permeability core sample taken from an Iranian aquifer was cleaned by methanol injection for 24 hours. Then it was dried in oven at 90°C for 12 hours. After that the core was vacuumed for 8 hours and saturated by two pore volume of the synthetic brine with 210000 ppm salt concentration. After that natural gas was injected at a constant flow rate into the core plug saturated with brine, and at the gas breakthrough time experiments were stopped and the storage capacity of sample was measured by comparing its weight difference before and after the test. Obtained results illustrate that the injection pressure plays an important role in the gas storage process, and increasing the pressure improves the sweep efficiency and water withdrawal. In other words, by doubling the injection pressure from 80 to 160 bar the gas storage capacity enhances about 7%.

**Index Terms**—Natural gas, storage, aquifer, pressure effect.

## I. INTRODUCTION

Underground gas storage (UGS) is a concept which has evolved the effective balancing of a variable demand market. Historically, UGS was introduced for the first time in 1915 at an operating gas field in Canada. But rapidly UGS facilities were developed, and recently researchers have focused on underground natural gas storing during the low consumption

seasons [1]. In other words, gas storage is now considered as a key element for the gas supply market and has been used to satisfy a number of needs [2]. The whole natural gas storage process is comprised of injecting the gas into a subsurface reservoir during periods that demand falls below the gas supply. When consumption exceeds the supply, the gas will be withdrawn from the reservoir, and it is possible to have an effective delivery during the demand peak [3]. This process can also be adapted to produce oil or condensate and can be considered as an improved oil recovery (IOR) method [4].

Depleted oil and gas reservoirs, salt caverns and aquifers are major candidates for storing natural gas. Aquifers are underground water bearing formations which may extend over distances of several miles. When a closed anticlinal structure exists in an aquifer, it is possible to inject and store natural gas in the upper portion of the aquifer [5]. Because of the strong water drive in these reservoirs, it is reasonable to consider the important parameters in this process. But there are few related researches in the literatures, so the effective parameters are not well studied [6]. There are various parameters engaged in the gas storage process such as injection pressure, flow rate, brine salinity, temperature and reservoir rock properties. Salinity and temperature are not affected in a huge aquifer during gas storage [7], [8] but injection pressure and gas flow rate are more operative and interesting to be studied. Usually when encountering a flow of gas, the pressure of the system may affect the gas phase behavior very much. In the case of natural gas, increase of pressure changes the gas behavior toward the liquid flow. Abdollahi *et al.* [9] developed a compositional simulation model and showed that the injection pressure of gas is very effective on storage capacity during the gas storage process. Also other researchers have performed different simulations on natural gas storage process. Golghanddashti *et al.* [10] studied the gas storage in a depleted gas reservoir with edge aquifer at ambient pressure and high flow rates. Also Chun *et al.* investigated the gas storage process at atmospheric pressure. Sohrabi *et al.* [11] evaluated the multiphase flow and gas phase sweep efficiency during water alternating gas process. Billiotte *et al.* [12] studied numerically the injection withdrawal cycles and the flow rate effect in underground gas storage reservoir, and they have simulated air-water displacement in a micromodel.

As literature illustrates there has not been any experimental study on high pressure natural gas storage in saline aquifers. So in this study for the first time the influence of gas injection pressure on storage of natural gas in saline aquifers has been investigated experimentally. Three core flood experiments have been done on a core plug, and the fully brine saturated

Manuscript received August 11, 2017; revised November 20, 2017. This work was supported by the Natural Gas Storage Company of Iran.

E. Kazemi Tooseh is with National Iranian Oil Company, Tehran, Iran (e-mail: esmaeelkazemi69@gmail.com).

A. Jafari is with Tarbiat Modares University, Tehran, Iran (e-mail: ajafari@modares.ac.ir).

A. Teymouri is with National Iranian Gas Company, Tehran, Iran (e-mail: teymouri@nigc.ir).

sample is turned to a gas storage reservoir and the storage capacity of rock is calculated in each experiment.

## II. EXPERIMENTAL PROCEDURE

One core sample with length and diameter 3 and 1.5 inches, respectively was taken from an Iranian aquifer reservoir candidate for natural gas storage. The porosity and permeability of the core sequentially are 8.32% and 0.09 md. Table I specifies the core plug characteristics used in this research.

TABLE I: SPECIFICATION OF ROCK CORE USED IN THIS STUDY

Porosity (%)	Air Permeability (md)	Length (inch)	Diameter (inch)
8.32	0.09	3	1.5

Injected gas is the domestic gas which mainly consists of methane, and its combination is analyzed by the gas chromatography analysis. In order to measure non hydrocarbon gases along with hydrocarbon gases, TCD detector is deployed, and the gas chromatography analysis is done using TGF gas chromatograph model no.2550TG. Result of gas chromatography analysis is shown in Fig. 1. The injected gas consists of 98.98% methane and 1.02% CO<sub>2</sub>. The analysis is repeated twice in order to be sure that measurements are accurate. As it is shown in Fig. 1, there are two groups of peaks, the first two peaks refer to methane and the last one belongs to carbon dioxide. It should be noted that the first two peaks are adjacent because of high concentration of methane in the injected gas.

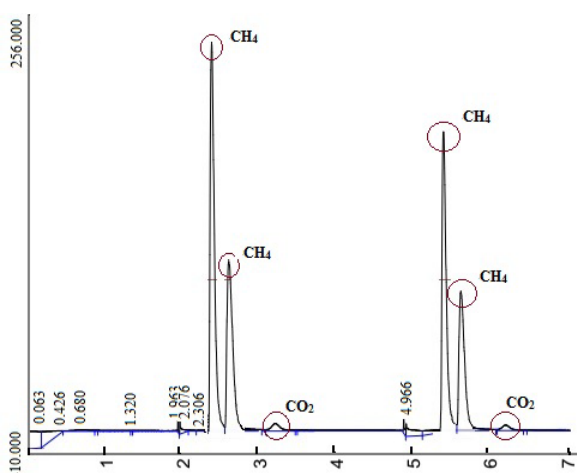


Fig. 1. Results of TCD gas chromatography.

In order to ensure that the feed gas composition is the same as studying reservoir condition (domestic gas), natural gas was provided from the domestic gas line in laboratory. Also in order to fill the gas transfer vessel, natural gas was passed and pressurized through compressor and gas booster. The pressure of domestic gas line is about 1 bar, so in order to fill the feed vessel a multi cycle injection method was designed. At first, gas was passed through a compressor and pressurized up to 3 bar, and then it was passed through the booster to get a

pressure equal to 30 bar. The pressurized gas was stored in a transfer vessel and it was displaced to another one after injecting water to the bottom part by pump. The cycle was repeated for three times to get a fully charged transfer vessel by high pressure natural gas. Fig. 2 shows the gas charging setup.

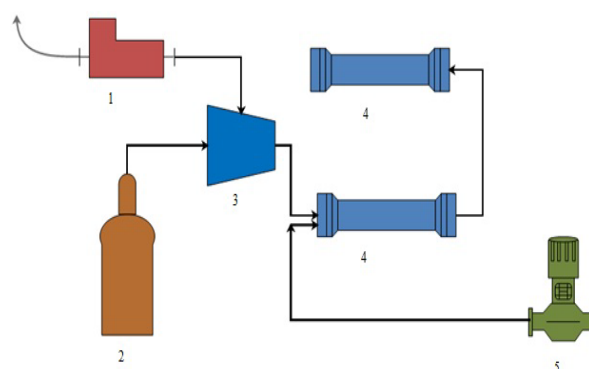


Fig. 2. Schematic of the designed setup for providing natural gas from the domestic gas line (1. Air Compressor, 2. Nitrogen Cylinder, 3. Gas Booster, 4. Transfer Vessel, 5. Pump).

Gas production rate was measured by using a simple water displacement setup. The setup consists of a cylinder with length equal to 1 meter and diameter equal to 9 cm. First it was vacuumed and filled with water. When gas entered the cylinder, water was displaced and the produced gas volume was measured by recording the water level change. Also production rate was measured by dividing the produced volume to water displacing time.



Fig. 3. Gas storage setup used in this study.

The main experimental setup mainly consists of a high pressure positive displacement pump, gas and water transfer vessels, core holder, hydraulic over burden pressure pump, heater, mixing valve, pressure transducers, back pressure regulator and separator. Fig. 3 shows the experimental setup used in this research. In each experiment the core sample was cleaned by injecting two pore volume of methanol, and then it was dried in oven at 90°C for 12 hours. After that the sample was vacuumed for 8 hours (because of its low permeability) and saturated by two pore volumes of the synthetic brine with density equal to 1.095 gr/cc and compositions illustrated in Table II.

The saturated core plug weight was measured, then it was

wrapped in aluminum foil in order to inhibit the gas flow out of the core sample and the synthetic brine was injected at the constant rate 0.05 cc/min in order to increase the pressure to the test value. Finally natural gas was injected in a typical flow rate condition and gas-water displacement under high pressure equilibrium occurred. The temperature of the system was set to 46 °C, which is the same as the studying reservoir condition. After injecting two pore volumes of gas and no water production, the sample was held under the constant pressure for 24 hours. Meanwhile gas production rate was measured, and the calculated rates were transformed to experiment pressure by using the ideal gas law (Eq. (1)). In addition, the gas effective permeability was calculated for each experiment using Darcy law (Eq. (2)).

TABLE II: BRINE COMPOSITION USED HERE

Ion Name	Na <sup>+</sup>	Ca <sup>2+</sup>	K <sup>+</sup>	Mg <sup>2+</sup>	Cl <sup>-</sup>	SO <sub>4</sub> <sup>2-</sup>
Concentration (ppm)	30820	45740	640	1580	130820	400

At the end, core rock weight was measured and storage capacity was calculated by the mean of weight difference before and after the test using equations (3) and (4). It should be mentioned that for having an accurate estimation of stored gas volume, weight measurement suggests the best case. As noted by many authors [13]-[15], natural gas solubility is very little in water even at high pressure, so trapping in aqueous phase is out of concern in this topic and the only way for gas storage is water removal.

$$PV = ZnRT \quad (1)$$

where  $Q$  is flow rate in cc/s,  $K$  is permeability in darcy,  $A$  is cross section in cm<sup>2</sup>,  $\mu$  is viscosity,  $dP$  is pressure difference and  $L$  is the length.

$$Q = \frac{KA dP}{\mu L} \quad (2)$$

where  $Q$  is flow rate in cc/s,  $K$  is permeability in darcy,  $A$  is cross section in cm<sup>2</sup>,  $\mu$  is viscosity,  $dP$  is pressure difference and  $L$  is the length.

$$V_b = \frac{m_b}{\rho_b} \quad (3)$$

$$m_b = m_1 - m_2 \quad (4)$$

In these equations,  $V_b$ ,  $m_b$  and  $\rho_b$  are volume, mass and density of produced brine,  $m_1$  and  $m_2$  stands for saturated core weight and core weight after the gas injection. Using these two equations yield volume of produced brine in the experiment. Then the stored gas volume will be the same as produced brine volume.

### III. RESULTS AND DISCUSSION

At first two experiments were done in order to investigate

the retention time effect on the gas storage. For the first experiment core sample was held under experimental condition for 5 days and in the second experiment retention time duration was set to 1 day. After measuring the storage gas volume no significant difference was observed. So 1 day retention time was selected for remaining experiments, and all measurements were done based on 1 day retention time. Table III shows the results of two experiments, and as the table illustrates the storage volume difference between two tests is about 1% which is negligible.

TABLE III: RETENTION TIME EFFECT ON GAS STORAGE CAPACITY

Retention Time	Flow Rate (cc/min)	Pressure (bar)	Storage Volume (cc)	Storage (%)
5 days	0.05	160	0.987	13.67
1 day	0.05	160	0.913	12.64

The effect of injection pressure on natural gas storage was investigated by injecting the gas at three typical pressures. It is worthy to note that due to low permeability of the core sample, the injection flow rate is very low, and it was set to 0.05 cc/min. Much care should be taken into account when the injection flow rate is constant. Injection gas flow rate could affect gas flow and gas storage volume. At high flow rates there is less time to fully observe the effectiveness of gas pressure on brine displacement. So choosing a suitable flow rate is very important for investigating the injection pressure effect. Rock permeability is one of the main factors for selecting the injection rate. Here the injection rate 0.05 cc/min has been chosen in order to have a continuous flow while considering the gas behavior under high pressure in the porous medium.

Three constant flow rate experiments were done at 46 °C, and they were performed at the injection pressures 80, 120 and 160 bar. Core weight measurements presented that there is more weight loss at higher pressures. In addition, as it can be seen in Table IV, higher injection pressure leads to higher gas production rate. On the other hand gas viscosity increases by increasing the injection pressure.

TABLE IV: GAS PRODUCTION RATE AND EFFECTIVE PERMEABILITY MEASUREMENT

$P$ (bar)	$dp$ (atm)	$\mu$ (cp)	$Q$ (cc/s)	$K$ (md)
80	0.435	0.0135	0.0117	0.0121
120	0.694	0.015	0.0143	0.0103
160	1.12	0.0168	0.0218	0.0109

Comparison of obtained results illustrated in Table IV and Table V confirms that more effective permeability would not certainly yield more storage percentage. Because there are various factors controlling the permeability such as gas phase and flow behavior. It can be observed that effective permeability at 80 bars is more than others, but the storage percentage is lower in this experiment.

Natural gas which mainly consists of methane shows a gaseous phase behavior even at high pressures. As the injection pressure enhances, density and viscosity of the gas

phase increases. This leads to lower mobility and a better piston-like displacement. So in the case of gas injection into an aquifer, by increasing the flooding pressure the gas phase sweep efficiency enhances. In other words, as Table V illustrates, by improving the injection pressure from 80 to 160 bar the storage capacity enhances from 5.78% to 12.64%. According to the results, enhancing the injection pressure from 120 to 160 bar has increased the stored gas volume about 5% while pressure enhance from 80 to 120 bar has improved the storage volume about 2%. It can be concluded that higher pressures have more effect on the gas phase behavior and at 160 bar the gas flow is getting closer to a liquid-like piston displacement.

TABLE V: INJECTION PRESSURE EFFECT ON GAS STORAGE CAPACITY

Experiment No.	Flow Rate (cc/min)	Pressure (bar)	Storage Volume (cc)	Storage (%)
1	0.05	80	0.417	5.78
2	0.05	120	0.552	7.64
3	0.05	160	0.913	12.64

It should be mentioned that by increasing the injection pressure, the cap rock failure pressure should be taken into account. If the reservoir pressure increases too much, integrity of cap rock weakens and there will be a path for gas leakage out of the reservoir.

#### IV. CONCLUSION

In order to perform natural gas storage properly, more attention should be paid to all the aspects of this process. As water and gas displacement across a reservoir is affected by operating conditions, in this study the injection pressure was studied through core flood experiments. Obtained data showed that increasing the pressure improves the sweep efficiency and water withdrawal. In this study increasing the injection pressure has improved the gas storage volume of the rock about 7%. But there would be a limit for pressure and choosing the injection pressure depends on many factors.

#### ACKNOWLEDGMENT

The authors appreciate Natural Gas Storage Company of Iran for the valuable support and encouragement during this research.

#### REFERENCES

- [1] A. Khaksar, A. White, K. Rahman, *et al.*, "Geomechanical evaluation for short term gas storage in depleted reservoirs," presented at the 46th US Rock Mechanics/Geomechanics Symposium. Chicago, Illinois, USA, June 24-27, 2012.
- [2] K. Aminian and S. D. Mohaghegh, *Natural Gas Storage Engineering*, first edition, Oxford: Eolss Publishers, 2009.
- [3] D. L. Katz and R. L. Lee, *Natural Gas Engineering: Production and Storage*, first edition. New York: McGraw-Hill Economics Department, 1990.
- [4] M. Soroush and N. Alizadeh, "Underground gas storage in partially depleted gas reservoir," presented at Canadian International Petroleum Conference, Calgary, Canada, June 12-14, 2007.
- [5] W. K. Sawyer, M. D. Zuber, and A. D. Bues, "Reservoir simulation and analysis of the sciota aquifer gas storage pool," presented at SPE Eastern Regional Meeting, Pittsburgh, Pennsylvania, USA, November 9-11, 1998.
- [6] L. Chun, W. Jieming, X. Hongcheng, *et al.*, "Study on fluids flow characteristics of water-gas mutual flooding in sandstone underground gas storage with edge water," presented at International Petroleum Technology Conference, Beijing, China, March 26-28, 2013.
- [7] P. Sadirli, A. Jafari, S. Sadeghnejhad, *et al.*, "Simulation and sensitivity analysis of natural gas storage in aquifers in presence of horizontal well," presented at the Fourth Conference on Reservoir Engineering and Upstream Industries, Tehran, Iran, 28 May, 2015.
- [8] P. Sadirli, A. Jafari, S. Sadeghnejhad, *et al.* "Simulation of natural gas storage process in aquifers," presented at the First National Conference on Oil and Gas Fields Development, Tehran, Iran, January 28-29, 2015.
- [9] A. Abdollahi, M. Riazi, and S. Ayatollahi, "Investigation of gas storage feasibility in an iranian aquifer," presented at the First Technical Conference and Exhibition on Petroleum, Tehran, Iran, May 14-16, 2013.
- [10] H. Golghanddashti, M. Saadat, S. Abbasi, *et al.*, "Experimental investigation of salt precipitation during gas injection into a depleted gas reservoir," presented at the International Petroleum Technology Conference. Bangkok, Thailand, February 7-9, 2011.
- [11] M. Sohrabi, D. H. Tehrani, A. Danesh, *et al.*, "Visualization of oil recovery by water-alternating-gas injection using high-pressure micromodels," *SPE J.*, vol. 9, no. 3, pp. 290-301, 2004.
- [12] J. A. Billiotte, H. D. Moegen, and P. Oren, "Experimental micromodeling and numerical simulation of gas/water injection/withdrawal cycles as applied to underground gas storage," *SPE Advanced Technology Series* vol. 1, no. 1, pp. 133-139, 1993.
- [13] Z. Duan and S. Mao, "A thermodynamic model for calculating methane solubility, density and gas phase composition of methane-bearing aqueous fluids from 273 to 523k and from 1 to 2000 bar," *Geochim. Cosmochim. Acta*, vol. 70, no. 13, pp. 3369-3386, 2006.
- [14] Z. Duan, N. Møller, J. Greenberg, *et al.*, "The prediction of methane solubility in natural waters to high ionic strength from 0 to 250 c and from 0 to 1600 bar," *Geochim. Cosmochim. Acta*, vol. 56, no. 4, pp. 1451-1460, 1992.
- [15] R. Sun, W. Hu, and Z. Duan, "Prediction of nitrogen solubility in pure water and aqueous nacl solutions up to high temperature, pressure, and ionic strength," *J. Solut. Chem.*, vol. 30, no. 6, pp. 561-573, 2001.



**Esmael Kazemi Tooseh** born in 1990. Kazemi holds a BS degree in petroleum engineering from Petroleum University of Technology, Ahvaz, Iran at 2013 and a MS degree in petroleum engineering from Tarbiat Modares University, Tehran, Iran at 2016.

He has worked on gas storage project in one of Iran's gas storage reservoirs. He is currently with National Iranian Oil Company.



**Arezou Jafari** holds a BS degree in chemical engineering from Isfahan University of Technology, Isfahan, Iran and a MS degree in chemical engineering from Sharif University of Technology, Tehran, Iran and a PhD degree in chemical engineering (transport phenomena in porous media) from Lappeenranta University of Technology, Finland.

She is an assistant professor at Tarbiat Modares University. Her research area includes fluid flow in porous media, CFD simulation of fluid flow and chemical processes, enhanced oil recovery, gas storage and reservoir simulation.



**Ali Teymouri** holds a BS degree in petroleum engineering from Petroleum University of Technology in 1995 and a MS in reservoir engineering from University of Calgary in 2002.

He is a senior reservoir engineering who has been working in different subsidiaries of National Iranian Oil Company as reservoir engineer, petro-physics, researcher, execution activities to grow personal and professional brands. After spending nearly a two decades working in upstream activities, he knows what truly drives oil and gas fields' recovery through challenges.

# Life Cycle Assessment of Biodiesel Production from Microalgae: A Mass and Energy Balance Approach in Order to Compare Conventional with *in Situ* Transesterification

Gorkem Uctug, Divya Naginlal Modi, and Ferda Mavituna

**Abstract**—The aim of this work was to perform life cycle analyses (LCA) based on detailed process mass and energy balances for the production of biodiesel from microalgae in order to compare the conventional transesterification with *in situ* transesterification. GaBi software was used to perform the LCA. The material balances revealed that a slightly lower biodiesel yield was obtained for *in situ* transesterification process (5.06 kg/day) when compared to the conventional one (5.5 kg/day). GaBi results showed that the global warming potential (GWP) of the conventional transesterification process was higher than *in situ* transesterification by 140 kg CO<sub>2</sub> equivalent (per tonne of biodiesel produced). No substantial difference was noted however, for acidification (4.15 vs. 4.34 kg SO<sub>2</sub> equivalent), eutrophication (0.641 to 0.666 kg PO<sub>4</sub>-equivalent) and human toxicity potential (72.3 vs. 77 kg dichlorobenzene equivalent) between the two processes per kg of biodiesel produced. The results of the LCA analysis also show that electricity production was the major contributor for all the environmental impacts. When both the global warming potential and biodiesel yield were taken into account, it could be concluded that biodiesel production via *in situ* transesterification was a better option.

**Index Terms**—Biodiesel, environmental impact, life cycle analysis, microalgae, transesterification.

## I. INTRODUCTION

The increasing demand for energy, the growing fears of climate change and other environmental issues and soaring prices of fossil fuels due to depleting fuel reserves are the main drivers for finding alternative sources of energy which are environmentally friendly [1], [2]. Extensive research has shown that biofuels are capable of replacing conventional fossil fuels in the transportation sector [3] and they have lower carbon emissions. Hence, biofuels are deemed capable of decreasing greenhouse gas emissions arising from the transportation industry [4]. Furthermore, biofuels contribute in reducing the dependency on conventional fuel sources in many countries [4] and they are equally considered to represent and compromise between meeting energy needs without causing further environmental damage [2]. Biodiesel is attracting interest due to several reasons, some of which are the following [5]-[7]:

i) it is biodegradable and has no toxicity characteristics,

Manuscript received August 4, 2017; revised November 20, 2017.

Gorkem Uctug is with the Izmir University of Economics, Faculty of Engineering and Computer Science, Turkey (e-mail: gorkem.uctug@ieu.edu.tr).

Ferda Mavituna and Divya Naginlal Modi are with the University of Manchester, School of Chemical Engineering and Analytical Science, Turkey (e-mail: ferda.mavituna@manchester.ac.uk, divya.naginlal@gmail.com).

- ii) it has a lower contribution to air emissions,
- iii) it can be produced from renewable precursors,
- iv) it has negligible sulfur content, superior flash point and higher combustion efficiency
- v) and it can be used in vehicles without modifying the engine due to the fact that biodiesel has the same physical and chemical characteristics as diesel.

Biodiesel can be produced via a variety of feedstocks, which are classified according to availability of use for other purposes. First generation feedstock (palm, rapeseed, soybean, coconut) have edible oils that are suitable for human consumption, second generation feedstock consists of oils that are inappropriate for human consumption (jatropha, karanja, jojoba, mahua, waste cooking oil, grease, animal fats), and finally third generation feedstock is defined as new products obtained from biological reactions/processes, such as microalgae [7]. Currently, the two most common feedstocks which are being used for producing biodiesel are rapeseed (in Europe) and soybean (in the United States). However, a debate is ongoing as to whether these two feedstocks should be primarily used as food or as a fuel source [8]. An alternative feedstock for biodiesel production can be algae. Amongst the numerous advantages associated with the latter, the most important one is that algae cannot be used as a food source so the problem of resource allocation between food and energy supply does not apply to the case of biodiesel production from algae [9]. However, it has been reported that it is imperative to have technological breakthroughs in the processing of algae so as to lower the environmental impacts below that of fossil fuel-based diesel [10], [11].

There have been several life cycle assessment (LCA) studies on algal biodiesel production but these have not considered mass and energy balances. The scope of this paper therefore, is to apply the mass and energy balance principle to perform a “gate to gate” LCA on biodiesel production from microalgae. The objectives of our study are as follows:

- vi) To build two hypothetical models of microalgal biodiesel production. The former model is based upon the information available from literature on biodiesel production from *Chlorella* using raceway ponds of seawater in India with the conventional transesterification. The model consists of using an alternative route that uses *in situ* transesterification, which is believed to be more efficient. These models are considered herein so as to determine whether *in situ* transesterification has a lower environmental impact.
- vii) To perform a mass and energy balance on the models for the process. The aim of performing these balances is to

build the inventory analysis which will then be used to perform the LCA.

viii) To analyse several examples of environmental impact based on the data obtained from the mass and energy balances and comparison among such instances so as to determine the best route of biodiesel production from microalgae.

## II. METHODOLOGY

### A. Biodiesel Production from Microalgae

There are several major and minor processes associated with the production of biodiesel from microalgae. These processes are summarised in Table I.

TABLE I: MAJOR AND MINOR PROCESSES IN BIODIESEL PRODUCTION FROM MICROALGAE

Process Classification	Unit Process
Major	Cultivation
	Harvesting
	Oil extraction
	Transesterification and <i>in situ</i> transesterification
	Anaerobic digestion
Minor	Transportation of biomass within the industry through a belt conveyor
	Separation of algal residue from oil
	Hexane and methanol recovery from oil
	Neutralisation of catalyst
	Separation of glycerol from biodiesel
	Purification of biodiesel

Since the main novelty of this paper is to compare two different transesterification methods, we believe that a special focus should be given to transesterification. Transesterification can be defined as the process whereby triacylglycerols (TAGs) are converted into fatty acid methyl esters (FAME) in the presence of an alcohol and a catalyst [12].

*In situ* transesterification, on the other hand, consists of performing oil extraction and conversion of oil into biodiesel through a single step. The advantages of *in situ* transesterification over conventional transesterification is the reduction in the manufacturing cost due to the elimination of certain unit processes such as oil extraction using hexane, and simplicity of system design and operation [13], [14]. However, *in situ* transesterification has certain disadvantages as well such as the decrease in the biodiesel yield and the increased consumption of chemicals due to the requirement of a higher ratio alcohol-oil ratio [15].

### B. Mass and Energy Balance Approach

Since there are no known existing commercial plants which produce biodiesel from microalgae [16], the models used in this research were built based on the information available from the literature, especially for the cultivation of the microalgae as shown in Table II. In this paper, the inputs and outputs were determined using a chemical engineering approach, that is, mass and energy balances rather than just collecting data about the process. Although biodiesel production from microalgae is still in its infancy on the commercial scale, much research has been carried out about the unit operations involved in the process. In this study, two scenarios of mass and energy balances have been carried out.

The first scenario (also referred to as the baseline scenario) consists of using the conventional method of producing biodiesel whereas the second scenario (*in situ* transesterification) involves using a more advanced technology so as to minimise cost and process units. Detailed information about the mass and energy balances can be found elsewhere [17].

TABLE II: DATA FOR THE MASS AND ENERGY BALANCE CALCULATIONS

Parameters	Values	References
Maximum specific growth rate	0.041 h <sup>-1</sup>	[18]
Initial dissolved CO <sub>2</sub> concentration	0.013 mol·m <sup>-3</sup>	
Michaelis- Menten constant of CO <sub>2</sub>	0.00021 mol·m <sup>-3</sup>	
Surface area of raceway pond	10,000 m <sup>2</sup>	[19, 20]
Depth of raceway pond	20 cm	[20]
Biomass concentration in pond	0.1 g·L <sup>-1</sup>	[18]
CO <sub>2</sub> utilization efficiency	90%	[21, 22]
Amount of CO <sub>2</sub> consumed by microalgae daily	540 kg	[22]
CO <sub>2</sub> loss	25%	[11, 23]
Ratio of C:N :P	100:16:1	[23]
Amount of water lost due to evaporation per square metre	0.0062 m <sup>3</sup>	[24]
CO <sub>2</sub> utilization efficiency	90%	[21, 22]
Organic carbon content of microalgae	50%	[25]

### C. Life Cycle Assessment (LCA) Methodology

The scope of this study consists of analysing 1 kg of algal biodiesel produced at factory gate through the conventional esterification method and *in situ* transesterification. System expansion is applied in this study for both production routes, as follows; algal residue is anaerobically digested to produce biogas and is in turn combusted to generate electricity which is used in the cultivation process. Similarly, glycerol is combusted in a furnace to generate heat which is used within the biodiesel production process. The environmental impacts were calculated by using GaBi software with CML2001 methodology. The main reason behind this choice is that the same methodology has been adopted by several authors [11], [16] who previously carried out LCA research on biodiesel. The biodiesel production is assumed to take place in India using raceway ponds with seawater.

The system boundary for the production of biodiesel through the conventional method and *in situ* transesterification are represented by Fig. 1 and Fig. 2, respectively. The following unit processes have not been considered in this project:

- construction of the biodiesel plant;
- transportation of raw materials and of process equipment;
- manufacturing process of raw materials (except electricity) and process equipment;
- transportation of biodiesel to the filling station, and;
- combustion of the biodiesel produced.

Detailed information about the LCA inventory can be found elsewhere [17].

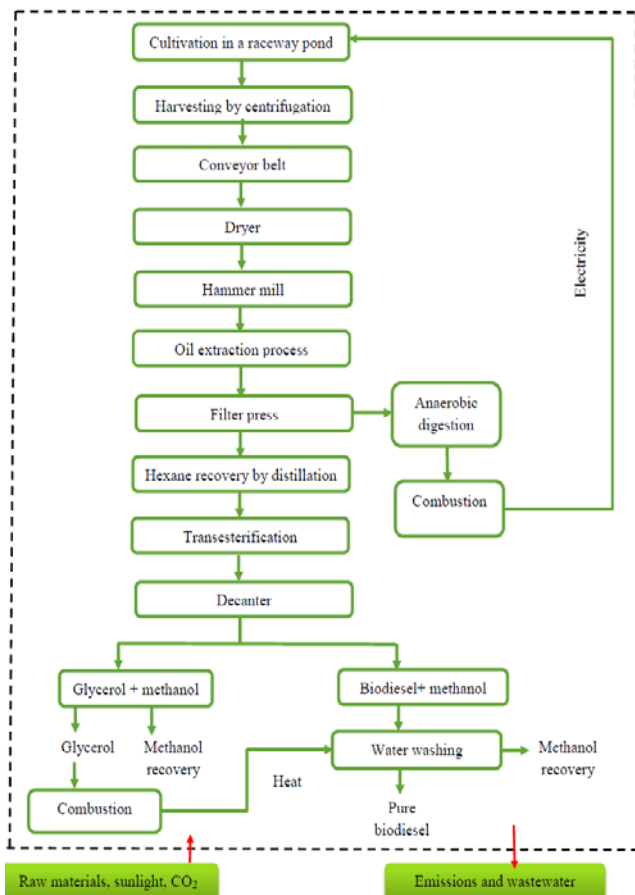


Fig. 1. System boundary for conventional algal biodiesel production.

In the two models salt water algae such as the genus *Chlorella* is used. The cultivation is based on open raceway ponds with the injection of carbon dioxide (flue gas). Paddlewheels are used in order to provide mixing of the dissolved carbon dioxide and other nutrients, sodium nitrate and diammonium phosphate solution. The operating period for the raceway pond is assumed to be 10 hours. During the night, it is assumed that the algae will not grow.

Algal oil was assumed to consist only of linoleic acid (C18:2) since it has been observed to be the most abundant fatty acid present in microalgae [26]. Linoleic acid was therefore used in the estimation of the stoichiometric carbon requirement by microalgae for the formation of the fatty acids.

### III. RESULTS AND DISCUSSION

Fig. 3 below shows the comparative impact results for

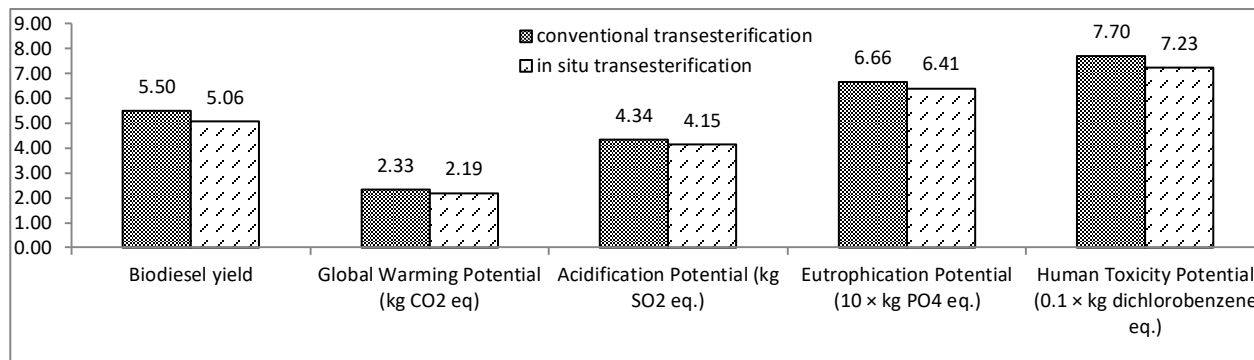


Fig. 3. Yield and impact scores for conventional and *in situ* transesterification.

conventional and *in situ* transesterification, as well as the yield scores for each technology.

#### A. Global Warming Potential

Based on Fig. 3, it is estimated that irrespective of the method of biodiesel production considered, an average of 2.26 kg CO<sub>2</sub> eq. per kilogram of biodiesel produced is emitted. The results from the GaBi software revealed that in both scenarios, electricity production is the major process which contributes most to the release of GHG gases. In this work, electricity production has been modelled using coal as its precursor material. Using coal as a raw material for electricity production leads to the release of massive amounts of CO<sub>2</sub>, CH<sub>4</sub> and NO<sub>x</sub>. The CO<sub>2</sub> emission, which is reported in the GaBi software to contribute to global warming, is, in fact, the excess CO<sub>2</sub> not consumed by the microalgae and, consequently, released into the atmosphere. In order to further increase the amount of CO<sub>2</sub> consumed by microalgae, new approaches to facilitate CO<sub>2</sub> consumption by the algae must be developed.

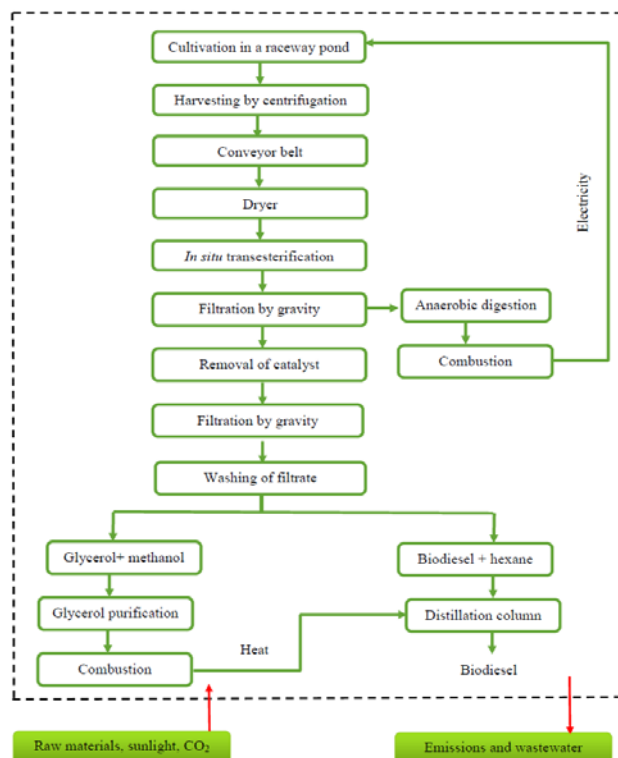


Fig. 2. System boundary for in-situ transesterification in algal biodiesel production.

### B. Acidification Potential

The range of acidification potential of microalgal biodiesel production was found to vary between 4.15 to 4.34 kg SO<sub>2</sub>-eq. per kilogram of biodiesel produced. The GaBi analysis proved that electricity and cultivation of microalgae are the major contributors to the effect of acidification. The emissions produced during electricity generation which contribute to the effect of acidification include NO<sub>x</sub>, hydrogen chloride (HCl) and NH<sub>3</sub>. Fertilisers are believed to be the main cause for NH<sub>3</sub> emissions [11]. It can be observed that there is a very small difference in the acidification potential between *in situ* transesterification and conventional transesterification. Hence, it can be argued that this difference is relatively insignificant on an industrial scale, for example for the production of 1000 kg of biodiesel. The marginal difference is due to the fact that the electricity consumption in *in situ* transesterification is less than in conventional transesterification.

### C. Eutrophication Potential

Regardless of the method of biodiesel production considered, the eutrophication potential varies between 0.666 to 0.641 kg PO<sub>4</sub><sup>3-</sup> eq. per kilogram of biodiesel produced. The major contributors of eutrophication are electricity production and cultivation of microalgae. GaBi revealed that NH<sub>3</sub> is the major pollutant leading to the effect of eutrophication. Similar findings have been observed in earlier studies [27].

### D. Human Toxicity Potential

From Fig. 3, it can be speculated that there is a minimal difference of about 6.1% between the two scenarios. If the above scenarios are modelled for large scale biodiesel

production, the savings in terms of human toxicity potential in *in situ* transesterification are not substantial. Human toxicity is caused mostly through emissions into air, which is equal to 68.2 kg DCB eq. and 64.1 kg DCB eq. for conventional and *in situ* transesterification, respectively (both are expressed in units of kilogram of biodiesel produced). A stage contribution analysis of the GaBi results showed that electricity production is the sole key contributor to human toxicity. This result conforms to earlier findings [27]. The pollutants released from the production of electricity consist mostly of heavy metals (41.3%) such as arsenic (+V) and selenium, inorganic emissions to air (23.2%) and organic emissions to air (23.5%) for *in situ* transesterification. This result is in agreement with findings in earlier studies [27] that emissions of heavy metals are responsible for human toxicity.

### E. Comparison to Other Studies

Although there is a considerable number of studies concerning the LCA of microalgal biodiesel in the literature, direct comparison of our results to the results published in those studies proved to be impossible in most cases due to either differences in system boundaries or in functional units. For instance, many studies define the functional unit as the unit amount of energy produced in a vehicle. Furthermore, the type of LCA methodology used (endpoint vs. midpoint) also limits the scope of comparisons of the respective results. Finally, even if the system boundaries, functional units, and methodologies are similar, the impacts calculated in one study may have been overlooked in another. It was therefore only possible to compare the global warming potential results with four other studies. Results of these comparisons are presented in Fig. 4.

Fig. 4. Comparison of Global Warming Potential (GWP) values against other studies.

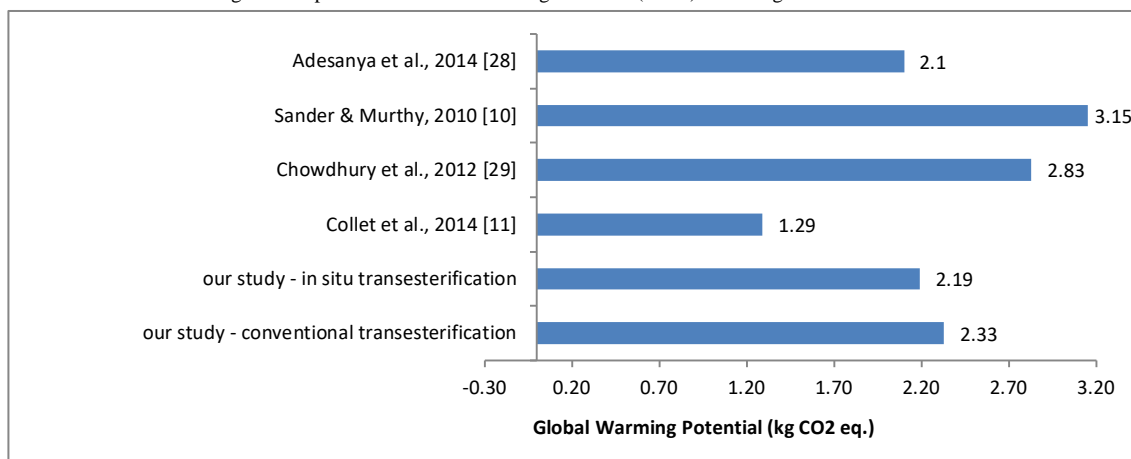


Fig. 4 shows that our results are close to, albeit not the same as, the findings reported in earlier studies. The main differences arise from the environmental qualities of the sources used for electricity generation. For instance, Collet and colleagues [11] used the European electricity mix data, which has much lower GWP impact than the Indian electricity mix, and we believe this to be the main reason behind the considerable difference between their results and ours.

Last but not least, we would like to explain the absence of a sensitivity analysis in this study. Since the present approach

is based on a detailed mass and energy balance, we believe that all the inventory data are of high quality and therefore we deem any sort of sensitivity analysis unnecessary.

## IV. CONCLUSION

In this study, two hypothetical models; conventional and *in situ* transesterification, were developed as potential methods of producing biodiesel from microalgae. The two systems considered for biodiesel production consist of unit operations that were modelled in the best possible realistic way. It can be

stated that *in situ* transesterification have never been considered in previous LCA studies on microalgal biodiesel production. A combination of the technologies applied in the downstream processing of first and second generation biodiesel feedstocks were applied to the microalgal biodiesel production systems. Mass and energy balances were performed and used to build the inventory for the LCA on biodiesel production. The material and energy balances carried out indicated that the biodiesel production process has a relatively low efficiency. However, algae can have up to 100 times more oil content when compared to first and second generation feedstocks (energy crops). Also, *in situ* transesterification has a slightly lower biodiesel yield than the conventional transesterification method. An analysis on the possible environmental impacts that may arise from the biodiesel production process has been carried out. The LCA analysis revealed the following:

- *In situ* transesterification has been proved to perform better across all the impact categories considered in the present work. This is due to the fact that the conventional transesterification process has slightly higher energy consumption.
- The global warming potential of *in situ* transesterification is lower than that of the conventional transesterification. The former has a GWP of 2190 kg CO<sub>2</sub>-eq. whereas the latter has a GWP of 2330 kg CO<sub>2</sub>-eq.
- The difference observed amongst the environmental impacts (besides global warming potential) is marginal and consequently, it may not make a significant difference on the consequences of acidification, eutrophication and human toxicity.
- In both scenarios, the effect of acidification has been found to be caused mainly by electricity production and cultivation of microalgae. The use of fertilisers in the cultivation medium has been observed to be responsible for the acidification effect due to the release of NH<sub>3</sub>.
- Results given by GaBi revealed that eutrophication is mostly a result of electricity generation and the cultivation process of microalgae. NO<sub>x</sub> and NH<sub>3</sub> are the major pollutants released from each of these processes, respectively.

Algal photosynthetic and primary carbon metabolism play a very important role not only in the process economics but also in the LCA-indicated sustainability issues for future considerations of algal hydrocarbon and/or biodiesel production. Strain improvement either through natural mutant identification or genetic manipulations, with the proper containment precautions, should be the alternatives to consider as far as future work is concerned.

#### REFERENCES

- [1] L. Zhu, *et al.*, "Biodiesel production from algae cultivated in winter with artificial wastewater through pH regulation by acetic acid," *Applied Energy*, vol. 128, pp. 103-110, 2014.
- [2] United Nations. (2014). The state of the biofuels market: Regulatory, Trade, and Development Perspectives. [Online]. Available: [http://unctad.org/en/PublicationsLibrary/ditcted2013d8\\_en.pdf](http://unctad.org/en/PublicationsLibrary/ditcted2013d8_en.pdf)
- [3] J. Malça, A. Coelho, and F. Freire, "Environmental life-cycle assessment of rapeseed-based biodiesel: Alternative cultivation systems and locations," *Applied Energy*, vol. 114, pp. 837-844, 2014.
- [4] DNV 2010 Biofuels 2020. A policy driven logistics and business challenge. [Online]. Available: [http://www.dnv.com/binaries/Biofuels%202020%20position%20paper\\_tcm4-](http://www.dnv.com/binaries/Biofuels%202020%20position%20paper_tcm4-)
- [5] I. Bankovic-Ilic, O. Stamenkovic, and V. Veljkovic, "Biodiesel production from non-edible plant oils," *Renewable and Sustainable Energy Reviews*, vol. 16, pp. 3621-3647, 2012.
- [6] S. Farell and E. Cavanagh, "An introduction to life cycle assessment with hands-on experiments for biodiesel production and use," *Education for Chemical Engineers*, vol. 9, pp. 67-76, 2014.
- [7] P. Nautiyal, K. Subramanian, and M. Dastidar, "Production and characterization of biodiesel from algae," *Fuel Processing Technology*, vol. 120, pp. 79-88, 2014.
- [8] X. Deng, L. Yajun, and X. Fei, "Microalgae: A promising feedstock for biodiesel," *African Journal of Microbiology*, vol. 3, issue 13, pp. 1008-1014, 2009.
- [9] S. Medipally, F. Yusoff, S. Banerjee, and M. Shariff, "Microalgae as sustainable renewable energy feedstock for biofuel production," *BioMed Research International*, vol. 2015, pp. 1-13, 2015.
- [10] K. Sander and G. Murthy, "Life cycle analysis of algal biodiesel," *International Journal of Life Cycle Assessment*, vol. 15, pp. 704-714, 2010.
- [11] P. Collet, *et al.*, "Biodiesel from microalgae- life cycle assessment and recommendations for potential improvements," *Renewable Energy*, vol. 71, pp. 525-533, 2014.
- [12] A. Koutinas and S. Papanikolaou, "Biodiesel production from microbial oil," in *Handbook of biofuels production*, R. Luque, J. Campelo, and J. Clark, Eds., Cambridge: Woodhead Publishing Ltd., 2016, p. 177.
- [13] I. Rawat, R. R. Kumar, T. Mutanda, and F. Bux, "Biodiesel from microalgae: A critical evaluation from laboratory to large scale production," *Applied Energy*, vol. 103, pp. 444-467, 2015.
- [14] H. He, X. Guo, and S. Zhu, "Comparison of membrane extraction with traditional extraction methods for biodiesel production," *Journal of the American Oil Chemists' Society*, vol. 83, pp. 457-460, 2006.
- [15] P. Hidalgo, *et al.*, "Improving the FAME yield of *in situ* transesterification from microalgal biomass through particle size reduction and cosolvent incorporation," *Energy & Fuels*, vol. 29, pp. 823-832, 2014.
- [16] L. Lardon, *et al.*, "Life cycle assessment of biodiesel production from microalgae," *Environmental Science & Technology*, vol. 43, issue 17, pp. 6475-6481, 2009.
- [17] N. M. Divya, "Life cycle assessment of biodiesel production from microalgae," MSc dissertation, The University of Manchester, Manchester, UK, 2015.
- [18] H. Lian, V. Subramanian, and Y. Tang, "Experimental analysis and model-based optimization of microalgae growth in photo-bioreactors using flue gas," *Biomass and Bioenergy*, vol. 41, pp. 131-148, 2012.
- [19] A. Pandey, D. Lee, Y. Chisti, and C. Soccol, *Biofuels from Algae*, USA: Elsevier, 2014.
- [20] M. Borowitzka, "Microalgae in outdoor ponds," in *Algal Culturing Techniques*, R. Andersen, Ed., United Kingdom: Elsevier Academic Press, 2005.
- [21] A. Demirbas and M. Demirbas, *Algae Energy: Algae as a New Source of Biodiesel*, London: Springer, 2010.
- [22] S. Sudhakar, S. Suresh, and M. Premalatha, "An overview of CO<sub>2</sub> mitigation using algae cultivation technology," *International Journal of Chemical Research*, vol. 3, issue 3, pp. 110-117, 2011.
- [23] J. Rogers, *et al.*, "A critical analysis of paddlewheel-driven raceway ponds for algal biofuel production at commercial scales," *Algal Research*, vol. 4, pp. 76-88, 2014.
- [24] N. Sazdanoff, "Modeling and simulation of the algae to biodiesel fuel cycle," B. Eng. Thesis, Ohio State University, 2006.
- [25] P. Schlagermann, *et al.*, "Composition of algal oil and its potential as biofuel," *Journal of Combustion*, vol. 2012, pp. 1-14, 2012.
- [26] J. Lee, *et al.*, "Comparison of several methods for effective lipid extraction from microalgae," *Bioresource Technology*, vol. 101, issue 1, pp. 75-77, 2010.
- [27] J. Hou, P. Zhang, X. Yuan, and Y. Zheng, "Life cycle assessment of biodiesel from soybean, jatropha and microalgae in China conditions," *Renewable and Sustainable Energy Reviews*, vol. 15, pp. 5081-5091, 2011.
- [28] V. Adesanya, E. Cadena, S. Scott, and A. Smith, "Life cycle assessment on microbial biodiesel production using a hybrid cultivation system," *Bioresource Technology*, vol. 163, pp. 343-355, 2014.
- [29] R. Chowdhury, S. Vjamajala, and R. Gerlach, "Reduction of environmental and energy footprint of microalgal biodiesel production through material and energy integration," *Bioresource Technology*, vol. 108, pp. 102-111, 2012.



**Fehmi Görkem Üçtuğ** was born in Ankara, Turkey in 1982. After graduating from Middle East Technical University – Chemical Engineering Department with a GPA of 3.85/4.00- with the First in Class award in 2004, he carried out his PhD studies at the University of Manchester, School of Chemical Engineering and Analytical Sciences between 2004 and 2008. His studies were funded by the Marie Curie Fellowship of

the 6<sup>th</sup> Framework Programme of the European Union. His thesis title was “Synthesis and characterisation of polyvinylalcohol-mordenite membranes and their applications in direct methanol fuel cells”.

After returning to Turkey, he completed his compulsory military service and then started working at Bahçesehir University – Energy Systems Engineering Department in 2010, where he had worked as an assistant professor until September 2016. He taught courses such as “Fundamentals of thermodynamics”, “Heat and mass transfer”, “Fuels and combustion”, “Energy economics”, “Sustainable energy”, “Fuel cell technologies”, “Introduction to energy systems engineering”, “Alternative and renewable energy systems”, “Capstone project”. He also was the vice-dean of the Faculty of Engineering and Natural Sciences between 2013 and 2016. Between September-December 2016, he worked as a visiting professor at the Sustainable Industrial Systems research group within the School of Chemical Engineering and Analytical Sciences of the University of Manchester.

Since February 2017, he has been working as an assistant professor at Izmir University of Economics (Turkey), Faculty of Engineering and Computer Science. His fields of interest include life cycle assessment, clean carbon technologies, direct methanol fuel cells, energy efficiency in buildings, and optimization.

**Divya Naginlal Modi** was born in Plaines Wilhems, Mauritius in 1991. After graduating from the University of Mauritius in chemical and environmental engineering with a GPA of 3.32/4 in 2014, she pursued her MSc degree in environment and sustainable technology at the University of Manchester, School of Chemical Engineering and Analytical Science in 2015. During her master’s degree, the title of her thesis was “Life cycle assessment of biodiesel production from microalgae”.

After returning to her home country, she was employed as a research assistant at the Mauritius Research Council in June 2016, which is the national body responsible for advising the Government of Mauritius on Science and Technology issues and it influences the direction of technological innovation by funding projects in areas of national priority and encouraging strategic partnerships. Her research projects at the Mauritius Research Council focus in the field of biotechnology. Her research interests are in the following areas: life cycle assessment, industrial ecology, sustainable development, biotechnology, renewable energy, recycling and waste to energy.



**Ferda Mavituna** is currently a professor of chemical and biochemical engineering in the School of Chemical Engineering and Analytical Science at The University of Manchester, UK. She obtained her degree of BSc in chemical engineering with the Distinction of High Honours and the First Prize in the Department of Chemical Engineering, Middle East Technical University (METU), in Ankara, Turkey in 1973. Her degrees of MSc in advanced chemical engineering and PhD in chemical engineering were awarded by the Victoria University of Manchester, UK in 1974 and 1979, respectively. She was chosen for the IChemE and SERC Special Award during 1978-1980 in order to write the biochemical engineering and biotechnology handbook with professor Bernard Atkinson (Macmillan Publishers Ltd). Ferda became a lecturer in the Chemical Engineering Department of UMIST, Manchester in 1980. She was awarded the Senior CIBA-GEIGY Fellowship in 1989 for sabbatical at ETH Zurich. Her research was supported by both industrial companies, notably Albright and Wilson and Kaneka as well as the research councils. Her main research covers specialty chemicals production, such as pharmaceuticals by freely suspended and immobilised microbial, plant and animal cell cultures. In her research, Ferda uses both experimental and theoretical/computational approaches such as kinetics, mass transfer and metabolic flux balance analysis. She has also taught a wide range of chemical engineering and bioprocess engineering courses at graduate and undergraduate levels.



# **Enzyme Engineering and Technology**



# An Amperometric Biosensor Based on Fumarate Reductase for Enzymatic Properties and Electrical Behavior

Yemin Yu, Yonghong Hu, Tao Li, Wenge Yang, Yuhao zhang, and Renlun Deng

**Abstract**—In this paper, the production of fumarate reductase was studied. Through ultrasonic separation, gel chromatography and 65% ammonium sulfate fractionation, the fumarate reductase specific activity reached to 106 U/mg, the purification ratio was 12.8 times and the recovery was 24%. Fumarate reductase was fixed on electrode, which was modified polyethyleneimine reductive graphene composites, through covalent bonding and electrostatic adsorption. The electrode was used to replace coenzyme NADH in the cell inside metabolism, constructing a fumarate reductase catalytic system based on electrical driving.

The results showed that fumaric acid reductase immobilized on the electrode not only maintained a certain biological activity, but also could catalyze the metabolism of fumaric acid. Thus, the electrical catalysis of fumarate reductase/polyethyleneimine reductive graphene composites/glassy carbon electrode and the substrate of fumaric acid based on fumarate reductase were studied, providing a scientific theoretical basis for the production of succinic acid in vitro.

**Index Terms**—Fumarate reductase, fumaric acid, succinic acid, electronical catalytic behavior.

## I. INTRODUCTION

Bio-based chemicals are series of products that are derived from renewable biomass and catalyzed by biological cells or enzymatic proteins. Succinic acid is ranked by the US Department of Energy's 12 kinds of biological-based bulk chemicals, the large-scale production process is one hot focus at home and abroad, compared with the traditional chemical synthesis process, bio-high technology has the advantage of small pollution.

Succinic acid ( $C_4H_6O_4$ , CAS number 110-15-6, molecular weight 118.09, Fig. 1), is an important chemical raw material and main "C4 platform compound" that can be converted to 1,4-butanediol, tetrahydrofuran, 6,4-butyrolactone and other four-carbon chemicals. It has a wide range of use in medicine, food and surfactant industry [1]. Succinic acid is an important member of the tricarboxylic acid cycle, and the metabolic regulation of the living body plays a pivotal role. As a surfactant, cleaning additive, ion chelating agent, acidifying

agent and antidote, etc., in food, medical care and health care products, Electroplating and other industries occupy a very important position. At present, many of the chemical products are based on benzene as raw materials. As one petrochemical products, benzene is not renewable. Hence, from the consideration of long-term, it is very meaningful to find one kind of right renewable raw materials to replace benzene. With the development of catalytic processes, succinic acid can also be converted to more chemical products, such as succinic acid hydrogenation of butanediol can be carboxylated adipic acid. In the food field, succinic acid is an ideal sour agent. Succinic acid sodium salt can improve the quality of soy sauce, soy sauce, liquid seasoning and refining products. In the pharmaceutical industry, succinic acid is one active ingredients of traditional Chinese medicine amber, been involved in energy metabolism and affecting excitability. One interesting thing is that succinic acid can also be used as a plant growing agent.

Fumarate reductase is an enzyme that changes the fumaric acid to succinic acid by achieving H from NADH and is important in microbial metabolisms a part of anaerobic respiration (Fig. 2, 3). The enzyme is widely found in gram-negative bacteria, facultative anaerobic gram-positive bacteria, as well as some green algae, protozoa, parasitic worms and low ocean eukaryotes [2], [3]. In other words, fumarate reductase couples the reduction of fumarate to succinate to the oxidation of quinol to quinone, in a reaction opposite to that catalysed by the related complex II of the respiratory chain (succinate dehydrogenase). Fumarate reductase is a staple enzyme in the tricarboxylic acid cycle. The reverse enzyme is a succinate dehydrogenase. As a key enzyme in many biological anaerobic respiration, it plays very important role. It not only can catalyze the reduction of fumaric acid to succinic acid but also can be a potential shoe gene for the treatment of many diseases because both the mammal and the human do not contain fumarate reductase in while the microbes causing various diseases contain. The fumarate reductase, which has been studied, can be divided into two types of membrane-bound and soluble. Most of the fumarate reductase belongs to the membrane-bound type, with three kinds of subunits, one catalytic subunit, one iron family of subunits and anchoring subunits that bind the catalytic subunit and iron cluster protein subunits to the membrane. The catalytic subunit contains active sites, while the iron cluster protein subunits pass electrons to the catalytic subunit by paving the subunits. This type of fumarate reductase mainly

Manuscript received September 30, 2017; revised November 30, 2017. This work was supported in part by the state key development program of China (2016YED0201002).

The authors are with College of Biotechnology and Pharmaceutical Engineering, State Key Laboratory of Materials-Oriented Chemical Engineering, Nanjing Tech University, Nanjing 211816, China (e-mail: 1253753161@qq.com, yonghonghu11@126.com).

in the anaerobic conditions and maintaining oxygen balance will be functional to produce succinic acid from fumaric acid.

However, the traditional chemical way of synthesizing succinic acid is limited due to cost and environmental pollution, making the limitation of wide range of applications when succinic acid is used as the basic chemical raw materials. Fermentation producing succinic acid has many advantages. First, it is reported that using a new microbial fermentation process and a new recovery process for electro dialysis and liquid-liquid extraction, whose cost is much lower than that of the traditional chemical production method. Thus, the traditional chemical way of synthesizing succinic acid will give way to fermentation. Secondly, because of the environment-friendly feature, the cost reduction is beneficial to the wide use range of applications of succinic acid as organic synthesis intermediates. Third, the fermentation production of succinic acid is based on renewable sources, such as glucose and carbon dioxide as the main raw material, the new process of producing benzene and other petrochemical products market prospects is social and environmental. This way not only gets out of the dependence on petrochemical raw materials, but also opens up a new utilization way of greenhouse gas carbon dioxide [4], [5]

At present, the research on fumarate reductase is mainly focused on the application of the enzyme, articles in the world talking about purification methods and the nature of the enzymology is not a lot. In the enzymatic fermentation, fumarate reductase plays a key role in the direct conversion of converting fumaric acid to succinic acid. Fumarate reductase as a key enzyme in the production of succinic acid, its research has become increasingly important. What's more, the enzymatic properties of fumarate reductase vary greatly depend on different strains. It is necessary to study the basic characteristics and enzymatic properties of fumarate reductase by using intracellular fumarate reductase to transform fumaric acid into succinic acid. In this study, the preliminary purification of fumarate reductase produced by *Brevibacterium ammoniagenes* was studied, which provided theoretical guidance for industrial application of fumarate reductase.

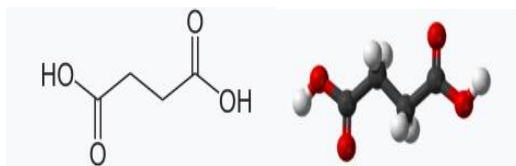


Fig. 1. Structure of succinic acid.

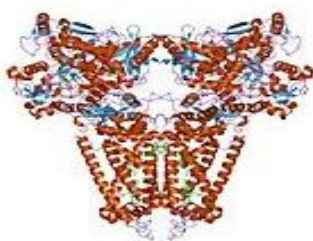


Fig. 2. Fumarate + fumarate reductase  $\Rightarrow$  succinic acid.

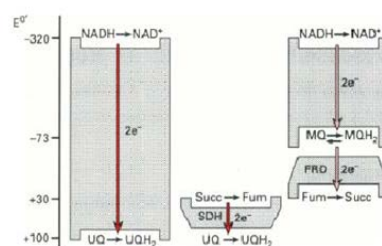


Fig. 3. Fumarate reductase catalyzes fumaric acid to succinic acid.

## II. EXPERIMENTAL MATERIALS AND METHODS

### A. Experimental Strains

*Brevibacterium ammoniagenes* MA-2, deposited in China Strain Collection Center.

### B. Medium

- Activation medium (g/L): peptone 10, beef extract 5, NaCl 5, agar 20, pH 7.0.
- Seed medium (g/L): glucose 20, corn steep liquor 15, urea 2,  $\text{KH}_2\text{PO}_4$  2,  $\text{MgSO}_4 \cdot 7\text{H}_2\text{O}$  0.5, pH 7.0.
- Fermentation medium (g/L): glucose 20, corn steep liquor 30, urea 2, fumaric acid 20,  $\text{KH}_2\text{PO}_4$  2,  $\text{MgSO}_4 \cdot 7\text{H}_2\text{O}$  0.5, pH 7.0.

### C. Species Culture Methods

- Activate strain: from the glycerol preservation tube in the refrigerator, Pick out a ring bacteria. Put 50mL activation medium in 250 mL flask. Under the conditions of 32 °C, 180 r / min, shake flask for 24 hours.
- Cultivate strain: Absorb 1mL of bacterial fluid from the activation medium, to 250mL Erlenmeyer flask with 50 mL seed medium. Under the conditions of 32 °C, 180 r/min, shake flask for 24 hours.
- Shake flask culture: Absorb 10% bulk of bacterial fluid from the seed medium, to 250 mL Erlenmeyer flask with 50 mL fermentation. Under the conditions of 32 °C, 180 r/min, shake flask for 48 hours.

### D. Optimization of Fermentation Medium for Fermentation

Determination of fumarate reductase activity: fumarate reductase catalyzes substrate fumaric acid to succinic acid. Succinic acid at 210 nm has a special absorption peak. According to the characteristics of the reaction to determine the concentration of succinic acid to measure fumarate reductase activity.

Specific methods: collect the *Brevibacterium ammoniagenes* MA-2 cells after the end of the fermentation, washed with stroke-physiological saline solution. Then use stroke-physiological saline solution to make bacteria suspension which per ml contain 0.1 g wet for the determination of fumarate reductase activity. 0.5 ml was added to 2.0 mL 1M fumarate (pH 7.0) solution containing 0.4% of cholic acid, reacting at 37 °C for 1 hour. The reaction mixture was boiled for 5 min and texted at 210 nm using an ultraviolet spectrophotometer. Enzyme activity units (U) are defined as:

in appropriate catalytic conditions, the amount of enzyme catalyzes fumaric acid to produce 1 $\mu$ mol succinic acid per hour.

We will study the effect of three medium components.

The effect of nitrogen source on the enzyme production: The contents of organic nitrogen (peptone, yeast extract, beef extract, corn steep liquor) and inorganic nitrogen (diammonium citrate, urea, (NH<sub>4</sub>)<sub>2</sub>SO<sub>4</sub>) were selected as the initial medium in the process of optimization of nitrogen source. The effect of each nitrogen source medium based on fumarate reductase activity was determined by shaking flask culture, and the appropriate nitrogen source was selected.

The effect of carbon source on the enzyme production: After select the optimal nitrogen source, the optimum carbon source fermentation conditions were as follows: glucose, sucrose, maltose, inositol, lactose and soluble starch. The effect of each carbon source medium based on fumarate reductase activity was determined after shaking flask culture. Thus, select the appropriate carbon source.

The effect of inorganic salt ions on enzyme production: Based on the optimal carbon source and nitrogen source, the fermentation medium was prepared by different inorganic salt ions MgSO<sub>4</sub>·7H<sub>2</sub>O, KH<sub>2</sub>PO<sub>4</sub>, NaCl, ZnSO<sub>4</sub>, CuSO<sub>4</sub> and CaCO<sub>3</sub>. After shaking flask culture, each inorganic salt medium was tested for fumarate reductase activity. Thus, select the appropriate concentration of inorganic salt ions.

Then, using the Plackett-Burman experiment, the factors influencing the activity of fumarate reductase were screened out from a number of independent single factors. Each variable had high (+) and low (-) 2 levels. The use the Design Expert software to analyze the experimental results, examine the significance of each factor, screening out the most important factors. Based on the initial shake flask fermentation test, 9 single factors related to fermentation were tested in the previous experiment, namely glucose, sucrose, soluble starch, corn steep liquor, ammonium sulfate, diammonium citrate, KH<sub>2</sub>PO<sub>4</sub>, MgSO<sub>4</sub>·7H<sub>2</sub>O, CaCO<sub>3</sub>, and the evaluation index was the activity of fumarate reductase in fermentation broth.

#### E. Acquisition of Fumarate Reductase

a) Obtaining strain: The fermentation broth containing the cells was filtered and washed with 0.05 mol/L K<sub>3</sub>PO<sub>4</sub> buffer for 3 times, and centrifuged at 2000 r/min for 20 minutes to collect precipitation.

b) Cell fragmentation: Add K<sub>3</sub>PO<sub>4</sub> buffer to wash the precipitation. Centrifugate to get precipitation. Repeat for two times. The lysate was added to the centrifuge tube at a rate of 50 mL fermentation liquid adding 2 mL lysate. Small magnetics were added under the conditions of 4°C, 1500 rpm for 3 hours. Then put into the -20°C refrigerator frozen. At last, in the ultrasonic cleaning machine, liquid was treated by ice bath and ultrasound for 30 minutes.

c) Ammonium sulfate precipitation [6], [7]: The solution obtained above was centrifuged to obtain a supernatant. Protamine sulfate solution, whose pH is 7.0, at a bulk of 20% of the supernatant, was added to the supernatant. The mixed solution was centrifuged after 1 hour. The supernatant was

graded by adding ammonium sulfate precipitation. A total of 7 ammonium sulfate gradients experiment is 0%, 15%, 25%, 35%, 45%, 55% and 65%. 50 mL of the 8 same volume of supernatant was added solid ammonium sulphate to the above different saturation, stirring for 40 minutes and then being stored for 24 hours. Through being centrifugated at 12000 r/min for 30 minutes, the supernatant was discarded and the fumarate reductase precipitate sediment was obtained.

d) Dialysis overnight. The precipitate obtained above was suspended with the phosphate buffer (pH=7.5). Using dialysis bag, dialysis the mixture for 48 h (molecular weight=30 kD). In this process, the dialysate was replaced every 6 hours. At last, the fumarate reductase was obtained and stored at 4°C for use.

#### F. Electrical Detection Of Fumaric Acid Reductase Method

##### 1) Preparation of polyethyleneimine reductive graphene composites (PEI-RGO) [8]-[10]

Firstly, 1.5 mL (concentration at 2 mg/mL) was diluted to 25.5 mL. Constantly stirring, reduced graphene was added to 4.5 mL (0.2 wt%) of polyethyleneimine solution. After 10 minutes, make a refluxed reaction at 135°C for 3.5 hours. Secondly, after the reaction, the product was naturally cooled and then centrifuged for 10 minutes at 13000 rpm/min. Thirdly, the product was washed by water for several times. Finally, the product was put in 2 mL water with ultrasonic shake and stored in a dry and cool place for use.

##### 2) Preparation of glassy carbon electrode (GCE)

The glassy carbon electrode (GCE) with a diameter of 3mm was polished successively on the suede with 1.0  $\mu$ m and 0.1  $\mu$ m Al<sub>2</sub>O<sub>3</sub> powder to make the surface of the GCE smooth as a mirror. The surface was washed with distilled water and then treated by ultrasonic at 50 times for 30 seconds. Finally the GCE was cleaned with distilled water and dried with nitrogen for use.

##### 3) Preparation of fumarate reductase/PEI-RGO/GCE

10  $\mu$ L PEI-RGO composite was added to the surface of the cleaned GCE. After drying at room temperature, 5  $\mu$ L fumarate reductase was added and stored at 4°C. Before the electrical test, 5  $\mu$ L 0.05% naphthol was added GCE to prevent the enzyme from leaking [11]-[15].

##### 4) Electronic test

In this work, electrical testing methods is mainly cyclic voltammetry (CV). The electrode working system is composed of a modified glassy carbon electrode (GCE), a platinum wire electrode (Pt) as a counter electrode, and a saturated calomel electrode (SCE) as a reference electrode. The range of potential scanning 1V - 1V and all electrical tests were carried out at room temperature. What's more, all electrical tests were performed in 10.0 mL 0.1 M pH 7.4 and anaerobic PBS buffer. Before these tests, high purity nitrogen was passed to the buffer for about 30 minutes to remove the dissolved oxygen [16].

The electrical-driven fumaric acid metabolism was performed 20  $\mu$ L 1 M umaric acid was injected into 10.0 mL

0.1 M pH 7.4 and anaerobic PBS buffer. The metabolic profile of fumarate and cyclic voltammetry curves were recorded.

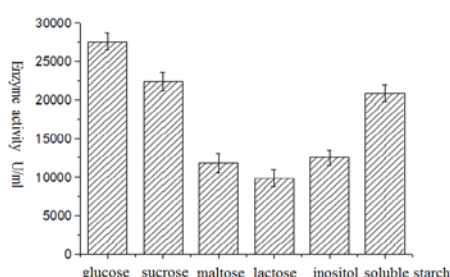


Fig. 4. The effect of carbon source on the enzyme production.

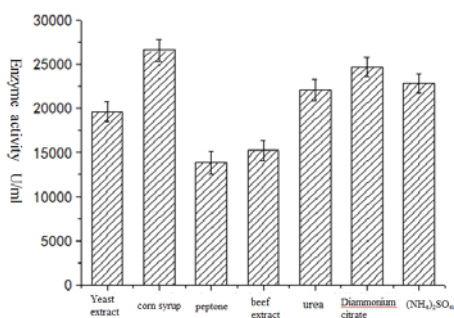


Fig. 5. The effect of nitrogen source on the enzyme production.

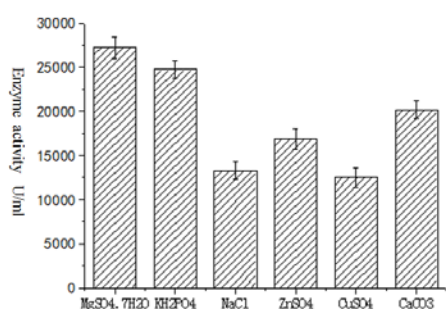


Fig. 6. The effect of inorganic salt ions on enzyme production.

### III. RESULTS AND DISCUSSION

#### A. Optimization of Fermentation Medium for Fermentation

The effect of carbon source on the enzyme production (Fig. 4): Select glucose, sucrose, soluble starch as a carbon source, the enzyme activity is higher.

The effect of nitrogen source on the enzyme production (Fig. 5): Select the organic nitrogen source of corn steep liquor and inorganic nitrogen source diammonium citrate, ammonium sulfate as the best compound nitrogen source for the production of *Brevibacterium ammoniagenes*.

The effect of inorganic salt ions on enzyme production (Fig. 6): Select MgSO<sub>4</sub>·7H<sub>2</sub>O, KH<sub>2</sub>PO<sub>4</sub>, CaCO<sub>3</sub> as inorganic salt ions source, the enzyme activity is higher.

The Plackett-Burman experiment design result in Table I. Table II is analyzed using Design-Expert software. The results are shown in Table II.

Thus, three factors (maize pulp, glucose, MgSO<sub>4</sub>·7H<sub>2</sub>O) has greatest impact on enzyme activity.

TABLE I: PLACKETT-BURMAN EXPERIMENT DESIGN

Std	Run	variable										Enzyme activity U/mL	
		A	B	C	D	E	F	G	H	I	J		K
1	6	1	1	-1	1	1	-1	-1	-1	-1	1	-1	23357
2	10	-1	1	1	-1	1	1	1	-1	-1	-1	1	19265
3	4	1	-1	1	1	-1	1	1	1	-1	-1	-1	26923
4	12	-1	1	-1	1	1	-1	1	1	1	-1	-1	23287
5	1	-1	-1	1	-1	1	1	-1	1	1	1	-1	21393
6	7	-1	-1	-1	1	-1	1	1	-1	1	1	1	23979
7	2	1	-1	-1	-1	1	-1	1	1	-1	1	1	23386
8	5	1	1	-1	-1	-1	1	-1	1	1	-1	1	23328
9	3	1	1	1	-1	-1	-1	1	-1	1	1	-1	20393
10	11	-1	1	1	1	-1	-1	-1	1	-1	1	1	24252
11	8	1	-1	1	1	1	-1	-1	-1	1	-1	1	21743
12	9	-1	-1	-1	-1	-1	-1	-1	-1	-1	-1	-1	17816

TABLE II: VARIANCE ANALYSIS OF PLACKETT-BURMAN

Source of variance	F Text	Prob>F	significance
glucose	758.93	0.0231	3
sucrose	9.93	0.1957	8
Soluble starch	14.39	0.1641	7
corn syrup	2875.49	0.0119	1
Ammonium sulfate	128.65	0.0560	6
Diammonium citrate	473.13	0.0292	4
KH <sub>2</sub> PO <sub>4</sub>	242.14	0.0409	5
MgSO <sub>4</sub> ·7H <sub>2</sub> O	2297.49	0.0133	2
CaCO <sub>3</sub>	1.410×10 <sup>-3</sup>	0.9708	9

#### B. Enzymatic Ammonium Sulfate Fractionation Salt Precipitation

The supernatant was ultrasonic treatment by ammonium sulphate with different saturation, and the supernatant enzyme activity was detected. The results are shown in Table III and Fig. 7.

Fig. 7 showed that fumarate reductase begins to when ammonium sulfate saturation level is greater than 15%. When ammonium sulfate saturation level was 65%, all fumarate reductase precipitated out. Therefore, the first step is to remove the contaminating protein with ammonium sulphate at a saturation of 0% to 15%. After centrifugation, ammonium sulfate was added to the supernatant to reach to a saturation of 65%, the fumarate reductase protein precipitate.

TABLE III: THE RESULT OF AMMONIUM SULFATE FRACTION PRECIPITATION

Different saturation of (NH <sub>4</sub> ) <sub>2</sub> SO <sub>4</sub> (%)	0	15	25	35	45	55	65
Enzyme activity(%)	100	94.6	86.8	52.7	36.7	12.9	0

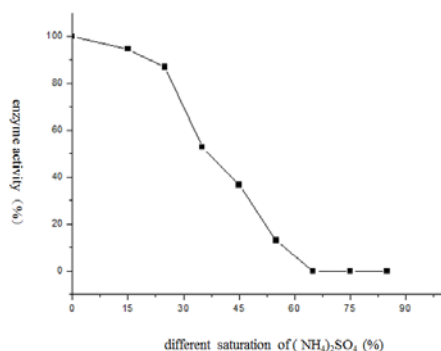


Fig. 7. The relationship between different saturation of  $(\text{NH}_4)_2\text{SO}_4$  and enzyme activity.

### C. Preliminary Results of Enzyme Purification

Through ultrasonic separation, gel chromatography and 65% ammonium sulfate fractionation, the fumarate reductase specific activity reached to 106 U / mg, the purification ratio was 12.8 times and the recovery was 24% in Table IV.

TABLE IV: THE PURIFICATION PROCURES OF THE FUMARASE REDUCTASE

project	all enemy activity (U)	all protein (mg)	specific activity (U/mg)	purificati on ratio	recover y ratio (%)
ultrasonic separation	27210	3309	8.24	1	100
65% ammonium sulfate fractionation	15640	213	73.22	8.8	57
gel chromatograp hy	6499	61	106	12.8	24

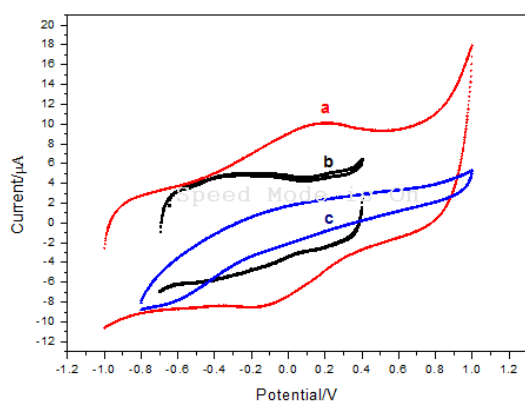


Fig. 8. (a) Fumarate reductase/PEI-RGO/GCE; (b) PEI-RGO/GCE; (c) GCE in 0.1M pH 7.4 and anaerobic PBS buffer at  $100 \text{ mV} \cdot \text{S}^{-1}$ .

### D. Direct Electrical Study of Fumarate Reductase/PEI-RGO/GCE

Fig. 8 and Fig. 9 show the cyclic voltammograms of GCE, PEI-RGO/GCE and fumarate reductase/PEI-RGO/GCE in 10.0 mL 0.1 M pH 7.4 and anaerobic PBS buffer (scan rate at 100 mv/s). The curve (a) of fumarate reductase/PEI-RGO/GCE had a pair of obvious redox peaks

with peak potentials of -0.166V and 0.179V, respectively. The corresponding peak currents were  $-8.582 \mu\text{A}$  and  $9.966 \mu\text{A}$ . While the curve (c) and curve (b) had no redox peaks. Thus, it is indicated that fumarate reductase was capable of directing electron transfer rapidly and stably on the PEI-RGO /GCE surface, which was caused by fumarase reductase immobilized on the GCE. On the other hand, it is proved that fumarase reductase was successfully fixed on the GCE.

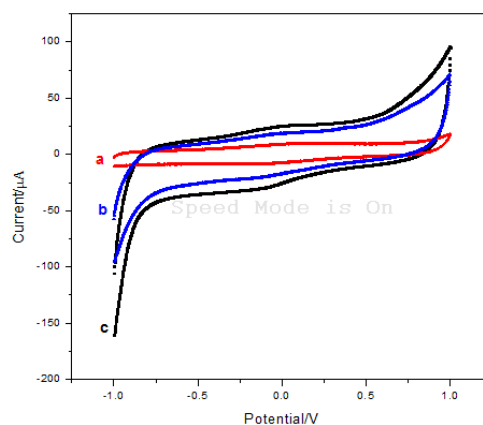


Fig. 9. Fumarate reductase/PEI-RGO/GCE in anaerobic (a); air saturation (b); air saturated with 0.1 M pH=7.4 PBS buffer (C).

### E. The Electrical Catalytic Behavior of Fumarate Reductase/PEI-RGO/GCE to Fumaric Acid

The electrical catalytic behavior of Fumarate reductase/PEI-RGO/GCE to fumaric acid is shown in Fig. 10. When dissolved oxygen is present, like curve (b), the cyclic voltammograms of direct electrical transfer of fumarate reductase/PEI-RGO/GCE changed and the reduction current significantly increased. By adding 100  $\mu\text{M}$  fumaric acid to the PBS buffer, the cyclic voltammograms of fumarate reductase/PEI-RGO/GCE also showed a significant change and the reduction peak current continued to increase. As there was only one pair of redox peak in the whole scanning range, and the peak potential coincided with the peak potential of the fumarate reductase/PEI-RGO/GCE under anaerobic conditions, indicated that the fumarate reductase immobilized on the electrode not only maintained a certain activity, but also can catalyze the metabolism of fumaric acid effectively.

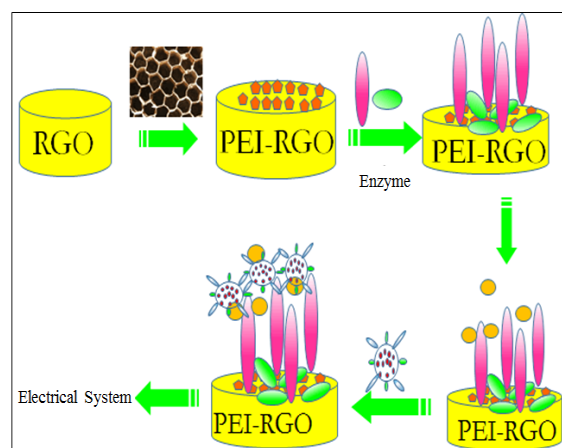


Fig. 10. System of fumarate reductase/PEI-RGO/GCE.

#### IV. CONCLUSION

Through ultrasonic separation, gel chromatography and 65% ammonium sulfate fractionation, the fumarate reductase specific activity reached to 106 U / mg, the purification ratio was 12.8 times and the recovery was 24%

Combined with good biocompatibility, excellent electrical conductivity and large surface area of graphene and the advantages of polyethyleneimine with excellent water solubility, excellent model ability, rich functional groups and other characteristics, the polyethyleneimine reductive graphene composites (PEI-RGO) showed good performance. Fumarate reductase was immobilized on the surface of PEI-RGO modified electrode by electrostatic adsorption. The GCE was used to replace the coenzyme NADH to provide electrons for the metabolism of fumarate reductase in vitro. At last, the curve of fumarate reductase/PEI-RGO/GCE had a pair of obvious redox peaks with peak potentials of -0.166V and 0.179V, respectively. The corresponding peak currents were -8.582 $\mu$ A and 9.966 $\mu$ A. The results show that through the electronic system, fumarate reductase can not only to achieve the electronic transmission between the electrodes, but also advance the accumulate metabolism of fumaric acid. This work provides a solid theoretical basis for fumarate reductase to product succinic acid in vitro.

#### ACKNOWLEDGMENT

This research work was financially supported by the state key development program of China (2016YED0201002). We thank the editor and the anonymous reviewers.

#### REFERENCE

- [1] J. G. Zeikus, M. K. Jain, and P. Elankovan, "Biotechnology of succinic acid production and markets for derived industrial products," *App Microbiol Biot*, vol. 51, no. 5, pp. 545-552, 1999.
- [2] G. Fuchs, E. Stupperich, and R. K. Thauer, "Function of fumarate reductase in methanogenic bacteria (Methanobacterium)," *Arch Microbiol*, vol. 119, no. 2, pp. 215-218, 1978.
- [3] J. B. Mckinlay, C. Vieille, and J. G. Zeikus, "Prospects for a bio-based succinate industry," *App Microbiol Biot*, vol. 76, no. 4, pp. 727-740, 2007.
- [4] C. Dongmei, L. Mi, X. Xu, L. Jusheng, Q. Jing, and L. Songqin, "Nanocomposites of graphene and cytochrome P450 2D6 isozyme for electrochemical-driven tramadol metabolism," *Langmuir*, vol. 30, no. 39, pp. 11833-11840, 2014.
- [5] B. Derkus, E. Emregul, C. Yucesan, and K. C. Emregul, "Myelin basic protein immunosensor for multiple sclerosis detection based upon label-free electrochemical impedance spectroscopy," *Biosens Bioelectron*, vol. 46, no.16, pp. 53-60, 2013.
- [6] R. R. Gokarn, M. A. Eiteman, and E. Altman, "Expression of pyruvate carboxylase enhances succinate production in *Escherichia coli* without

- affecting glucose uptake," *Biotechnol Lett*, vol. 20, no.8, pp. 795-798, 1998.
- [7] G. A. Hebert, P. L. Pelham, and B. Pittman, "Determination of the optimal ammonium sulfate concentration for the fractionation of rabbit, sheep, horse, and goat antisera," *J. Gen. Appl. Microbiol*, vol. 25, no. 1, pp. 26-36, 1973.
- [8] Y. Yuan, X. Gou, R. Yuan, Y. Chai, Y. Zhuo, X. Ye, and X. Gan, "Graphene-promoted 3, 4, 9, 10-perylenetetracarboxylic acid nanocomposite as redox probe in label-free electrochemical aptasensor," *Biosens Bioelectron*, vol. 30, no. 1, pp. 123-127, 2011.
- [9] M. J. Fernandez-Merino, L. Guardia, J. I. Paredes, S. Villar-Rodil, P. Solis-Fernandez, A. Martinez-Alonso, and J. M. D. Tascon, "Vitamin C is an ideal substitute for hydrazine in the reduction of graphene oxide suspensions," *J. Phys. Chem. C.*, vol. 114, no. 14, pp. 6426-6432, 2010.
- [10] M. Huang, X. Xu, H. Yang, and S. Liu, "Electrochemically-driven and dynamic enhancement of drug metabolism via cytochrome P450 microsomes on colloidal gold/graphene nanocomposites," *Rsc. Advances*, vol. 2, no. 33, pp. 12844-12850, 2012.
- [11] J. Lu, W. Wei, L. Yin, Y. Pu, and S. Liu, "Flow injection chemiluminescence immunoassay of microcystin-LR by using PEI-modified magnetic beads as capturer and HRP-functionalized silica nanoparticles as signal amplifier," *The Analyst*, vol. 138, no. 5, pp. 1483-1489, 2013.
- [12] T. G. Park, J. H. Jeong, and S. W. Kim, "Current status of polymeric gene delivery systems," *Adv. Drug Deliver Rev.*, vol. 58, no. 4, pp. 467-86, 2006.
- [13] B. Willner, E. Katz, and I. Willner, "Electrical contacting of redox proteins by nanotechnological means," *Curr. Opin. Biotechnol*, vol. 17, no. 6, pp. 589-596, 2006.
- [14] Q. Xue, D. Kato, T. Kamata, Q. Guo, T. You, and O. Niwa, "Human cytochrome P450 3A4 and a carbon nanofiber modified film electrode as a platform for the simple evaluation of drug metabolism and inhibition reactions," *Analyst*, vol. 138, no. 21, pp. 6463-6468, 2013.
- [15] S. Wen, F. Zheng, M. Shen, and X. Shi, "Surface modification and PEGylation of branched polyethyleneimine for improved biocompatibility," *J. Appl. Polym. Sci.*, vol. 128, no. 6, pp. 3807-3813, 2013.
- [16] M. Sheng, Y. Gao, J. Sun, and F. Gao, "Carbon nanodots-chitosan composite film: a platform for protein immobilization, direct electrochemistry and bioelectrocatalysis," *Biosens Bioelectron*, vol. 58, no. 8, pp. 351-358, 2014.



**Yemin Yu** comes from Nanjing, Jiangsu Province, China. Now study in Nanjing Tech University, master's degree in second grade.

She does research as a postgraduate student in Huyonghong laboratory and has published two papers in important journal.



**Yonghong Hu** is with College of Biotechnology and Pharmaceutical Engineering, State Key Laboratory of Materials-Oriented Chemical Engineering, Nanjing Tech University, Nanjing 211816, China.

In the last five years, she has taken in hand more than 30 Provincial and ministerial level projects included 867, 973, National Natural Science Foundation of China, transformation of achievements. She won the prize of national and provincial science and technology about 11 and the prize of the provincial teaching 12. In the past three years, more than 70 papers were published in important journals at home and abroad, and 59 articles were included in SCI. She applied for 36 national invention patents, and 17 patents were authorized. She has published 10 books.

# Depilling of Spun Polyester Fabric through Laundering with Detergent Containing Alkaline Cutinolytic Esterase

Taweeporn Sooksai, Hunsu Punnapayak, Sehanat Prasongsuk, and Usa Sangwatanaroj

**Abstract**—This research targets to remove fabric pill from spun polyester knitted fabric (pilling rate 1 out of 5) through laundering with a detergent containing alkaline cutinolytic esterase. After washing, fabric was graded for pilling rate, measured for color difference, and tested for weight loss and strength loss. Results indicated that fabric washed with detergent containing esterase had lower amount of pills (pilling rate 3-4) than that washed only with detergent (pilling rate 2-3). In addition, the former also showed better color appearance than the latter. However, the fabric weight loss and strength loss after washing with detergent containing esterase were slightly higher than that washing with only detergent.

**Index Terms**—*Fusarium* sp., cutinolytic esterase, laundry detergent, spun polyester, fabric pill.

## I. INTRODUCTION

Polyethylene terephthalate (PET) is a synthetic polyester fiber often used in textile industry (approximately 70%) because of its outstanding properties including high strength and durability, light weight, resistance to wrinkle, high abrasion resistance, and easy to care for. However, frequent wearing and washing spun polyester fabric (made from staple or short fibers) can lead to pilling (small ball of loose fibers) or fuzzing (loose fibers) on fabric surface that causes unpleasant look.

This is because during wearing and washing, loose fibers start to push out from the fabric surface, and over time, abrasion causes entanglements of loose fibers and finally develops them into spherical bundles anchoring on the fabric surface, known as fabric pill. Due to fiber high strength, it is not easy to remove fabric pill from surface of polyester fabric via regular washing.

Three methods are suggested for pill removal or depilling, consisting of physical (shear/shave), chemical (alkaline treatment), and biological (enzymatic treatment) methods. Enzymes have been used effectively in textile industries as well as to assist the development and improvement of modern household and industrial detergents. Surface treatment with enzymes are related to the field of enzyme technology and the

benefit of using enzyme is fast in reaction rate with highly specific reaction at mild condition.

Cellulase, lipase and protease enzymes have been widely used in various laundry detergent. Some research works have confirmed that cutinase, a lipolytic enzyme, can also be another choice for detergent [1]-[4] as well as for textile industries. Cutinase is known to catalyze the hydrolysis of polyester molecules at their ester bonds into carboxyl and hydroxyl groups. This reaction causes the decrease of the degree of polymerization of polyester chains, the weakness of fibers, and finally the removal of these fibers from polyester surface when additional mechanical action is applied.

*Andersen et al.* patented a method to treat polyester fabric with a polyester hydrolytic enzyme, a terephthalic acid diethyl ester hydrolytic enzyme (ETE hydrolytic enzyme) and/or an ethyleneglycol dibenzyl ester hydrolytic enzyme (BEB hydrolytic enzyme) in the presence of detergents, in order to reduce pilling propensity and to improve color clarification [5]. *Yoon et al.* treated polyester fabric with polyesterase-a serine esterase and found improvements of fabric's hydrophilicity, oily stain release, pill and polyester size removal, and cationic dye binding. However, treated fabric showed a decrease of fabric luster [6]. In 2005, *Mccloskey and Jump* [7] attempted to remove pills from polyester fabric surface through bio-polishing process using cutinase as well as to treat 50/50 polyester/cotton fabric with cutinase and a compatible cellulase, and found successful pill removal results. *Donelli et al.* treated polyester surface with a lipolytic enzyme (commercial cutinase) in order to improve its surface hydrophilicity and found increases of wettability and dyeability of treated polyester materials [8]. In addition, *Nimchua et al.* found a high cutinolytic esterase produced from *Fusarium solani* after cultivation in a medium with initial pH of 11.0 at 25°C for 4 days and used it for surface treatment of polyester fiber [9]. Cutinases had also been used in laundry detergents for depilling of polyester fabric [10]. Nowadays, designs of novel enzymes with enhanced activity on synthetic polymer substrates are still being screened and selected for industrial applications, especially in detergent industry.

In this study, a local produced cutinolytic esterase powder was added into a commercial powder detergent and the detergent was used for laundering spun polyester knitted fabric that has a pilling rate of 1 (highest amount of pills) in order to study the effect of esterase in detergent on pill removal efficiency.

## II. MATERIALS

Fabric for this study was a local produced red spun

Manuscript received August 8, 2017; revised November 5, 2017. This work was financial supported by Chulalongkorn University and the Department of Agriculture, Ministry of Agriculture and Cooperatives, Thailand.

T. Sooksai, H. Punnapayak, and S. Prasongsuk are with the Plant Biomass Utilization Research Unit, the Department of Botany, Faculty of Science, Chulalongkorn University, Bangkok, Thailand (e-mail: moferdream@gmail.com, phunsa@chula.ac.th, sehanat.p@chula.ac.th).

U. Sangwatanaroj is with the Department of Materials Science, Faculty of Science, Chulalongkorn University, Bangkok, Thailand (e-mail: usa.s@chula.ac.th).

polyester knitted fabric with single jersey construction. The commercial detergent used in this work was an alkaline powder detergent (sodium lauryl ether sulfate and alcohol ethoxylated), supplied by Unilever (Thailand) Co., Ltd. Cutinolytic esterase enzyme showed optimum activity at pH 9.0 and temperature 35°C was produced from *Fusarium falciforme* PBURU-T5 at the Plant Biomass Utilization Research Unit, Department of Botany, Chulalongkorn University, and was used in this research.

### III. EXPERIMENTAL

#### A. Preparation for Pilling Sample

Approximately 10 cm x10 cm or 1.3 g of fabric was mounted on polyurethane tube and placed in pilling box. Sample was spun in pilling tester for 4,500 revolutions at a constant speed of 30 rpm to obtain fabric with pilling rate 1 (rate 1 = maximum pill, rate 5 = minimum pill), according to the standard test method ISO 12945.

#### B. Ratio of Detergent to Fabric

The amount of detergent used in this work was at the lowest amount that could completely remove oily stain (staining procedure was based on the standard test method AATCC 130) from polyester fabric through one washing cycle. It was found that the required ratio of detergent to fabric to water was 1 g: 6.5 g: 50 ml, respectively

#### C. Ratio of Detergent to Enzyme

Detergent and enzyme were mixed well at various weight ratios of 1:0.05, 1:0.10, 1:0.15, and 1:0.20, respectively, and they were used for washing test.

#### D. Washing Procedure

Solutions of detergent and detergent containing enzyme were prepared according to the ratios previously mentioned. Fabric was washed in the prepared solution at 35°C for 1 hour per cycle using a launder-o-meter "Gyrowash" as a washing tester. After each washing cycle, fabric was water rinsed for 30 minutes and then air dried. Both normal washing test (without stainless steel ball) and accelerated washing test (with stainless steel balls) were conducted. The accelerated washing was performed by adding 10, 20, 30 and 40 stainless steel balls to the test. It was found that the washing condition using 20 stainless steel balls showed the best pill removal efficiency (pilling rate of after washed fabric was rated 3-4, before washing was rated 1). Additional experiment was also done to determine the relationship between numbers of washing cycle when washing with and without stainless steel ball, by washing fabric (pilling rate 1) without stainless steel ball at 35°C for several cycles (1 hour per cycle) until the fabric pilling rate improved to 3-4. It was found that 8 washing cycles at 35°C (1 hour per cycle) without stainless steel ball was comparable to 1 washing cycle using 20 stainless steel balls at same temperature and time per cycle.

#### E. Fabric Testing

##### 1) Pilling rate

Fabric was evaluated for pilling rate by eye-comparing its

surface appearance with 5 standard photographs of fabric (pilling rates 1 to 5) and grading to the nearest rate (i.e. 1,2,3,4,5) or between two rates (i.e. 1-2, 3-4), according to the standard test method ISO 12945-1. Fabric with pilling rate 1 is determined to have the highest amount of pills and fussy hairs while fabric with rate 5 has a smooth surface with the lowest amount of pills and hairs. Based on the requirement for exporting apparel to major markets, the pilling rate should be at least 3-4 [11].

##### 2) Surface appearance

Fabric surface was observed under an optical microscope to determine for the amount of pill and hair contents.

##### 3) Color measurement

Fabric before and after pilling as well as washing was measured for color values using a colorimeter Macbeth Color-Eye 7000 according to the AATCC Evaluation Procedure 6. Fabric color strength (K/S) or color depth was measured at fabric surface at wavelength 510 nm (red color) in which fabric with higher K/S showed darker color than that with lower K/S. In addition, fabric color difference ( $\Delta E^*$ ), lightness ( $L^*$ ) and color shade ( $a^*$ ,  $b^*$ ) were also measured. Fabric after pilling generally shows some color different from fabric before pilling because pills and fussy hairs on fabric surface are capable of changing the color appearance of fabric. On the contrary, when pills and hairs are removed, the color difference between fabrics should be minimized. In his work, fabric after pilling (both before and after washing) was color evaluated to see how much its color was different from that of fabric before pilling (pilling rate 5,  $\Delta E^* = 0$ ). The washing process that could produce fabric with  $\Delta E^*$  closed to 0 would be the optimal washing process for pill removal in this work. Measurement of fabric lightness and color shade was also done in order to respectively evaluate the brightest white ( $L^* = 100$ ) or darkest black ( $L^* = 0$ ) of fabric color as well as to see the color shade of fabric ( $a^* > 0$  is red,  $a^* < 0$  is green,  $b^* > 0$  is yellow,  $b^* < 0$  is blue,  $a^* = 0$  and  $b^* = 0$  is true neutral gray).

##### 4) Weight loss

Fabric dry weight before and after washing was determined using an infrared balance in order to analyze for % fabric weight loss after pill removal through washing.

##### 5) Strength loss

Fabric was tested for bursting strength (kPa) using a hydraulic-type bursting strength tester, according to the standard test method ASTM D 3786. Its strength before and after washing was measured and results were used for calculation of % fabric strength loss after pill removal through washing.

### IV. RESULTS AND DISCUSSION

Originally spun polyester fabric had a pilling rate of 5 (lowest pill content) but after pilling, its pilling rate was down to 1 (highest pill content) shown as fabric (a) in Table I and in Fig. 1(a). When fabric with pilling rate 1 "fabric (a)" was washed with detergent at 35°C for 1 cycle (1 hour), the pilling rate of fabric still remained at 1 (see Table I and also Fig. 1 (b)) and this indicated that washing fabric (a) with detergent did

not promote the pill removal at all.

Once fabric (a) was washed for 1 cycle with detergent containing various amounts of esterase enzyme, the fabric pilling rate or pilling resistance was improved and maximized to 2-3 when the ratio of detergent to enzyme of 1:0.10 was used for the washing process. This result confirmed that an addition of local produced esterase into the detergent could support the depilling efficiency of the detergent itself through enzyme catalyzing the hydrolysis of the polyester chains as already mentioned in the introduction. However, the required pilling rate for exported apparel was set at 3-4 [11] and this was also the target pilling rate of the fabric after washing in this work. Therefore, it could be concluded that the normal washing process (washing without stainless steel ball) using detergent: enzyme 1:0.10 at 35°C for more than 1 cycle was needed for increasing the fabric pilling rate to 3-4. It was found that 8 normal washing cycles using detergent: enzyme 1:0.10 could increase the fabric pilling rate to 3-4 and this result was comparable to one accelerated washing cycle using detergent: enzyme 1:0.10 and 20 stainless steel balls that could produce fabric with pilling rate 3-4 as shown in Table I and Fig. 1(d).

TABLE I: FABRIC PILLING RATE AND % WEIGHT LOSS AFTER WASHING

Fabric washing condition	Pilling rate	% Weight loss
Before pilling, no wash	5	-
After pilling, no wash: fabric (a)	1	0
Washing (a) with detergent	1	0.73
Washing (a) with detergent: enzyme 1:0.05	1-2	2.09
Washing (a) with detergent: enzyme 1:0.10	2-3	2.60
Washing (a) with detergent: enzyme 1:0.15	2	2.52
Washing (a) with detergent: enzyme 1:0.20	2	2.42
Washing (a) with detergent: enzyme 1:0.10 and 10 stainless steel balls	2	2.44
Washing (a) with detergent: enzyme 1:0.10 and 20 stainless steel balls	3-4	2.78
Washing (a) with detergent: enzyme 1:0.10 and 30 stainless steel balls	2-3	2.16
Washing (a) with detergent: enzyme 1:0.10 and 40 stainless steel balls	2-3	2.59
Washing (a) with detergent and 10 stainless steel balls	2	1.89
Washing (a) with detergent and 20 stainless steel balls	2-3	1.36
Washing (a) with detergent and 30 stainless steel balls	2-3	2.37
Washing (a) with detergent and 40 stainless steel balls	2-3	2.60
Washing (a) with detergent: enzyme 1:0.10 for 8 cycles	3-4	2.68

Table I also showed slight fabric weight loss of 0.73-2.78% after washing spun polyester fabric with detergent as well as with detergent containing enzyme. It was found that fabric washing with detergent containing enzyme lost more weight than fabric washing with only detergent. This weight loss could have come from losing of fibers or from pill/hair removal during washing with detergent and esterase enzyme.

Results from Table I indicated that the optimal ratio between this alkaline powder detergent and the local produced alkaline cutinolytic esterase (PBURU-T5) should be at 1:0.10

and it's required for 8 normal washing cycles (1 hour/cycle) at 35°C for efficiently remove pills from spun polyester fabric (improve fabric pill resistance from pilling rate 1 to the required pilling rate 3-4) through washing with this optimal composition of detergent: enzyme mixture.

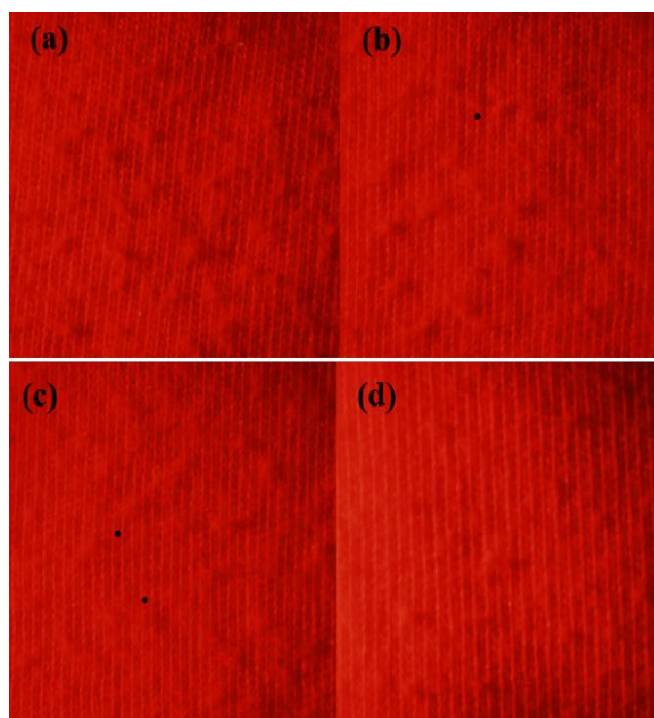


Fig. 1. Optical microscope images of fabric pills (a) after pilling/no wash, pilling rate 1, (b) washing fabric (a) with detergent, pilling rate 1, (c) washing fabric (a) with detergent and 20 stainless steel balls, pilling rate 2-3, (d) washing fabric (a) with detergent: enzyme 1:0.10 and 20 stainless steel balls, pilling rate 3-4.

Table II Showed color values of fabric after pilling and after some washing conditions using detergent and detergent containing enzyme, comparison to color values of fabric before pilling. All fabrics in this Table showed similar yellowish red color ( $L^*$ ,  $a^*$  and  $b^* > 0$ ). Pilling and washing reactions did not change much of the lightness ( $L^*$ ) and color shade ( $a^*$  and  $b^*$ ) of fabrics. It was found that fabric before pilling had the lowest color strength ( $K/S = 24.4$ ) or the lightest color. Once the fabric was pilled to rating 1 (fabric (a)), its color strength significantly increased 3 units ( $K/S = 27.4$ ) to a darker shade and showed a noticeable color difference of 1.82 ( $\Delta E^* \geq 1$ , eyes detectable) when compared with the color of fabric before pilling ( $\Delta E^* = 0$ ). As fabric (a) with pilling rate 1 was washed with detergent as well as with detergent containing enzyme, the color strength ( $K/S$ ) and color difference ( $\Delta E^*$ ) decreased from those of fabric (a) and the values were more closed to those of fabric before pilling (pilling rate 5,  $K/S = 24.4$ ,  $\Delta E^* = 0$ ) than to those of fabric after pilling (no washing). This could be explained that washing fabric with detergent in the presence or absence of enzyme could promote the fabric pill removal and decrease the change of color appearance, with a higher efficiency of pill removal when detergent containing enzyme was used. It was clear to say that fabric washed with detergent: enzyme 1:0.10 (with and without 20 stainless steel balls) showed the lowest color strength and unnoticeable color difference ( $\Delta E^* < 1$ ) and

the values were the closest to those of fabric before pilling, especially when washing fabric with detergent: enzyme 1:0.10 and 20 stainless steel balls. This could mean that an addition of esterase enzyme into the commercial detergent could assist the pill removal efficiency of the detergent itself.

TABLE II: FABRIC COLOR VALUES: LIGHTNESS (L\*), RED+/GREEN- (A\*), YELLOW+/BLUE- (B\*), COLOR DIFFERENCE ( $\Delta E^*$ ) AND COLOR STRENGTH (K/S)

Fabric washing condition	L*	a*	b*	$\Delta E^*$	K/S
Before pilling, no wash	36.6	55.5	29.4	0	24.4
After pilling, no wash: fabric (a)	36.8	55.8	30.3	1.82	27.4
Washing (a) with detergent	37.1	56.4	30.5	1.51	26.8
Washing (a) with detergent:enzyme 1:0.10	37.1	56.1	30.0	0.96	25.6
Washing (a) with detergent:enzyme 1:0.10 and 20 stainless steel balls	37.0	55.6	29.8	0.59	25.2
Washing (a) with detergent and 20 stainless steel balls	37.2	55.7	29.7	1.10	25.9

TABLE III: FABRIC BURSTING STRENGTH AND % STRENGTH LOSS AFTER WASHING.

Fabric washing condition	Bursting strength (kPa)	% Strength loss
After pilling, no wash (pilling rate 1)	1010	0
After pilling (pilling rate 1) and washing with detergent:enzyme 1:0.10 and 20 stainless steel balls (pilling rate 3-4)	926	8.3

Finally, the after washed fabrics were tested for their bursting strength shown in Table III and found that strength loss of 8 % was observed when detergent: enzyme was used. However, polyester knitted fabric was considered to be one of the strongest fabrics in the world textile market. Its bursting strength was reported to be several times higher than fabrics made of viscose, acrylic, as well as cotton fibers [12]. Therefore, in this work the 8% bursting strength loss of polyester fabric after 8 normal washing cycles using detergent:enzyme 1:0.10 (one accelerated washing cycle using detergent:enzyme 1:0.10 and 20 stainless steel balls) was not a big concern for textile users.

## V. CONCLUSION

This research discovered that a commercial detergent containing esterase could be used successfully for depilling of spun polyester knitted fabric (pilling rate 1) through 8 normal laundering cycles. The after washed fabric showed pilling rate of 3-4 with slight weight loss and strength loss.

## ACKNOWLEDGMENT

Authors thank a research grant of Chulalongkorn University and the Department of Agriculture, Ministry of Agriculture and Cooperatives, Thailand for research supports.

## REFERENCES

- [1] Unilever, "Enzyme-containing surfactant compositions," U.S. Patent 94 04771, 1994a.
- [2] Unilever, "Eukaryotic cutinase variant with increased lipolytic activity," U.S. Patent 94 11303, 1994b.

- [3] M. R. Egmond and C. J. van Bommel, "Impact of structural information on understanding lipolytic function," *IEEE Trans. Methods in Enzymology*, vol. 284, pp. 119-129, 1997.
- [4] J. S. Okkels, "Preparing polypeptide variants with improved functional properties," U.S. patent 97 09664, 1997.
- [5] B. K. Anderson, K. Borch, M. Abo, and B. Damgaard, "A method of treating polyester fabrics," U.S. Patent 59 97584, 1999.
- [6] M. Y. Yoon, J. Kellis, and A. J. Poulou, "Enzymatic modification of polyester," *IEEE Trans. AATCC Rev.*, vol. 2, pp. 33-36, 2002.
- [7] S. G. McCloskey and J. M. Jump, "Bio-polishing of polyester and polyester/cotton fabric," *IEEE Trans. Textile Research Journal*, vol. 75, pp. 480-484, 2005.
- [8] I. Donelli, P. Taddei, P. F. Smet, D. Poelman, V. A. Nierstrasz, and G. Freddi, "Enzymatic surface modification and functionalization of PET: A water contact angle, FTIR, and fluorescence spectroscopy study," *IEEE Trans. Biotechnology and Bioengineering*, vol. 103, pp. 845-856, 2009.
- [9] T. Nimchua, D. E. Eveleigh, U. Sangwatanaroj, and H. Punnapayak, "Screening of tropical fungi producing polyethylene terephthalate-hydrolyzing enzyme for fabric modification," *IEEE Trans. Journal of Industrial Microbiology and Biotechnology*, vol. 35, pp. 843-850, 2008.
- [10] G. M. Guebitz and A. Cavaco-Paulo, "Enzymes go big: Surface hydrolysis and functionalisation of synthetic polymers," *IEEE Trans. Trends in Biotechnology*, vol. 26, pp. 32-38, 2008.
- [11] *Textiles, Carpet, Feather and Down Testing Price List*, Intertek Testing Services Ltd., Shanghai, China, 2008, pp. 1-31.
- [12] Z. Degirmenci and E. Coruh, "The influences of loop length and raw material on bursting strength air permeability and physical characteristics of single jersey knitted fabrics," *IEEE Trans. Journal of Engineered Fibers and Fabrics*, vol. 12, pp. 43-49, 2017.



**Taweeporn Sooksai** is currently a full time PhD candidate in Biotechnology, Faculty of Science, Chulalongkorn University. She has been working as a scientist at the Department of Agriculture, Ministry of Agriculture and Cooperative, Thailand for almost 5 years. Her research interests are in the areas of biotechnology and postharvest technology.



**Hunsa Punnapayak** is a professor of the Department of Botany, Faculty of Science, Chulalongkorn University. His research interests include biomass and crop residue utilization, biotransformation, fungal enzymes and fermentation. He has published more than 34 academic papers with 289 citations.



**Sehanat Prasongsuk** is an associate professor of the Department of Botany, Faculty of Science, Chulalongkorn University. His research interests include Plant and Fungal Biotechnology, Plant and Crop Residues utilization, Fungal enzymes and metabolites, Mushroom and its Applications and Biopulping and Biobleaching. He has published more than 26 academic papers with 172 citations.



**Usa Sangwatanaroj** is an assistant professor of the Department of Materials Science, Faculty of Science, Chulalongkorn University. Her research interests include productions and applications of enzymes for textile applications (retting, desizing, scouring, bio-stoning, and depilling), bacterial decolorization of dye effluent, as well as natural dyeing of cotton and silk.

# **Applied Chemistry and Microcapsule Technology**



# Encapsulation, Properties, and Thermal Study of Red Biocolorant from Selected Plants Obtained Through Physical Extraction

Renny Indrawati, Diah Mustika Lukitasari, Yuyun Yuniati, Heriyanto, and Leenawaty Limantara

**Abstract**—The human perception on food is closely associated with its color. Since the standard manufacturing procedure often causes partial even total degradation of natural pigments, resulting in color fading, the addition of colorants becomes necessary. Natural colorant, produced from plants or animals, has health promoting effects, better safety, and need not any specific toxicity evaluation. However, the extraction method will be crucial in determining the properties of this biocolorant. In the present study, red biocolorant was prepared from selected local plants i.e., red spinach, red cabbage, beetroot, and dragon fruit, through physical extraction in order to avoid the using of organic solvents. Then, we applied the encapsulation technique and evaluated its coloring and antioxidant properties, as well as its stability against thermal treatment. The results showed that the encapsulated biocolorant of red spinach and beetroot exhibited red hue at pH range 2-11, whereas those of red cabbage and dragon fruit indicated color alteration at different pH. The prominent red hue intensity was found at pH 4 for encapsulated beetroot extract, which endured up to 10 days at aqueous buffered solution when stored in the dark at 20°C. In addition, it underwent merely low degradation (~30%) during incubation at 60°C for 30 minutes. The antioxidant activity of encapsulated biocolorant of beetroot was comparable to that of red cabbage, being higher than the others.

**Index Terms**—Biocolorant, coloring properties, encapsulation, red, thermal stability.

## I. INTRODUCTION

It is widely known that color is one of the prime factors in food choice, besides its physical appearance and odor. The appetite stimulators are red and yellow, while the most potential suppressor is blue [1]. Food industries have extensively used both synthetic and natural colorants in order to embellish their products, either giving new color or just improving the color after processing treatment that might cause fading. Although the properties of synthetic colorants are unrivaled, the health-aware consumers and regulatory

Manuscript received August 30, 2017; revised November 8, 2017. This work was supported by National Innovation System Research Grant, provided by Ministry of Research, Technology, and Higher Education of the Republic of Indonesia.

Renny Indrawati, Yuyun Yuniati, and Heriyanto are with Ma Chung Research Center for Photosynthetic Pigments and Chemistry Study Program, Universitas Ma Chung, Malang, Indonesia (e-mail: renny.indrawati@machung.ac.id).

Diah Mustika Lukitasari is with Ma Chung Research Center for Photosynthetic Pigments, Universitas Ma Chung, Malang, Indonesia.

Leenawaty Limantara is with Ma Chung Research Center for Photosynthetic Pigments, Universitas Ma Chung, and Universitas Pembangunan Jaya, Jakarta, Indonesia.

authorities have unavoidably led the worldwide movement towards more natural colors in food [2]. The Royal Society of Chemistry recently published that over than ninety percent of European new products released during 2011 – 2016 have applied natural colors [3].

According to our latest market survey at several supermarkets in East Java, Indonesia, the use of non-synthetic colorant was dominant in baby food and (100%) and dairy products (60%), while its utilization on other categories was less than 20%, even none for instant meals. Our finding was in line with the common concept of human perception. The yellow beta-carotene (23%) and red carmine (21%) were predominantly employed beside the other natural sources such as annatto, curcumin, caramels, chlorophylls, and anthocyanins [4]. In fact, there is the ‘carmine problem’ which is related to its nauseating animal origin, aluminium content, microbiological issues, as well as its ability for inducing severe allergic reactions led to several public scandals [5]. Consequently, there is an urgent need for potential substitutes, coming from pigments or plant origin.

Some plants have been mentioned as the possible alternative for production of red biocolorant, i.e. dye sorghum (*Sorghum bicolor*), fruit of *Optunia stricta*, beetroot (*Beta vulgaris* L.), dragon fruit (*Hylocereus polyrhizus*), roselle (*Hibiscus sabdariffa*), and other plants of the Amaranthaceae [6]–[11]. Moreover, the subsequent concern is addressed to the preference of extraction and concentration method that should be able to compromise the instability of natural pigments, inexpensive, food-grade process, and environmental friendly. To the best of our knowledge, there is only a limited number of study in the production of red biocolorant which relied on solvent-free extraction and nonthermal processing.

In the present work, we encapsulated the red biocolorant, physically extracted from red spinach, red cabbage, beetroot, and dragon fruit, and then evaluate its properties and thermal stability. The encapsulation procedure is followed by lyophilization to give concentrated red biocolorant in powder form. Reconstitution of red biocolorant in buffered solution was intended to verify the influence of pH on its coloring properties and thermal stability. The antioxidant assay was carried out to examine the potency of these red biocolorants as functional food ingredients.

## II. MATERIALS AND METHODS

### A. Materials

The red spinach (RS), red cabbage (RC), beetroot (BR), and

dragon fruit (DF) were originated from locally grown plants sold at local grocery in Malang, East Java, Indonesia. Maltodextrin DE 10-12% (Yishui Dadi Corn Developing Co. Ltd., China) was used for encapsulating material. Solvents and reagents were commercially available from Merck Co. & Inc., USA and Sigma Aldrich Co., Germany. Chemicals for buffered solution were obtained from Lianyungang Chameleon Technology Co. Ltd., China (citric acid and sodium hydrogen phosphate) and Amresco Inc., USA (sodium azide).

#### B. Extraction and Encapsulation Procedure

All plants samples were rinsed with tap water, blotted dry, peeled (beetroot and dragon fruit), and cut. Then, physical extraction was performed by means of slow juicer HH-SBF11 (Hurom, USA) without any water addition. The collected extract was homogenized with Maltodextrin (5 % w/v), and kept frozen overnight prior to lyophilization for 48 hours at  $-49^{\circ}\text{C}$  under low pressure 0.04 MPa (Labconco-Freezone 2.5 L Benchtop, USA). The dried encapsulated extract (moisture content below 10 %) was ground to give red biocolorant in powder form, stored at freezer ( $-18^{\circ}\text{C}$ ) until it was used for further analysis.

#### C. Preparation of McIlvaine Buffer

The McIlvaine buffer was prepared according to [12] with slight modification. Citric acid (less than 2 % w/v), sodium hydrogen phosphate (less than 2 % w/v), and sodium azide (0.02% w/v) were dissolved in distilled water to create a series of buffered solutions at pH 2 – 11.

#### D. Tinctorial Strength and Stability Evaluation

The encapsulated red biocolorant (0.1 % w/v) was redissolved in McIlvaine buffer in order to evaluate the coloring capacity, measured as tinctorial strength = [maximum absorbance  $\times$  100]/sample weight. The biocolorant in buffered solutions were stored in Climate Chamber ICH110 (Mettler, Germany) at  $20^{\circ}\text{C}$  with 15 % relative humidity for certain period of time under darkness. Thermal study was carried out at  $60^{\circ}\text{C}$  for 30 minutes using waterbath in duplicate samples.

Spectroscopy measurement was accomplished by means of Spectrophotometer UV-1800 (Shimadzu, Japan), while the color measurement was performed using Colorflex EZ No.45/0 (HunterLab, USA). Hue was calculated as the angle having tangent  $b^*/a^*$ . Change of colors was calculated as  $\Delta E$  from the Hunter  $L^*$ ,  $a^*$ , and  $b^*$  values using determined equation [13].

#### E. Antioxidant Assays

Antioxidant activity and  $\text{IC}_{50}$  value of encapsulated extract was determined against DPPH (2,2-diphenyl-1-picrylhydrazyl-hydrate) free-radical [14]. The encapsulated biocolorant was first dissolved in water at 1000 ppm, then a series of dilution was prepared using methanol, followed with addition of  $0.2 \mu\text{M}$  DPPH solution. Samples were incubated for 30 minutes in the dark at room temperature, and the remaining DPPH radicals was quantified using absorption set at 517 nm. The  $\text{IC}_{50}$  value represents the weight of sample

required to scavenge 50 % of the available DPPH radicals.

### III. RESULTS AND DISCUSSION

#### A. Encapsulated Red Biocolorant

Red biocolorant from plant origin could be empowered due to the presence of some natural red pigments, i.e. lycopene, anthocyanins, betalains, and betacyanins. Compared to other pigment groups with different color appearance, most of red pigments have high polarity and exhibit favorable solubility in water. Since the main constituent of some parts of the plants is water, those pigments may be concurrently squeezed out from the intact structure via free and bound water. The red spinach, red cabbage, beetroot, and dragon fruit were chosen and subjected to physical extraction by means of slow juicing instrument, which is applicable to parts of plants that do not have rigid structure and contain enough water. Furthermore, the extract was encapsulated and lyophilized in order to reduce the water content and hence increase its shelf life.

In the present work, four types of powdered biocolorant were generated from the selected raw materials. The red spinach and beetroot gave vivid red powder, while red cabbage and dragon fruit provided purplish red powder. The particle attribute was investigated by using Scanning Electron Microscopy (SEM), revealing the typical irregular shape of freeze dried material with average particle dimensions ranging from  $54.61 \pm 9.50 \mu\text{m} \times 85.80 \pm 10.92 \mu\text{m}$ . Since the microcapsules may range from 0.2 – 5000 $\mu\text{m}$  in size [15], our encapsulated biocolorant could be attempted as microencapsulation of plant pigments. As detailed by [16], one reason for using microencapsulation technologies is to facilitate the heat- and light-labile ingredients like many pigments, so that their shelf life and release time could be tuned. Despite the fact that spray drying may produce more homogenous form of microcapsules, the high temperature of inlet promoted partial change of the heat-labile pigments which led to faster degradation [17], [18]. Freeze drying (lyophilization) was chosen as nonthermal processing which indicated lower degradation.



Fig. 1. Color disparities of encapsulated red biocolorant prepared from red spinach (a), beetroot (b), red cabbage (c), and dragon fruit (d), redissolved in buffered aqueous solution at pH 2 – 11 and after storage ( $20^{\circ}\text{C}$ , dark).

#### B. Coloring and Antioxidant Properties

Fig. 1 shows the color disparities of encapsulated

biocolorant in McIlvaine buffer at various pH. The hue and color intensity were exceptionally influenced by pH value as well as pigments composition of each raw materials.

The extract of red spinach and beetroot gave appealing red color in buffered solution at wide pH range, yet the intensity was slightly decreased on very acidic and basic condition. The extract of dragon fruit showed almost comparable intensity shift with purplish hue. On the other hand, the color of red cabbage extract was interestingly varied depends on the pH value, having the highest intensity of bluish hue in basic environment. Quantitative measurement for this finding was depicted as tinctorial values in Fig. 2. The encapsulated biocolorant of red spinach, beetroot, and dragon fruit denoted a polynomial relationship between pH and its tinctorial strength with the maximum at slightly acid to neutral region (pH 4–8), whereas that of red cabbage was fairly different, having the tinctorial maxima at pH 2 (red) and about pH 9–10 (blue). Overall, encapsulated red biocolorant from beetroot exhibited superior tinctorial strength, meaning that the stronger coloration could be released by the equal dyes concentration.

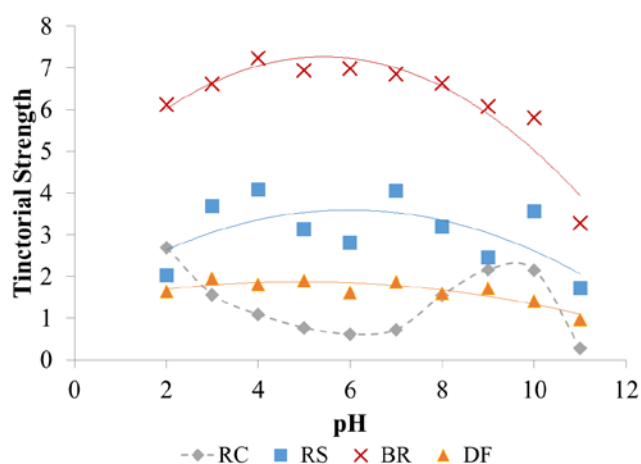


Fig. 2. Tinctorial strength of encapsulated red biocolorant prepared from red spinach (RS), beetroot (BR), red cabbage (RC), and dragon fruit (DF) at concentration of 0.1 % (w/v) in buffered aqueous solution at pH 2–11.

The red spinach, beetroot, and red dragon fruit are known to have dominance of betalains on its stems, leaves, and roots. It consists of red-violet betacyanins and yellow betaxanthins groups, which absorb light near the maxima at 535 nm and 480 nm, respectively [19]–[21]. The diversity in composition and content of pigment fractions on both groups, as determined by genetic information, steps of growth/maturity, as well as environmental factors, will result in color variety. Instead of betalains, the anthocyanins group dominates in the biocolorant extract from red cabbage [22]. In accordance with the characteristic of anthocyanins, cabbage extract had red color at acidic solution, almost transparent at neutral, and turned to blue and even green at alkaline solution. Although all red biocolorant of the present work may exhibit similar color in their powder form, each revealed distinct coloring properties.

It is also interesting to know that most natural pigments also play a biological role as antioxidant. Table I listed the  $IC_{50}$

value of encapsulated red biocolorant, in which a lower  $IC_{50}$  indicates greater antioxidant activity. The biocolorant of red spinach and beetroot obtained through physical extraction possessed higher antioxidant activity than those of red cabbage and dragon fruit, gaining more preeminence besides their excellent red color and strong coloration.

TABLE I:  $IC_{50}$  VALUES OF ENCAPSULATED RED BIOCOLORANT ON DPPH-RADICAL SCAVENGING ACTIVITY

Origin of Encapsulated Red Biocolorant	$IC_{50} \pm SE$ (ppm)
Red Spinach (RS)	$1558.00 \pm 22.29$
Beetroot (BR)	$1921.88 \pm 1.76$
Red Cabbage (RC)	$4560.23 \pm 266.98$
Dragon Fruit (DF)	$5299.99 \pm 1521.25$

\*Values obtained from regression lines with a good coefficient of determination ( $r^2 \geq 0.85$ ), SE standard error.

Moreover, the stability of these biocolorant was monitored during certain storage period at ambient temperature. The fluctuation of hue in pH 4 to 8 became our focus since most samples had stronger coloration, as well as food and drugs environment also generally cover this range. Fig. 3 revealed that the change of hue was significantly affected by pH and time of storage. The acidic solution at pH 4 was the most favorable condition for all biocolorant, causing mild change of hue during storage. The hue of red spinach and dragon fruit extract tend to increase as time changes, whereas that of red cabbage extract was found to decrease at pH 6–8. A distinctive characteristic was found at beetroot extract, which showed superior stability at pH 4 (10 days), 7 (8 days), and 8 (8 days), but brought out poor stability at pH 5 (2 days) and 6 (4 days). The color of encapsulated beetroot extract was easily changed to brownish yellow at pH 5 and 6, unlike the consistent red hue in the other pH values. The increase of lightness ( $L^*$ ) value was detected in all samples, revealing the occurrence of pigments degradation and naturally color fading.

Previous study of the red spinach done by [23] had emphasized the stability of anthocyanin fraction from its fruit, which was more stable at pH 5 and 6 rather than at pH 4. However, the dominance of anthocyanin groups might not be appeared in the encapsulated red biocolorant from red spinach. According to [24], the stability of betanine fraction from beetroot had great stability at pH 3.5, even also signifying greater antiradical activity which not easily degraded under illumination treatment, being in line with our detection. In addition, it was supposed that the natural acidic environment of dragon fruit (pH 5) should be most favorable to retard degradation of its pigments. In fact, the study of [9] revealed that the color of dragon fruit juice could be maintained up to 80% after 3 weeks dark storage at  $4^{\circ}C$  in pH 3. Our findings complemented the foregoing research that mostly employed solvent-based extraction, so that might not necessarily be applied directly in the food and pharmaceutical industries. Yet the stability evaluation of isolated pigment would be a worthwhile basis to explain our data.

### C. Thermal Study

The thermal study was aimed to estimate the effect of middle heating treatment to the color change of encapsulated

red biocolorant in buffered solution. This information could be the reference to avoid significant color adjustment after thermal processing. We observed the color change as  $\Delta E$  value which consider the shift of lightness ( $L^*$ ), redness ( $a^*$ ), as well as yellowness ( $c^*$ ) value. Thus, smaller value of color difference ( $\Delta E$ ) manifested preferable stability.

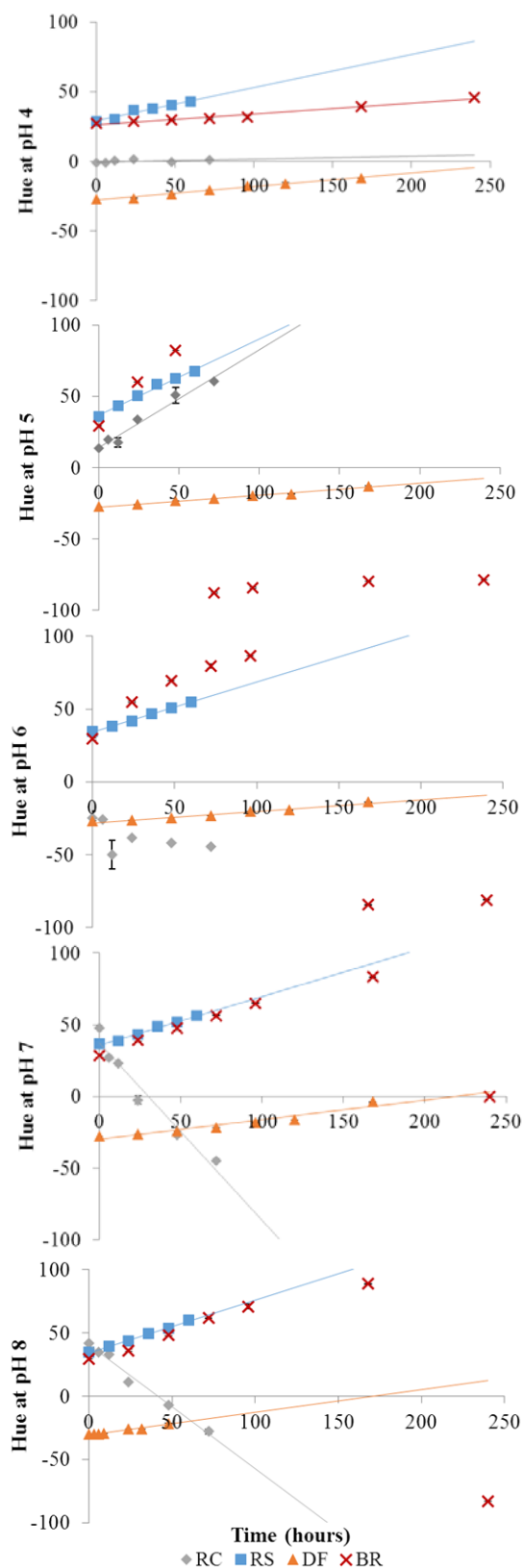


Fig. 3. The hue evolution of encapsulated red biocolorant prepared from red spinach (RS), beetroot (BR), red cabbage (RC), and dragon fruit (DF) in buffered aqueous solution at pH 4 – 8 within dark storage in 20°C.

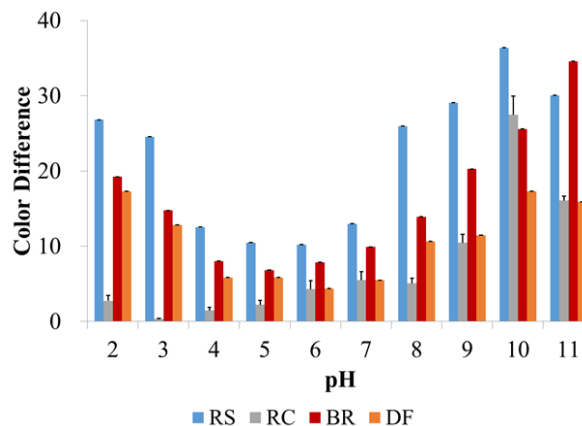


Fig. 4. Color difference ( $\Delta E$ ) of encapsulated red biocolorant prepared from red spinach (RS), beetroot (BR), red cabbage (RC), and dragon fruit (DF) in buffered aqueous solution at pH 2–11, after thermal treatment at 60°C for 30 minutes.

The thermal study gave a consistent result concerning pH-dependent stability of these encapsulated red biocolorant. Fig. 4 yet again revealed that most red biocolorant on the present work exhibited distinguished stability at pH range 4 to 8. Although the extract of red spinach showed vivid red color when reconstituted, it experienced greatest discoloration after incubated for 30 minutes at 60°C. The extract of beetroot underwent a slightly smaller color change than that of red spinach. Although the red powder produced from dragon fruit and red cabbage had lesser color difference, both did not consistently displayed red hue. The extract of dragon fruit could be a candidate for purple colorant, whereas that of red cabbage is rather fitted as blue colorant with an alkaline treatment.

#### D. Future Prospect and Outlook

In the point of view of chemistry, indeed there is nothing more stable than the synthetic dye. Nevertheless, the use of biocolorant has several advantages i.e., it is inescapable safe colorant for both the body and environment, exploited from renewable sources and hence supporting appropriate use of local wisdom, could be extracted without bearing any toxic chemical waste, and possesses health benefit upon its consumption. Additionally, the instability of biocolorant could be useful as bio-indicator, such as detection of food spoilage that causes pH alteration, adequacy of food processing or heat treatment, as well as biosensor of shelf life detection in intelligent packaging system. In case the minimal discoloration is needed, incorporation of biocolorant from several raw materials could be an option. For instance, the extract of red spinach may correct the instability of beetroot extract during prolonged storage at pH 5 and 6, and then a little amount of dragon fruit extract could support its color within heating treatment. Elucidation of most stable pigment fraction among those materials is also being the part of our current project.

#### IV. CONCLUSION

Four types of vivid red powder were effectively produced through simple physical extraction and lyophilization step

from red spinach, beetroot, red cabbage, and dragon fruit. Considering the coloring capacity, hue, and antioxidant activity, red spinach and beetroot met the superior candidate of eco-friendly red biocolorant. The beetroot extract showed good stability during dark storage up to 10 days in 20°C, especially at pH 4, 7, and 8. The extract of red spinach and dragon fruit could be incorporated in order to accomplish its discoloration at pH 5 and 6 as well as in thermal processing.

## REFERENCES

- [1] S. Singh, "Impact of color on marketing," *Management Decision*, vol. 44, no. 6, pp. 783-789, March 2006.
- [2] N. Geldenhuys, "Taking natural to a new level: Colours & flavours," *South African Food Review*, vol. 41, no. 10, pp. 22-24, October 2011.
- [3] S. Houlton. (February 2016). The natural food dye revolution. *Chemistry World*. [Online]. 15(2). Available: <https://www.chemistryworld.com/feature/the-natural-food-dye-revolution/9322.article>
- [4] R. Indrawati, G. C. Kombaitan, K. Anggraeni, M. M. Yusuf, Y. Yuniati, and L. Limantara, "How extensive the artificial dyes color our food?" *Proceeding of Natural Pigments Conference for South-East Asia*, ed. Yuzo Shioi, vol. 3, pp. 108-109, 2016.
- [5] R. Carle and R. M. Schweiggert, *Handbook on Natural Pigments in Food and Beverages*, 1st ed. Kidlington, U.K.: Woodhead Publishing, 2016, ch. 18, pp. 385.
- [6] F. U. G. Akogou, A. P. P. Kayode, H. M. W. den Besten, and A. R. Linnemann, "Extraction methods and food uses of a natural red colorant from dye sorghum," *Journal of the Science of Food and Agriculture*, June 2017.
- [7] J. M. Obon, M. R. Castellar, M. Alacid, and J. A. Fernandez-Lopez, "Production of a red-purple food colorant from *Optunia stricta* fruits by spray drying and its application in food model systems," *Journal of Food Engineering*, vol. 90, pp. 471-479, July 2008.
- [8] N. Lopez, E. Puertolas, S. Condon, J. Raso, and I. Alvarez, "Enhancement of the extraction of betanin from red beetroot by pulsed electric fields," *Journal of Food Engineering*, vol. 90, no. 1, pp. 60-66, January 2009.
- [9] K. K. Woo, F. H. Ngou, L. S. Ngo, W. K. Soong, and P. Y. Tang, "Stability of betalain pigment from red dragon fruit (*Hylocereus polyrhizus*)," *American Journal of Food Technology*, vol. 6, no. 2, pp. 140-148, 2011.
- [10] Y. Z. Cai, M. Sun, and H. Corke, "Characterization and application of betalain pigments from plants of the Amaranthaceae," *Trends in Food Science & Technology*, vol. 16, pp. 370-376, 2005.
- [11] K. Duangmal, B. Saicheua, and S. Sueeprasan, "Colour evaluation of freeze-dried roselle extract as a natural food colorant in a model system of a drink," *Food Science and Technology*, vol. 41, no. 8, pp. 1437-1445, November 2008.
- [12] G. A. Molina, A. R. H. Martinez, M. C. Valadez, F. G. Hernandez, and M. Estevez, "Effects of tetraethyl orthosilicate (TEOS) on the light and temperature stability of a pigment from *Beta vulgaris* and its potential food industry applications," *Molecules*, vol. 19, no. 11, pp. 17985-18002, 2014.
- [13] R. Indrawati, A. Chomiuk, Indriatmoko, M. A. S. Adhiwibawa, D. Siahaan, T. H. P. Brotosudarmo, and L. Limantara, "Stability of palm carotenes in an organic solvent and in a food emulsion system," *International Journal of Food Properties*, vol. 18, no. 11, pp. 2539-2548, April 2015.
- [14] F. Dehbi, A. Hasib, M. Bouaziz, A. Ouattmane, H. Elbatal, A. Jaouad, and S. Sayadi, "Effect of phenolic compounds and betalain pigments on the antioxidant capacity on Moroccan prickly pear juices," *Nature & Technology*, pp. 2-7, June 2013.
- [15] S. Krishnan, A. C. Kshirsagar, and R. S. Singhal, "The use of gum arabic and modified starch in the microencapsulation of a food flavoring agent," *Carbohydrate Polymers*, vol. 62, no. 4, pp. 309-315, December 2005.
- [16] A. Gaonkar, N. Vasisht, A. Khare, and R. Sobel, *Microencapsulation in the food industry*, 1st ed. Waltham, USA: Academic Press, 2014, ch. 1, pp. 3-12.
- [17] K. Selim, M. Tsimidou, and C. G. Biliaderis, "Kinetic studies of degradation of saffron carotenoids encapsulated in amorphous polymer matrices," *Food Chemistry*, vol. 71, no. 2, pp. 199-206, November 2000.
- [18] B. Nemzer, Z. Pietrzowski, A. Sporna, P. Stalica, W. Thresher, T. Michalowski, and S. Wybraniec, "Betalainic and nutritional profiles of pigment-enriched red beet root (*Beta vulgaris* L.) dried extracts," *Food Chemistry*, vol. 127, pp. 42-53, 2011.

- [19] S. S. Kumar, P. Manoj, N. P. Shetty, M. Prakash, and P. Giridhar, "Characterization of major betalain pigments –Gomphrenin, betanin and isobetanin from *Basella rubra* L. fruit and evaluation of efficacy as a natural colourant in product (ice cream) development," *Journal of Food Science and Technology*, vol. 52, no. 8, pp. 4994-5002, August 2015.
- [20] K. M. Herbach, F. C. Stintzing, and R. Carle, "Impact of thermal treatment on color and pigment pattern of red beet (*Beta vulgaris* L.) preparations," *Journal of Food Science*, vol. 69, no. 6, 2004.
- [21] O. P. S. Rebecca, A. N. Boyce, and S. Chandran, "Pigment identification and antioxidant properties of red dragon fruit (*Hylocereus polyrhizus*)," *African Journal of Biotechnology*, vol. 9, no. 10, pp. 1450-1454, March 2010.
- [22] J. Y. Lin, C. Y. Li, and I. F. Hwang, "Characterisation of the pigment components in red cabbage (*Brassica oleracea* L. var.) juice and their anti-inflammatory effects on LPS-stimulated murine splenocytes," *Food Chemistry*, vol. 109, no. 4, pp. 771-781, August 2008.
- [23] E. F. Ozela, P. C. Stringheta, and M. C. Chauca, "Stability of anthocyanin in spinach vine (*Basella rubra*) fruits," *Ciencia e Investigacion Agraria*, vol. 34, no. 2, pp. 115-120, 2007.
- [24] M. A. Pedreno and J. Escibano, "Correlation between antiradical activity and stability of betanin from *Beta vulgaris* L roots under different pH, temperature and light conditions," *Journal of the Science of Food and Agriculture*, vol. 81, no. 7., pp. 627-631, May 2001.



**Renny Indrawati** was born in Malang, East Java, Indonesia, on May 29, 1986. She received the undergraduate degree (bachelor in food technology) with a cum laude honor from Brawijaya University, Indonesia, in 2008. She began her career in research by joining Ma Chung Research Center for Photosynthetic Pigments (MRCPP) as a research assistant in 2009, and she is deeply interested in the development of functional food related to natural pigments. In 2011, she graduated with a summa cum laude honor from Satya Wacana Christian University, Indonesia, majored in Chlorophyll and Carotenoid. She subsequently finished the second master degree by research (master of international natural science) in 2012 at Kwansei Gakuin University, Japan.

Currently, she is a researcher at MRCPP as well as a lecturer assistant at Chemistry Study Program, Universitas Ma Chung, Indonesia. She has been involved in some prestigious national research grants, such as Excellent Research on National Strategy, Competitive Research Grant, and National Innovation System Research Grant. Her current research interest lies in the fabrication and stability studies of functional food colorants from natural resources.

Ms. Indrawati is an author and co-author of Indonesian peer-reviewed papers as well as several international publications. She has been awarded for a double degree scholarship by Indonesian Government to pursue her graduate study for two years and a half. She received the award as one of the best presenters in Natural Pigments Conference for South-East Asia in three consecutive years.



**Diah Mustika Lukitasari** was born in Malang, Indonesia, in 1990. She received bachelor and master degree in science and food technology from the Brawijaya University, in 2012 and 2015, respectively. Her major field of study is functional food and dietary supplement.

In 2012, she was a practical work assistant for manual laboratories of work and general microbiology in the Department of Agricultural Technology, Brawijaya University, Indonesia. In 2016, she joined Ma Chung Research Center for Photosynthetic Pigments (MRCPP), Universitas Ma Chung, Indonesia, as a research assistant. She has experienced in several research field, including the development of functional food, immunology of dietary supplements, microencapsulation of pigment, food colourants, and antioxidant activity of natural compounds.



**Yuyun Yuniati** received her doctoral degree in chemical engineering from Institute of Technology Sepuluh Nopember Surabaya, Indonesia, in 2013. Currently, she is a head of Chemistry Study Program at Universitas Ma Chung, Indonesia. She is a member research fellow in Ma Chung Research Center for Photosynthetic Pigments (MRCPP). She has focused her research in the field of functional food development, processing technology, kinetic and catalysis, as well as industrial chemistry.



**Heriyanto** received his B.Sc in Chemistry from Satya Wacana Christian University, Indonesia, in 2004. In 2008 and 2009, He obtained M.Sc as a double degree program in Biology from Satya Wacana Christian University, Indonesia and in Chemistry from Kwasei Gakuin University, Japan. Currently, he is a Ph.D student in the Faculty of Biochemistry, Biophysics and Biotechnology, Jagiellonian University, Poland.

He worked as a research assistant from 2004 to 2009 and then continues his work as a researcher at Ma Chung Research Center for Photosynthetic Pigments (MRCPP), Universitas Ma Chung, Indonesia. Since 2015, he has been invited as a lecturer in the Department of Chemistry, Universitas Ma Chung, Indonesia. He has an experience in the analysis of natural pigments for almost 14 years. His research interests include pigment analysis, analytical chemistry, spectroscopy and chromatography, as well as biochemistry of photosynthetic pigments.



**Leenawaty Limantara** finished her graduate study in Kwasei Gakuin University, Japan, majored in the physical chemistry related to photosynthetic pigments in light harvesting antenna. She has been involved in several post-doctoral research in Japan, United States, United Kingdom, and Germany.

She is an invited lecturer and principal investigator in Ma Chung Research Center for Photosynthetic Pigments, Universitas Ma Chung. She has been engaged in many studies related to chlorophyll since 1991 and received many research grants from both national and international institutions. Currently, she is the rector of Universitas Pembangunan Jaya, Jakarta, Indonesia.

Dr. Limantara has published her work in many international journals, chapters of books, reviews, and national peer-reviewed journals. She is the founder as well as chairwoman of the Association of Pigment Researchers in Indonesia. She is also the first Indonesian Ambassador Scientist for the Alexander von Humboldt Foundation, Germany.

# Influence of Shell Number on Loading Capacity of Microcapsules Containing Fragrance

A. K. Aldred, W. Chokbundit, and K. Saengsorn

**Abstract**—Microcapsules of single-shell melamine-formaldehyde (MF) and double-shell urea-formaldehyde/melamine-formaldehyde (UF/MF) microcapsules loading with fragrance of varied concentrations were prepared using in situ polymerization. The microcapsules were analyzed using Scanning electron microscope (SEM) and Fourier transform infrared spectrometer (FT-IR). Loading capacity of fragrance in the microcapsules in term of percent weight of fragrance was determined using soxhlet extraction. From SEM images, shapes and sizes of single shell MF microcapsules were different depending on concentrations of fragrance and SDS added in the preparation procedure. FT-IR spectra of double-shell UF/MF microcapsules loaded fragrance presented absorption band of C=O at  $1674\text{ cm}^{-1}$  as found in that of fragrance. Percent weight of fragrance in single-shell UF and double-shell UF/MF microcapsules substantially increased with increased concentration of fragrance. Additionally, loading capacity of fragrance in double-shell UF/MF microcapsules were higher than those in single-shell MF microcapsules at the same concentration of fragrance. This would lead to higher prolongation of fragrance release from double-shell UF/MF microcapsules than single-shell MF microcapsules and fulfill the end use applications.

**Index Terms**—Fragrance, loading capacity, melamine-formaldehyde, microcapsules, urea-formaldehyde.

## I. INTRODUCTION

Microencapsulation of active ingredients is an attractive way to create functional products. Their stability, storage as well as degradation protection are benefits to fulfill the appropriate applications. Microcapsules containing fragrance have been adopted to produce sensational-durable materials and used in wide ranges of application such as food, agriculture, papers, textiles, medical and consumer products. Stabilization and protection of the core ingredients using porous polymer shell are its advantage of microencapsulation technique for ingredient delivery and long lasting release. Encapsulation of active ingredients, including flavors in polymer shell of urea-formaldehyde [1]–[4] and melamine-formaldehyde has been versatile [5]–[8]. Control of fragrance diffusion by barrier system of various types has been employed in fragrance prolongation, for instance, cyclodextrin host [9]–[10], solid-lipid nanoparticles [11], amphiphilic-crosslinked polymer network [12], double emulsion system [13], synthetic polymers formed by miniemulsion polymerization [14], coacervation with various

carbohydrates [15]–[17], polymer blends [18] and multilayer microcapsules [19]. However, increasing in capacity of fragrance in urea-formaldehyde and melamine-formaldehyde is necessary to prolong the release period.

To increase loading capacity of fragrance, microcapsules of increased shell number using in situ polymerization was developed, in this investigation. Morphologies and chemical structures of the microcapsules loaded fragrance were analyzed using SEM and FT-IR, respectively. Percent weight of fragrance in the microcapsules was determined using soxhlet extraction.

## II. PROCEDURE

### A. Materials

Urea was supplied by BHD Prolabo, ammonium chloride was supplied by RFCL Limited, resorcinol was provided by Himedia. Hydrochloric acid and sodium dodecyl sulphate (SDS) were supplied from Merck, melamine was supplied by Aldrich. 36 % Formaldehyde and sodium carbonate was provided by Analar, poly(vinyl alcohol) was supplied from Ajax Finechem. Acetic acid was supplied by Carlo Erba and fragrance was purchased from Honghuad.

### B. Preparation of Single-Shell Melamine-Formaldehyde (MF) Microcapsules

Single-shell MF microcapsules were prepared by in situ polymerization in an O/W emulsion emulsion using the procedure described in other literatures [4], [20]–[22]. Briefly, emulsion of 15 ml fragrance in sodium dodecyl sulphate (SDS) solution was firstly prepared by dissolving various weights of SDS in 100 ml of distilled water (to provide 2, 4, 5 and 6 % w/v) SDS. The emulsion was stirred with a magnetic stirrer at  $70\text{ }^{\circ}\text{C}$  for 1 hr. Pre-polymer of melamine and formaldehyde was subsequently prepared as follows. 2.50 g melamine and 4.52 ml formaldehyde was dissolved in 100 ml distilled water; pH of the solution was adjusted to 8–9 by 10 % w/v sodium carbonate solution. Condensation reaction of melamine and formaldehyde was taken place and was carried out at  $70\text{ }^{\circ}\text{C}$  for 1 hr under magnetic stirrer. After that, the emulsion was dropwisely added to the pre-polymer solution, pH of the mixture was adjusted to 4–5 by 10 % v/v acetic acid. 10 ml of 0.3 % w/v poly (vinyl alcohol) was subsequently added, the reaction was further carried out at  $70\text{ }^{\circ}\text{C}$  for 1 hr using an overhead stirrer at a speed of 1000 rpm. Single-shell MF microcapsules were received; they were filtered under vacuum suction and then dried in a laboratory oven at  $60\text{ }^{\circ}\text{C}$  for 2 hrs.

Manuscript received October 18, 2017; revised December 5, 2017.

A. K. Aldred, W. Chokbundit, and K. Saengsorn are with Maejo University, Faculty of Science, ChiangMai Thailand 50290 (e-mail: arunee.k@mju.ac.th, wijitra260@hotmail.com, saengsorn23@hotmail.co.th).

Another set of single-shell MF microcapsules loaded fragrance was prepared in the similar manner using various volumes of fragrance (5, 10, 15, 20, 25, 30, 35 and 40 ml) in SDS solution of 5 % w/v.

### C. Preparation of Double-Shell Urea-Formaldehyde/Melamine-Formaldehyde (UF/MF) Microcapsules Loaded Fragrance

Microcapsules of urea-formaldehyde (UF) were firstly prepared from urea and formaldehyde solution containing resorcinol and ammonium chloride by in situ polymerization in an O/W emulsion as following procedure [1], [2]. Urea of 5.00 g, ammonium chloride of 0.50 g and resorcinol of 0.50 g were weighed and dissolved in 260 ml distilled water, respectively. 10.00 ml of 5 % w/v poly(vinyl alcohol) was added, pH of the solution was subsequently adjusted to 3.5 with 10 % v/v hydrochloric acid. After that, 12.60 ml of 0.06 M formaldehyde solution was added into the solution which was stirred at 1000 rpm by an overhead stirrer. In situ polymerization of urea and formaldehyde was taken place and it was carried out at 55 °C for 4 hr. Urea-formaldehyde microcapsules were received; they were filtered under vacuum suction and then dried in a laboratory oven at 60 °C for 2 hrs.

Urea-formaldehyde (UF) was used as microcapsules inner layer for the preparation of double-shell microcapsules. The outer layer of double-shell microcapsules was melamine-formaldehyde which was further prepared using the similar procedure mentioned above. The preparation of double-shell microcapsules shell urea-formaldehyde/melamine-formaldehyde (UF/MF) was performed as the following procedures.

Emulsion of fragrance in SDS solution was firstly prepared by dissolving 5.00 g SDS in 100 ml of distilled water. A series of 5, 10, 15, 20, 25, 30, 35 and 40 ml fragrance was added into SDS solution. The emulsion was stirred with a magnetic stirrer at 70 °C for 1 hr. Urea-formaldehyde microcapsules, as inner microcapsule shell were added into the emulsion of fragrance in SDS, the mixture was stirred with an overhead stirrer at a speed of 1000 rpm for 1 hr.

Pre-polymer of melamine and formaldehyde was subsequently prepared, 2.50 g melamine and 4.52 ml formaldehyde was dissolved in 100 ml distilled water, pH of the solution was adjusted to 8–9 by 10 % w/v sodium carbonate solution. Condensation reaction of melamine and formaldehyde was carried out at 70 °C for 1 hr under magnetic stirrer. After that, the emulsion with urea-formaldehyde microcapsules was dropwisely added to the pre-polymer solution, pH of the mixture was adjusted to 4–5 by 10 % v/v acetic acid. 10 ml of 0.3 % w/v poly(vinyl alcohol) was subsequently added, the reaction was further carried out at 70 °C for 1 hr using an overhead stirrer at a speed of 1000 rpm. Double-shell microcapsules of urea-formaldehyde/melamine-formaldehyde (UF/MF) were received; they were filtered under vacuum suction and then dried in a laboratory oven at 60 °C for 2 hrs.

To compare functional groups of the resultant single-shell MF and double-shell UF/MF microcapsules loaded fragrance analyzing by FT-IR, UF microcapsules and melamine/formaldehyde resin were prepared in the similar

manner without loading of fragrance.

### D. Analyses of Microcapsules Containing Fragrance

Characterization of fragrance and microcapsules were performed by means of a Fourier transform infrared spectrometer (Perkin-Elmer, USA). The samples were prepared as KBr disc and analyzed over wavelengths of 400–4000  $\text{cm}^{-1}$ . Surface morphology of the microcapsules was examined under a Scanning electron microscope (Jeol Co., Japan). The microcapsules were sprinkled onto a double sized tape, coated with gold using sputtering technique and examined under the microscope.

### E. Determination of Fragrance Loading Capacity

Fragrance loading capacity in term of percent weight of fragrance was performed using soxhlet extraction as explained in another literature [1]. A known weight of microcapsules ( $W_c$ ) was placed in a known weight thimble ( $W_{ti}$ ). The refluxed procedure was performed in 50 ml hexane for 1 hr using soxhlet extraction. After draining of hexane, the thimble with extracted microcapsules was then dried in a laboratory oven and cooled down in a desiccators, the final weight of thimble was noted ( $W_{tf}$ ). Percent weight of fragrance was calculated using equation (1). The determination of percent weight of fragrance in microcapsules was in triplicate.

$$(1) \quad \% \text{Weight of fragrance} = \frac{(W_c + W_{ti}) - W_{tf}}{W_c} \times 100$$

## III. RESULTS AND DISCUSSION

### A. Characterization of Microcapsules

Single-shell melamine-formaldehyde microcapsules containing fragrance prepared from varied amount of SDS gave different sizes and shapes as seen in Fig. 1. When 2–5 % w/v SDS was used, spherical microcapsules were received (Fig. 1. (a)–(c), respectively) while 6 % w/v SDS provided rod-shape single shell melamine-formaldehyde microcapsules (Fig. 1.(d)). The results attribute to effect of concentration of SDS on shape of its micelles which was sphere when low concentration was used, but rod micelles were formed at high concentration of SDS.

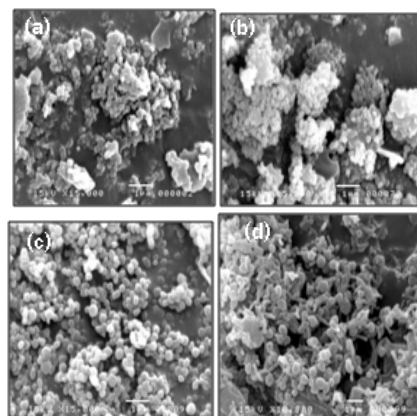


Fig. 1. Single shell melamine-formaldehyde microcapsules loaded with 15 ml of fragrance using (a) 2 % w/v SDS (b) 4 % w/v SDS (c) 5 % w/v SDS and (d) 6 % w/v SDS.

SEM images of double-shell microcapsules (UF/MF) loaded fragrance are present in Fig. 2. Shape of single shell microcapsules (UF) loaded 5 ml of fragrance is sphere (Fig. 2. (a)), its sizes are approximately 5  $\mu\text{m}$ . Being double-shell microcapsules (UF/MF) loaded different amounts of fragrance, they have the same size as that of single shell microcapsules (UF) (Fig. 2. (a)–(d)). However, coalescence of the microcapsules is observed when over 25 ml of fragrance was used; the larger double-shell microcapsules (UF/MF) were observed for 40 ml of fragrance (Fig. 2. (e)–(f)). This would be affected by loss of emulsifying potential of SDS when high volumes of fragrance were used in the preparation of microcapsules.

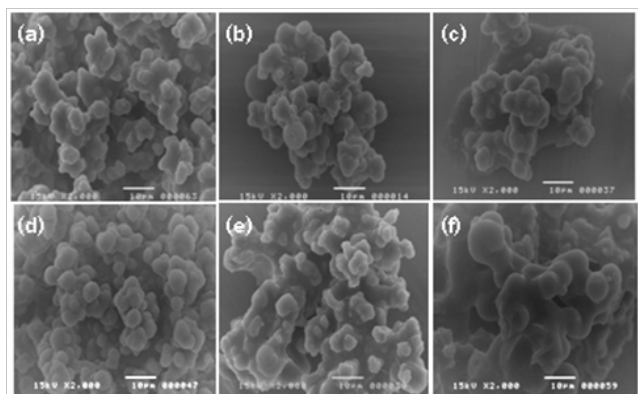


Fig. 2. (a) MF loaded with 5 ml of fragrance (b) UF/MF loaded 5 ml (c) 15 ml (d) 25 ml (e) 35 ml and (f) 40 ml of fragrance.

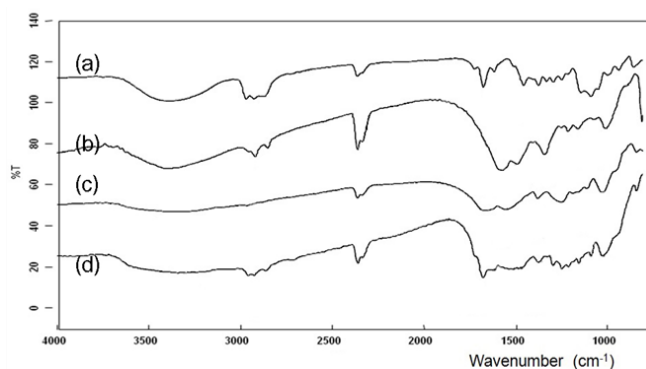


Fig. 3. FT-IR spectra of (a) fragrance (b) melamine-formaldehyde resin (c) urea-formaldehyde microcapsules and (d) double-shell (UF/MF) microcapsules loaded with 25 ml of fragrance.

TABLE I: PERCENT WEIGHT OF FRAGRANCE IN SINGLE-SHELL MF AND DOUBLE-SHELL UF/MF MICROCAPSULES WITH INCREASED FRAGRANCE

Vol. of fragrance (ml)	Percent weight of fragrance of fragrance (%)	
	MF	UF/MF
5	14.05 $\pm$ 2.62	36.82 $\pm$ 1.07
10	17.35 $\pm$ 2.53	48.78 $\pm$ 2.80
15	20.72 $\pm$ 2.01	44.89 $\pm$ 1.29
20	24.62 $\pm$ 2.33	64.36 $\pm$ 2.22
25	27.04 $\pm$ 2.13	77.16 $\pm$ 2.61

FT-IR spectrum of fragrance is shown in Fig. 3. Strong absorption band of C=O stretching in fragrance was observed at 1678  $\text{cm}^{-1}$  (Fig. 3(a)), while it is found at 1650  $\text{cm}^{-1}$  for urea-formaldehyde microcapsules (Fig. 3(b)) [23] and it is absent for MF resin (Fig. 3(c)). Strong absorption band of C=O stretching is also observed at 1678  $\text{cm}^{-1}$  in FT-IR spectrum of double-shell UF/MF microcapsules loaded with

25 ml of fragrance (Fig. 3(d)) [24]. The result demonstrates that fragrance was trapped in double-shell UF/MF microcapsules during preparation.

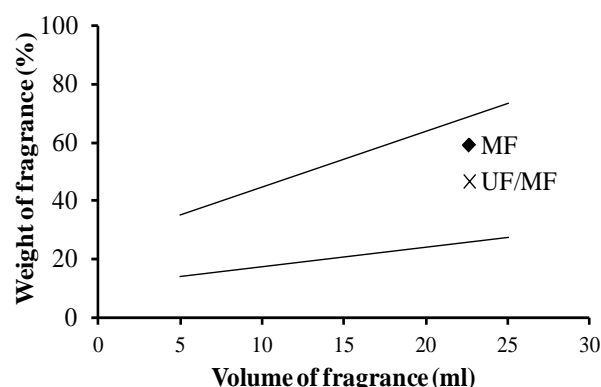


Fig. 4. Percent weight of fragrance single-shell MF and double-shell UF/MF microcapsules.

### B. Loading Capacity of Fragrance

Loading capacity of fragrance in term of percent weight performed by soxhlet extraction are presented in Table I and Fig. 4. The fragrance was loaded in single-shell MF microcapsules. Percent weight of fragrance in single shell MF microcapsules found to be increased with increased fragrance volumes from 5, 10, 15, 20 to 25 ml. Increase in percent weight of fragrance with increased volumes of fragrance is also observed in double-shell UF/MF microcapsules. Additionally, the values of double-shell UF/MF microcapsules are found to be higher than those of single-shell MF microcapsules. These are affected by the adsorption of fragrance by shell of microcapsules. In the preparation of double-shell UF/MF microcapsules, fragrance molecules were firstly adsorbed on surface of urea-formaldehyde shell (as inner layer). Mechanical agitation accelerated the transportation of fragrance molecules into the urea-formaldehyde shell in the second step of preparation. Fragrance molecules were subsequently encapsulated in deposited melamine-formaldehyde polymer (as the outer layer) after fragrance emulsion was added into its pre-polymer, other fragrance molecules were included in melamine-formaldehyde shell in the complete preparation procedure. Thus number of microcapsules shell has influence on loading capacity of microcapsules.

## IV. CONCLUSIONS

Single-shell MF and double-shell UF/MF microcapsules loaded fragrance were successfully prepared. SDS concentration affected to shape and size of single-shell melamine-formaldehyde microcapsules. Encapsulation of fragrance in microcapsules was indicated by the presence of C=O absorption band at 1674  $\text{cm}^{-1}$  in FT-IR spectra. The fragrance was able to be loaded in single-shell MF and double-shell UF/MF microcapsules. Double-shell UF/MF microcapsules showed greater percent weight of fragrance single-shell MF and they would affect to prolong release period of fragrance. Different released behaviors of fragrance from single-shell MF and double-shell UF/MF

microcapsules will be further studied to provide helpful information for textile applications.

#### REFERENCES

- [1] C. Suryanarayana, R. Chowdoji, and D. Kumar, "Preparation and characterization of microcapsules containing linseed oil and its used in self-healing coatings," *Progress in Organic Coatings*, vol. 63, pp. 72–78, 2008.
- [2] E. N. Brown, M. R. Kessler, N. R. Sottos, and S. R. White, "In situ poly(urea-formaldehyde) microencapsulation of dicyclopentadiene," *Journal of Microencapsulation*, vol. 20, no. 6, pp. 719–730, 2003.
- [3] H. Li, R. Wang, H. Hu, and W. Liu, "Surface modification of self-healing poly(urea-formaldehyde) microcapsules using silane-coupling agent," *Applied Surface Science*, vol. 255, pp. 1894–1900, 2008.
- [4] S. J. Park, Y. S. Shin, and J. R. Lee, "Preparation and characterization of microcapsules containing lemon oil," *Journal of Colloid and Interface Science*, vol. 241, pp. 502–508, 2001.
- [5] K. Hong and S. Park, "Melamine resin microcapsules containing fragrant oil: Synthesis and characterization," *Materials Chemistry and Physics*, vol. 58, pp. 128–131, 1999.
- [6] J. F. Su, X. Y. Wang, and H. Dong, "Influence of temperature on the deformation behaviors of melamine-formaldehyde microcapsules containing phase change material," *Materials Letters*, vol. 84, pp. 158–161, 2012.
- [7] F. Salaun and I. Vroman, "Influence of core materials on thermal properties of melamine-formaldehyde microcapsules," *European Polymer Journal*, vol. 44, pp. 849–860, 2008.
- [8] X. Fei, H. Zhao, B. Zhang, L. Cao, M. Yu, J. Zhou, and L. Yu, "Microencapsulation mechanism and size control of fragrance microcapsules with melamine resin shell," *Colloids and Surfaces A: Physicochem. Eng. Aspects*, vol. 469, pp. 300–306, 2015.
- [9] C. X. Wang and S. L. Chen, "Aromachology and its application in the textile field," *Fibres and Textiles in Eastern Europe*, vol. 13, pp. 41–44, 2005.
- [10] C. X. Wang and S. L. Chen, "Fragrance-release property of cyclodextrin inclusion compounds and their application in aromatherapy," *Journal of Industrial Textiles*, vol. 34, pp. 157–166, 2005.
- [11] E. B. Souto and R. H. Müller, "Cosmetic features and applications of lipid nanoparticles (SLN<sup>®</sup>, NLC<sup>®</sup>)," *International Journal of Cosmetics Science*, vol. 30, pp. 157–165.
- [12] G. O. Brown, C. Bergquist, P. Ferm, and K. L. Wooley, "Unusual, promoted release of guests from amphiphilic cross-linked polymer networks," *Journal of the American Chemical Society*, vol. 127, pp. 11238–11239, 2005.
- [13] A. Edris and B. Bergnsthäl, "Encapsulation of orange oil in a spray dried double emulsion," *Die Nahrung*, vol. 45, pp. 133–137, 2001.
- [14] K. Landfester, "Miniemulsion polymerization and the structure of polymer and hybrid nanoparticles," *Angewandte Chemie-International Edition*, vol. 48, pp. 4488–4508, 2009.
- [15] H. C. Paula, F. M. Sombra, R. D. F. Cavalcante, F. O. Abreu, and R. C. M. De Paula, "Preparation and characterization of chitosan/cashew gum beads loaded with *Lippia sidoides* essential oil," *Materials Science and Engineering C*, vol. 31, pp. 173–178, 2011.
- [16] J. Korus, P. Tomasik, and C. Y. Lii, "Microcapsules from starch granules," *Journal of Microencapsulation*, vol. 20, pp. 47–56, 2003.
- [17] A. Hambleton, M. J. Fabra, F. Debeaufort, C. Dury-Brun, and A. Voilley, "Interface and aroma barrier properties of iota-carrageenan emulsion-based films used for encapsulation of active food compounds," *Journal of Food Engineering*, vol. 93, pp. 80–88, 2009.
- [18] A. Sansukcharearnpon, S. Wanichwecharungruang, N. Leepi-patpaiboon, T. Kerdcharoen, and S. Arayachukeat, "High loading fragrance encapsulation based on a polymer-blend: Preparation and release behavior," *International Journal of Pharmaceutics*, vol. 391, pp. 267–273, 2010.
- [19] E. Ansarifard, M. Mohebbi, F. Shahidi, and A. Koocheki, "Novel Multilayer microcapsules based on soy protein isolate fibrils and high methoxyl pectin: Production, characterization and release modeling," *International Journal of Biological Macromolecules*, vol. 97, pp. 761–769, 2017.
- [20] H. Kage, H. Kawahara, N. Hamada, T. Kotake, and H. Ogura, "Operating conditions and microcapsules generated by *in situ* polymerization," *Advanced Powder Technol.*, vol. 13, no. 3, pp. 265–285, 2002.
- [21] H. Yuan, G. Li, L. Yanga, X. Yana, and D. Yanga, "Development of melamine-formaldehyde resin microcapsules with low formaldehyde emission suited for seed treatment," *Colloids and Surfaces B: Biointerfaces*, vol. 128, pp. 149–154, 2015.
- [22] J. F. Su, X. Y. Wang, and H. Dong, "Influence of temperature on the deformation behaviors of melamine-formaldehyde microcapsules containing phase change material," *Materials Letters*, vol. 84, pp. 158–161, 2012.
- [23] S. Chen, X. Lu, T. Wang, and Z. Zhang, "Preparation and characterization of urea-formaldehyde resin/reactive kaolinite composites," *Particuology*, vol. 24, pp. 203–209, 2016.
- [24] Z. Qiao and J. Mao, "Multifunctional poly(melamine-urea-formaldehyde)/grapheme microcapsules with low infrared emissivity and high thermal conductivity," *Materials Science & Engineering B*, vol. 226, pp. 86–93, 2017.



**Arunee Kongdee Aldred** is an associate professor at Maejo University, her PhD (2007) in chemistry is from University of Innsbruck.

She is interested in encapsulation of fragrance and bioactive compounds in synthetic and natural polymers for textiles and cosmetics applications. Chemical modification of polymers, textile fibers to enhance their special properties are also her interests.

Assoc. Prof. Dr. Aldred won many prizes for national and international researches and innovation competitions.

# Microencapsulation of Kabocha Pumpkin Carotenoids

Naomi M. Mulyadi, Tri D. Widyaningsih, Novita Wijayanti, Renny Indrawati, Heriyanto, and Leenawaty Limantara

**Abstract**—Kabocha pumpkin (*Curcubita maxima* [Duchesne ex Lamb.]) is a potential source of carotenoids. However, the usage of carotenoids is limited due to their instability and also their susceptible degradation against harmful conditions such as base and acidic conditions, oxidation, and illumination. In this study, kabocha carotenoids were incorporated into microencapsulation containing chitosan, sodium alginate and sodium tripolyphosphate. The objective of this study is to determine the formulation of coating agents, carotenoid stability in acidic conditions for mimicking the microencapsulation process, and to characterize the microencapsulated carotenoids including the determination of the efficiency of carotenoid incorporation into microencapsulates. A mixture of sodium alginate, chitosan and sodium tripolyphosphate (0.19 g : 1.92 g : 0.24 g, w/w/w) was the best of coating agents according to the physical characteristics and also its moisture content. Microcapsules obtained with and without addition of carotenoids were determined to be a microparticle size by SEM analysis. The products of microencapsulated carotenoids have the water content of around 5.4% to 7.1%. The highest efficiency of microencapsulation obtained was 91% at the carotenoid concentration of  $117.98 \mu\text{g} \cdot \text{g}^{-1}$  (0.5 %, w/v), although the efficiency was decreased with increasing carotenoids added to the microcapsules probably due to over loading of carotenoids used. The pattern of this efficiency was in line with  $L^*$  and  $^{\circ}\text{hue}$  values, whereas not only  $a^*$ ,  $b^*$ , and chroma values, but total carotenoids, and total provitamin A also increased.

**Index Terms**—Carotenoids, emulsion, kabocha (*Curcubita maxima* [Duchesne ex Lamb.]), microencapsulation, pumpkin.

## I. INTRODUCTION

Carotenoids have several functional benefits for human body. Carotenoids have roles in epithelisation process, influencing cell progression of the fibroblast, antioxidant, in protecting agent of UV radiation and decreasing the skin cancer risk. In addition, some types of carotenoids have a role as provitamin A [1]. However carotenoids are susceptibly degraded by harmful conditions, i.e. light radiation, high

Manuscript received August 5, 2017; revised November 8, 2017. This project was supported by the Indonesian Ministry of Research, Technology, and Higher Education through the National Innovation System Research Grant (IRPI-2017), IbIKK Community Service Grant (No. 101/SP2H/PPM/DRPM/IV/2017), and National Strategic Excellent Research (PUSNAS) Grant (No. 120/SP2H/LT/DRPM/IV/2017). The authors wish to thank Prof. Yuzo Shioi (Shizuoka University, Japan) for his valuable comments and critical reading of the paper.

Naomi M. Mulyadi, Tri D. Widyaningsih, and Novita Wijayanti are with the Department of Agricultural Product Technology, Brawijaya University, Malang, Indonesia.

Renny Indrawati and Heriyanto are with Ma Chung Research Center for Photosynthetic Pigments (MRCPP) and Chemistry Study Program, Universitas Ma Chung, Malang, Indonesia.

Leenawaty Limantara is with Ma Chung Research Center for Photosynthetic Pigments (MRCPP), Universitas Ma Chung, Malang, Indonesia and Center for Urban Studies, Universitas Pembangunan Jaya, Jakarta, Indonesia (email: leenawaty.limantara@upj.ac.id).

temperature, and the presence of acid or oxygen. These conditions may degrade their quality on disappearance of color, rancidity and decrease in bioactivity and food functional roles [2].

Some protecting techniques have been explored to protect pigments from the degradation. Encapsulation is a common way that protects bioactive molecules by entrapping them into other substances and also that changes the size of particles into nano- or microparticles. Microencapsulation is encapsulation which produces micro particles (1  $\mu\text{m}$  to 1000  $\mu\text{m}$ ) [3]. Microencapsulation has been applied in some kind of food products and usually uses spray-drying (high temperature) as a drying method while microencapsulation conducted by freeze dryer is still rare. The Freeze drying method produces the best quality for final product and does not change the bioactive composition in food because it uses low temperature. Suitable coating agents are needed in the encapsulation process, because the coating agents give protecting barrier to the bioactive compounds. Chitosan and sodium alginate are two kinds of coating agents that have been used for microencapsulation in pharmacy. These two agents give a good synergy in forming transparent, flexible, and strong film, and have high tensile strength [4], [5]. Preparation of microcapsule via emulsification with biopolymer combined with freeze drying technology is known to produce microspheres, having a particle size ranging between 20  $\mu\text{m}$  and 5 000  $\mu\text{m}$  [5].

Kabocha pumpkin (*Cucurbita maxima*) Duchesne is a potential carotenoids source. Kabocha has higher carotenoids content ( $285.91 \text{ mg} \cdot 100 \text{ g}^{-1}$ ) than local pumpkins ( $26.62 \text{ mg} \cdot 100 \text{ g}^{-1}$ ) [6]. In present study, the microencapsulation process of carotenoids from kabocha was conducted by freeze dryer. The best proportion of chitosan-sodium alginate-sodium tripolyphosphate (STPP) as coating agents of microencapsulated carotenoids would be chosen. The addition of different carotenoid concentrations was evaluated to determine microcapsules characteristics, such as color properties and encapsulation efficiency. The final product of microencapsulated kabocha carotenoids can be utilized as natural carotenoid powder with high stability.

## II. MATERIALS AND METHODS

### A. Materials and Reagents

Kabocha and sunflower oil (Golden Bridge, Malaysia) were purchased from Lai-Lai Fruit Market (Malang, Indonesia). Chitosan and Sodium Tripolyphosphate (STPP) (Changzhou Kamadi Trading Co., Ltd, Changzhou, China), sodium alginate (Qingdao Hyzlin Biology Development, China), tween 80 (Sigma Aldrich, St. Louis, United States), demineralized water with resistivity  $100 \times 10^4 \Omega \text{ cm}$ ,  $\text{N}_2$  gas (UHP grade, PT Samator, Surabaya, Indonesia) were used directly. Glacial

acetic acid, acetone, *n*-hexane are an analytical grade from Merck (Darmstadt, Germany).

### B. Sample Preparation

The fruit of Kabocha pumpkin was separated from the peel and then cut into small pieces. The pumpkin fruit was dried by a vacuum oven (VO-200, Memmert, Schwabach, Germany) at 50 °C and 2 mbar for 24 h. The dried fruit was ground using a grinder (M20, IKA-Werke, Selangor, Malaysia). The pumpkin powders were kept inside a desiccator in dark condition for future analysis.

### C. Carotenoids Extraction, Formulation of Coating Agents, and Stability Test in Emulsion System

Carotenoids were extracted from 20 g of dried kabocha powders with 30 mL of *n*-hexane by stirring for 40 min and then filtered through a filter paper. The extraction was repeated 2 times under a red light. The carotenoid extracts were dried by evaporation (Eyela SB-1100 rotary evaporator, Tokyo Rikakikai Co. LTD, Japan) and continued by the stream of nitrogen gas. The dried carotenoid extracts were kept at -30 °C.

Microencapsulation agents were comprised of sodium alginate, chitosan and STPP mixture (ACT) in 5 formulations (Table I). The microparticles with the ACT1 formulation were prepared by adding 96 mL of chitosan (2%, w/v) into 19.2 mL of sodium alginate solution (1%, w/v) and followed by addition of 4.8 mL of STPP solution (0.5%, w/v) and 0.96 mL of acetic acid. This mixture was homogenized three times by a UltraTurax Homogenizer T-18 (IKA) at 15 000 rpm for 5 min (1 rpm = 1/60 Hz). After storage at -15 °C for 24 h, the mixture was then lyophilized at -47 °C for 24 h by a freeze dryer (Labconco, Kansas City, USA). Other formulations of coating agents were prepared with the same manner as described above.

TABLE I: FORMULATIONS OF COATING AGENTS IN 120 G OF DEMINERALIZED WATER

Formula	Sodium alginate (1)		Chitosan (2)		STPP (3)		Mass Ratio of 1:2:3 (w/w/w)
	%	V	%	V	%	V	
ACT1	1.0	19.2	2.0	96.0	5.0	4.8	0.19:1.92:0.24
ACT2	2.0	37.5	4.0	75.0	2.0	7.5	0.75:3.00:0.15
ACT3	5.0	40.0	5.0	80.0	0.0	0.0	2.00:4.00:0.00
ACT4	2.0	40.0	2.0	80.0	0.0	0.0	0.80:1.60:0.00
ACT5	1.0	60.0	1.0	60.0	0.0	0.0	0.60:0.60:0.00

% = percentage (w/v); V = volume in mL; w = mass in g

Approximately 0.02 g of the dried carotenoid was dissolved in 0.2 mL of acetone and then titrated with 9.8 mL of acetic acid solution in different pH (pH 3 and pH 4) containing a Tween 80 solution (0.1%, w/v). The stability of the carotenoids was observed by recording the absorption spectrum in this emulsion at 0 min, 45 min, 100 min, and 150 min using 1700 UV-Vis Spectrophotometer (Shimadzu, Kyoto, Japan). The dried carotenoids in 10 mL of acetone were used as the control sample.

### D. Microencapsulation of Carotenoids

Preparation of carotenoids in emulsion system was adapted from the method of [7], while the microencapsulation of carotenoids was performed according to the method published elsewhere [8] with the slight modifications. Initially, the dried

carotenoids in the different masses were dissolved in trace amount of acetone (0.5 mL) and sunflower oil (1.5 mL) (the range of carotenoid concentration was 0.5 – 3.0%, w/v) and then added with Tween 80 (0.5 g) and sodium alginate (1%) in 19.2 mL of demineralized water. This emulsion was then homogenized at 1 500 rpm for 5 min. The carotenoid emulsion was mixed with chitosan (2%) in 96 mL of demineralized water and homogenized at 15 000 rpm for 1 min. Afterward STPP (5%, 4.8 mL) and acetic acid (2 mL) were added to this solution. The homogenization was continued for 5 min. To separate microencapsulated carotenoids from acidified water, the homogenized solution was centrifuged (Kubota, Tokyo, Japan) at 11 500 rpm and at 4° C for 20 min. The pellet of microencapsulated carotenoids was collected and stored at -15 °C for 24 h. The lyophilized process of microencapsulated carotenoids was performed by using a Freeze dryer (Labconco) at -47 °C for 24 h. The freeze-dried product was crushed in a mortar and sieved by a standard sieve (80 mesh).

### E. Characterization of Microcapsules

Microcapsules (0.001 g) were extracted with a mixture of acetone and water solution (8:2, v/v) and then centrifuged at 10 000 rpm for 15 min. The supernatant was then partitioned with *n*-hexane and the hexane layer was dried under the stream of nitrogen. The dried carotenoid extract was then re-dissolved in *n*-hexane and an absorption spectrum was recorded in the range of 250 – 600 nm. The efficiency of microencapsulation was then calculated based on the ratio of the absorption at the position of absorption maximum between the microencapsulated carotenoids and initially added carotenoids.

The L\*, a\*, and b\* values of the microcapsules were recorded by a Colorflex EZ (Hunter Associates Laboratory, Inc., Reston, USA). The hue and chroma values were also calculated. Total carotenoids and pro-vitamin A were estimated based on Gross formula [9] and NAS-NRC [10], respectively.

### F. Data Analysis

A SPSS 21 program with One-Way ANOVA (95%) and Duncan's Multiple Range Test was used for the statistical analysis.

## III. RESULTS AND DISCUSSION

### A. Determination of the Best Formula for Coating Agents

The composition of the coating agents is important for the final product. A high amount of sodium alginate produces a spongy structure due to the property of sodium alginate as a gel. Alginate contains gulunorat (G) and manuronat chains which the G chain will affect in the formation of gel [11]. The physical characteristics of formulations without the addition of STPP (ACT3, ACT4, and ACT5) revealed the sponge structure and formation of aggregates in the powders (Figure not shown). In addition, the moisture contents of these powders were higher than 10%. On the other hand, formulations with STPP (ACT1 and ACT2) produced dry and soft powders with lower moisture contents (less than 8%). However, the powders from the formulation of ACT2 were formed some aggregates with a sponge-like structure. Among 5 formulations tested, therefore, the best formulation of

coating agents was ACT1 in the following composition: sodium alginate: chitosan: STPP: demineralized water = 0.19 g:1.94 g:0.20 g:120 g. Besides the formulation, the process of microencapsulation is determined by the speed and duration of homogenization process, and other continuous procedures, i.e. centrifugation. Addition of ionic agent, such as STPP, can create cross interaction and improve the characteristic of the powder. STPP also facilitates chitosan to build crosslink with itself and addition of sodium alginate acts as a filler to strengthen the structure [8].

### B. Stability Test of Carotenoids

The solution used for the microencapsulation was found to have low pH with a range of pH 3.6 to pH 4.0, therefore, a stability test on carotenoids was needed to ensure the formulation. The stability of kabocha carotenoids in the emulsion system with different pH was evaluated from their absorption spectra (Fig. 1). The absorption of carotenoids in acetone as a control (Fig. 1 a) showed a slight increase in the intensity due to evaporation of acetone during measurements.

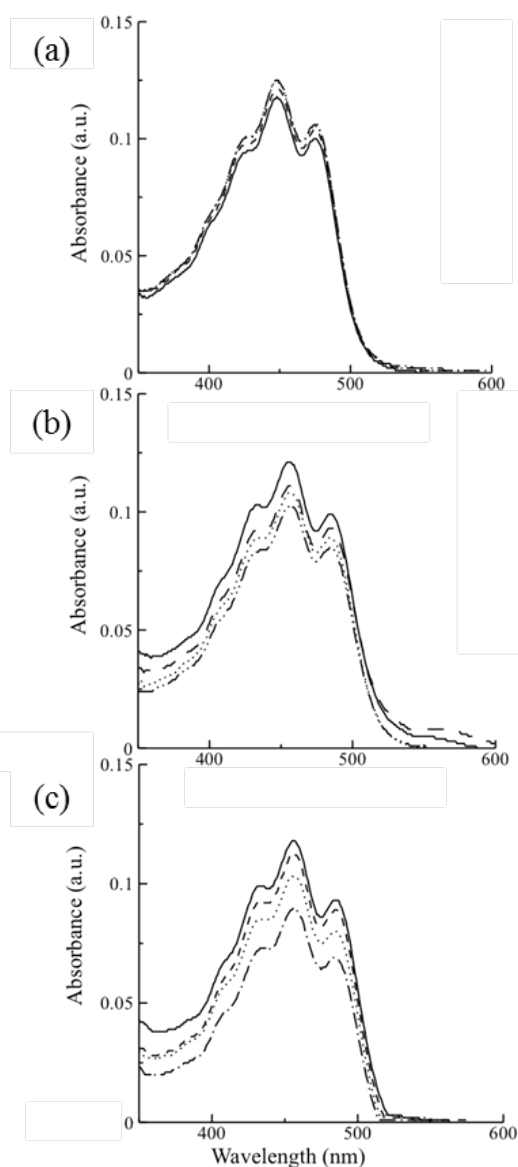


Fig. 1. Absorption spectra of kabocha carotenoids in acetone (a), emulsion systems at pH 4 (b) and pH 3 (c) incubated at room temperature for 0 min (—), 45 min (---), 100 min (.....) and 150 min (-.-.-).

In the emulsion with a low pH, it was shown that the

carotenoid spectra decreased in the intensity. After 150 min the absorbance of carotenoids has decreased to 18.8% and 15.2% in the emulsion with pH of 3 and 4, respectively. Based on the stability test, the maximum processing time for microencapsulation of carotenoids was set to be 60 min which least affects the carotenoid stability of 7.8% for both pH.

In Fig. 1, the spectra of carotenoids dissolved in acetone solution have 3 bands with absorption maxima at 424 nm, 448 nm, and 474 nm. In the emulsion system, the bands were red-shifted to about 6 nm to 8 nm. This shift is due to the aggregation process of carotenoids with their environment and it is usually called as a J-aggregation. Previously it was reported that a bathochromic shift of carotenoids occurred because of the interaction of carotenoids with the surfactants that produces an aggregate [12]. In the case of fucoxanthin, the presence of water caused the aggregation of fucoxanthin in acetone solution which shows the bathochromic shift up to 7 nm [13]. It was suggested that the presence of water in carotenoid solution might cause aggregation of carotenoids because there is a strong hydrophobic tensile strength [14].

### C. Characterization of Microencapsulated Carotenoids

The microencapsulated carotenoid powders have low moisture contents in the range of 5.41% to 7.08%. The moisture contents of the microencapsulated kabocha carotenoids were in line with the results reported before [15]. Moisture contents of microencapsulated powders dried by different methods of spray-freeze drying, freeze-drying, and spray-drying were 4.15% to 6.63%, 6.7% to 6.99% and 3.56% to 6.40%, respectively [15].

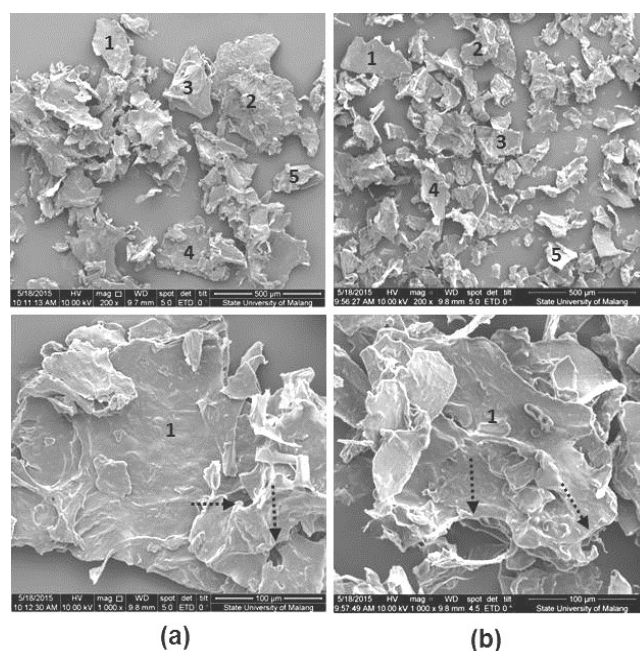


Fig. 2. SEM images of the empty microcapsules of ACT1 formulation (a) and the carotenoid-filled microcapsules with the addition of 3% carotenoids (b) observed at magnifications of 200 times (above) and 1000 times (below). Five specimens indicated with the numbers were used for calculating the average of diameter of microcapsules and the arrow indicates a porous structure of microcapsules.

SEM images of microcapsules depict the morphological characteristics of microparticles. The microencapsulated carotenoid powders have smaller diameter than that of empty one (Fig. 2, 200 times magnification). The large diameter of the empty microcapsules might be affected by the overlapped

powders during the SEM analysis and also the microcapsules have not been sieved. The average diameters of the empty and carotenoid-filled microcapsules were 337.88  $\mu\text{m}$  and 214.26  $\mu\text{m}$ , respectively, indicating that microencapsulation process has produced the micro-scale particles. Reference [5] revealed that microencapsulation by a freeze drying method produces a varied particle size of around 20 - 5000  $\mu\text{m}$ .

At the magnification of 1000 times (Fig. 2, below), carotenoid-filled microcapsules appeared a rougher surface than the empty microcapsules. It is suggested that the pigment has been entrapped to the coating agents. Other characteristics of microcapsules were irregular shape with porous and slab features and a variation in particle size probably due to the sample preparation during freeze drying and crushing steps. These SEM results were in agreement with other study by [16]. The morphology of freeze dried microcapsules was irregular shape having a slab-like structure. These morphological features came from the freeze dried matrix subjected to crush by mortar.

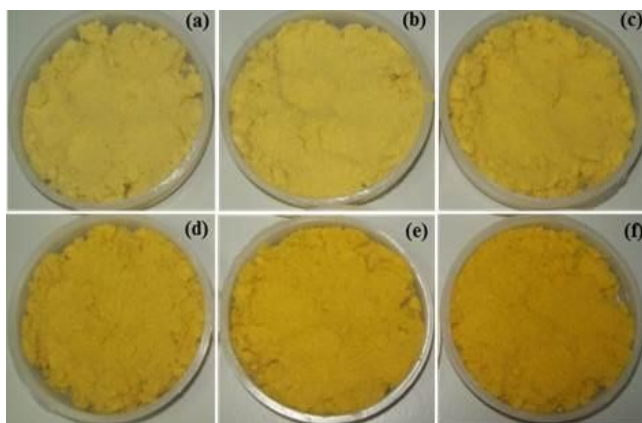


Fig. 3. Microencapsulated carotenoids powder with the ACT1 formulation using different addition of carotenoid concentrations, i.e. 0.5 % (a), 1.0 % (b), 1.5 % (c), 2.0 % (d), 2.5 % (e) and 3.0 % (f).

Color of the microencapsulated carotenoid powders was visually seen in the range from yellow to orange (Fig. 3). The addition of carotenoids significantly affected to the color change of the microencapsulated carotenoid powders. Table II summarizes color values, i.e.  $L^*$ ,  $a^*$ ,  $b^*$ ,  $C^*$  and  $^{\circ}\text{Hue}$ , from the samples. The positive correlations of  $a^*$ ,  $b^*$  and  $C^*$  with the amount of added carotenoids were seen because of increment of carotenoid concentration, while  $L^*$  and  $^{\circ}\text{Hue}$  gave a negative correlation. The results of color measurement were in agreement with the literatures [17], [18]. A study has reported that  $L^*$  value had a negative correlation to the addition of pigment, because higher pigment content will increase the darkness of sample as a consequence on decrease in  $L^*$  value. An  $L^*$  value had a strong correlation with the total carotenoids, whereas  $b^*$  and chroma values had a moderate correlation with total carotenoids and had a strong correlation with the increase in lutein. The degree of hue value had a negative correlation with total carotenoids [17]. Other report showed that  $a^*$ ,  $b^*$ , and  $C^*$  values also have a positive correlation with  $\beta$ -carotene content and total carotenoids [18].

Total carotenoids and pro-vitamin A of microencapsulated carotenoids powder increased with the increase in the carotenoid concentrations (Table III). Reference [9] reported the daily need for vitamin A in a man is 1 000 RE 8. It means that by consuming about 100 g of microencapsulated

carotenoids (the addition 2.5 % and 3.0 % carotenoids), it may fulfil the daily need for vitamin A. Based on SNI 7709–2012, maximum fortification of vitamin A to the vegetable oil is 45  $\text{IU}\cdot\text{g}^{-1}$ . The addition of 1.05 g to 4.20 g of the microencapsulated carotenoids to 1 g of vegetable oil is enough to achieve the standardization of food fortification. The increase in carotenoid concentration added in microencapsulation process caused the decrease in efficiency. Table III summarizes the percentage of encapsulation efficiency with the addition of several portions of carotenoids. This result showed the same trend with other reports. Reference [19] concluded that the loading carotenoids with high concentration did not provide better encapsulation efficiency. This phenomenon was also observed in other polymeric matrices that over loading of encapsulated materials caused some decrease in the encapsulation efficiency [20].

TABLE II: CHROMATIC VALUES OF THE MICROENCAPSULATED CAROTENOIDS FROM KABOCHA POWDERS WITH ACT1 FORMULATION

% Carotenoids (w/v)	$L^*$	$a^*$	$b^*$	$^{\circ}\text{Hue}$	$C^*$
0.5	76.21 $\pm 2.14^a$	3.64 $\pm 0.62^a$	48.91 $\pm 2.26^a$	85.76 $\pm 0.62^a$	49.05 $\pm 2.28^a$
1.0	76.61 $\pm 0.46^a$	7.85 $\pm 0.92^b$	60.33 $\pm 3.57^b$	82.59 $\pm 0.78^b$	60.84 $\pm 3.60^b$
1.5	74.74 $\pm 0.86^{ab}$	9.25 $\pm 0.35^c$	65.74 $\pm 3.39^c$	81.97 $\pm 0.66^b$	66.39 $\pm 3.31^c$
2.0	72.77 $\pm 0.60^b$	10.19 $\pm 0.10^c$	69.99 $\pm 3.33^d$	81.70 $\pm 0.36^{bc}$	70.73 $\pm 3.30^d$
2.5	70.34 $\pm 2.57^c$	11.66 $\pm 0.43^d$	72.34 $\pm 1.14^e$	80.85 $\pm 0.23^c$	73.28 $\pm 1.18^{de}$
3.0	70.34 $\pm 1.21^c$	14.02 $\pm 1.17^e$	74.69 $\pm 1.20^f$	79.37 $\pm 0.87^d$	76.00 $\pm 1.21^e$
Y	-1.49x + 78.72	1.84x + 3.00	4.83x + 48.42	-1.07x + 85.78	5.04x + 48.41
$R^2$	0.96	0.94	0.90	0.88	0.91

\*Means  $\pm$  SD. The difference notation shows that the data are significantly different at  $p \geq 0.05$ .

TABLE III: TOTAL CAROTENOIDS, PROVITAMIN A, AND MICROENCAPSULATION EFFICIENCY OF THE MICROENCAPSULATED CAROTENOIDS FROM KABOCHA POWDERS WITH THE ACT1 FORMULATION

% Carotenoids (w/v)	Total Carotenoids ( $\mu\text{g} \cdot \text{g}^{-1} \text{dw}^*$ )	Total Provitamin A		% Efficiency*
		RE/100 g dw*	IU/100 g dw*	
0.5	117.98 $\pm 10.41^a$	321.90 $\pm 28.39^a$	1 073.00 $\pm 94.64^a$	90.86 $\pm 6.17^a$
1.0	150.00 $\pm 11.70^b$	474.14 $\pm 36.99^b$	1 580.47 $\pm 123.28^b$	83.37 $\pm 7.82^{ab}$
1.5	207.38 $\pm 18.00^c$	691.03 $\pm 59.97^c$	2 303.42 $\pm 199.92^c$	78.20 $\pm 2.93^b$
2.0	235.51 $\pm 24.06^d$	822.68 $\pm 84.03^d$	2 742.26 $\pm 280.10^d$	62.51 $\pm 4.68^c$
2.5	279.17 $\pm 13.47^e$	1 045.88 $\pm 50.47^e$	3 486.27 $\pm 168.23^e$	58.55 $\pm 5.68^c$
3.0	318.29 $\pm 24.64^f$	1 287.00 $\pm 99.64^f$	4 290.01 $\pm 332.15^f$	54.72 $\pm 3.36^c$
0.5	117.98 $\pm 10.41^a$	321.90 $\pm 28.39^a$	1 073.00 $\pm 94.64^a$	90.86 $\pm 6.17^a$
1.0	150.00 $\pm 11.70^b$	474.14 $\pm 36.99^b$	1 580.47 $\pm 123.28^b$	83.37 $\pm 7.82^{ab}$

\*Means  $\pm$  SD. The difference notation shows that the data are significantly different at  $p \geq 0.05$ .

The centrifugation process also caused the decreasing in

microencapsulation efficiency. It was estimated that some pigments having high polarity were soluble in aqueous solution and dissolved into the supernatant. HPLC analysis was performed on microencapsulated carotenoid powders and the supernatant after centrifugation [21]. The results showed that the polar carotenoids, i.e., antheraxanthin, lutein, and zeaxanthin were present in higher amount in the supernatant than non-polar carotenoids such as  $\alpha$ - and  $\beta$ -carotene (1.1 to 1.9 times), while in the microencapsulated carotenoid powders, the relative concentration of non-polar carotenoids was 1.5 to 4.4 times higher than that of polar carotenoids. This result proved the loss of polar carotenoids in the supernatant during the centrifugation process. Centrifugation process is commonly used to separate bioactive compounds which have been entrapped into coating agents from untrapped one [8].

#### IV. CONCLUSION

Kabocha carotenoids can be entrapped with 2% chitosan, 1% sodium alginate and 5% STPP (1.92 g : 0.19 g : 0.24 g, w/w/w) to have a better microencapsulated products. The empty and carotenoid-filled microcapsules have an irregular shape, stable and porous structures, microsphere size with the average diameters between 214.26  $\mu\text{m}$  and 337.88  $\mu\text{m}$ . The concentration of carotenoids added to the microencapsulation influences the micro encapsulation efficiency, color values, total carotenoids and also provitamin A.

#### REFERENCES

- [1] A. C. Pinteá, B. S. Andrei, and C. Socaciu, "HPLC analysis of carotenoids in four varieties of *Calendula Officinalis* L. flowers," *Acta Biologica Szegediensis*, vol. 47, pp. 37–40, September 2003.
- [2] C. S. Boon, D. J. McClements, J. Weiss, and E. A. Decker, "Factors influencing the chemical stability of carotenoids in foods," *Critical Reviews in Food Science and Nutrition*, vol. 50, pp. 515–532, June 2010.
- [3] M. N. Singh, K. S. Y. Hemant, M. Ram, and H. G. Shivakumar, "Microencapsulation: A promising technique for controlled drug delivery," *Research in Pharmaceutical Sciences*, vol. 5, pp. 65–77, July 2010.
- [4] E. Rudnik, *Compostable Polymer Material*, Netherland: Elsevier, 2008.
- [5] N. J. Zuidam and E. Shimoni, "Overview of microencapsulates for use in food products or processes and methods to make them," in *Encapsulation Technologies for Active Food Ingredients and Food Processing*, N. J. Zuidam, Nedović, V. A., ed. New York: Springer, 2010.
- [6] S. R. Kim, T. Y. Ha, H. N. Song, Y. S. Kim, and Y. K. Park, "Comparison of nutritional composition and antioxidative activity for Kabocha squash and pumpkin," *Korean Journal of Food Science and Technology*, vol. 4, pp. 171–172, 2005.
- [7] W. Klaypradit and Y. W. Huang, "Chitosan-based encapsulation for tuna oil," Ph.D dissertation, The University of Georgia, Georgia, 2006.
- [8] S. Purwatiningsih, L. Ambarsari, Y. A. Sari, and Y. Nugraha, "Ketoprofen encapsulation optimization with chitosan-alginate cross-linked with sodium tripolyphosphate and its release mechanism determination using in vitro dissolution," *International Journal of Recent Research and Applied Studies*, vol. 14, pp. 141–149, 2013.
- [9] J. Gross, *Pigments in Vegetable: Chlorophylls and Carotenoid*, New York: Van Nostrand Reinhold, 1991.
- [10] NAS-NCR, *Recommended Dietary Allowances*, 8th ed. Washington D.C.: Food and Nutrition Board, 1974.
- [11] I. Donati, S. Holtan, Y. A. Mørch, M. Borgogna, M. Dentini, and G. Skjåk-Bræk, "New hypothesis on the role of alternating sequences in Calcium-alginate gels," *Biomacromolecules*, vol. 6, pp. 1031–1040, January 2005.
- [12] C. H. Lan, R. Fougere, and Y. Wache, "Increase in stability and change in supramolecular structure of  $\beta$ -karoten through

- encapsulation into polylactic acid nanoparticles," *Food Chemistry*, vol. 124, pp. 42–49, January 2011.
- [13] Heriyanto and L. Limantara, "Photo-stability and thermo-stability studies of fucoxanthin isomerization," *Proceedings of Natural Pigments Conference for South East Asia*, ed. L. Limantara, Heriyanto, E. Sadtono, pp. 73–78, 2010.
- [14] R. Giovannetti, L. Alibabaei, and F. Pucciarelli, "Kinetic model for astaxanthin aggregation in water-methanol mixtures," *Spectrochimica Acta Part A*, vol. 73, pp. 157–162, July 2009.
- [15] S. Y. Hundre, P. Karthik, and C. Anandharamkrishnan, "Effect of whey protein isolate and  $\beta$ -cyclodextrin wall system on stability of microencapsulated vanillin by spray-freeze drying method," *Food Chemistry*, vol. 174, pp. 16–24, May 2015.
- [16] S. Tandale, "Microencapsulation of vitamin C and garlic acid in whey protein concentrate by spray and freeze drying—Characterization and degradation kinetics," M.S. thesis, The University of Georgia, Georgia, 2007.
- [17] R. A. Itle and E. A. Kabelka, "Correlation between  $L^*a^*b^*$  color space values and carotenoid content in pumpkins and squash (*Cucurbita* spp.)," *Horticultural Science*, vol. 44, pp. 633–637, June 2009.
- [18] A. Seroczyńska, A. Korzeniewska, J. Sztangret-Wisniewska, K. Niemirowicz-Szczytt, and M. Gajewski, "Relationship between carotenoids content and flower or fruit flesh colour of winter squash (*Cucurbita maxima* Duch.)," *Folia Horticulturae*, vol. 18, pp. 51–61, April 2006.
- [19] P. Thamaket and P. Raviyan, "Preparation and physical properties of carotenoids encapsulated in chitosan cross-linked tripolyphosphate nanoparticles," *Food and Applied Bioscience Journal*, vol. 3, pp. 69–84, 2015.
- [20] N. Liu and H. J. Park, "Chitosan coated nanoliposome as vitamin E carrier," *Journal of Microencapsulation*, vol. 26, pp. 235–242, April 2009.
- [21] N. M. Mulyadi, "Identifikasi, komposisi, kandungan dan mikroenkapsulasi karotenoid kabocha (*Cucurbita maxima* L.) menggunakan kitosan-sodium alginat-STPP [Identification, composition, content and microencapsulated carotenoids of kabocha (*Cucurbita maxima* L.) using chitosan-sodium alginate-STPP]," Undergraduate thesis, Universitas Brawijaya, Malang, 2015.



**Naomi Megananda Mulyadi** was born in Tulungagung, Indonesia, on 30 January 1993. She graduated with honor from Brawijaya University, Indonesia, in 2015, obtained bachelor degree in food technology. She was interested on biochemistry, food analysis, as well as new product development. She has started to be an entrepreneur in food manufacture.



**Tri Dewanti Widyaningsih** was born in Yogyakarta, Indonesia, in 1961. She received bachelor degree in food processing from Gadjah Mada University, Yogyakarta, Indonesia, in 1985, master degree in community nutrition and doctoral degrees in functional food from Airlangga University, Surabaya, Indonesia in 1998 and 2011, respectively.

In 1998, she joined the Department of Agricultural Technology, Brawijaya University as a lecturer. Her current research interests include diet nutrition, functional food, bioactive compound, herbal supplement, food immunology, and food metabolism. She has been published a journal in *Journal of Food and Nutrition Research*, *International Journal of PharmTech Research*, *Food and Agricultural Immunology*, etc.

Dr. Widyaningsih was the head of food nutrition laboratories in the Department of Agricultural Technology, Brawijaya University, Indonesia. She was the recipient of Satyalancana Karya Satya awards, excellent lecturer awards, prospective innovation awards, and granted a patent (HAKI) for the grass jelly derivative product in the last ten years.



**Novita Wijayanti** was born in Jember, Indonesia, in 1980. She received bachelor and master degree in science and food technology from the Brawijaya University, Indonesia, in 2004 and 2013, respectively. Her major field of study is agricultural product technology and biotechnology of agroindustry.

In 2012, she joined the Department of Agricultural Technology, Brawijaya University as a lecturer. Her

current research interests include product development, functional food, dietary supplements, food chemistry, food serving management, physiology and metabolism of nutrients. She has been published a journal in national and international level.



**Renny Indrawati** was born in Malang, East Java, Indonesia, on 29 May 1986. She received the undergraduate degree (bachelor in food technology) with a cum laude honor from Brawijaya University, Indonesia, in 2008. She began her career in research by joining Ma Chung Research Center for Photosynthetic Pigments (MRCPP) as a research assistant in 2009, and she is deeply interested in the development of functional food related to natural pigments. In 2011, she graduated with a summa cum laude honor from Satya Wacana Christian University, Indonesia, majored in Chlorophyll and Carotenoid. She subsequently finished the second master degree by research (master of international natural science) in 2012 at Kwasei Gakuin University, Japan.

Currently, she is a researcher at MRCPP as well as a lecturer assistant at Chemistry Study Program, Universitas Ma Chung, Indonesia. She has been involved in some prestigious national research grants, such as excellent research on national strategy, competitive research grant, and national innovation system research grant. her current research interest lies in the fabrication and stability studies of functional food colorants from natural resources.

Ms. Indrawati is an author of Indonesian peer-reviewed papers as well as several international publications. She has been awarded for a double degree scholarship by Indonesian Government to pursuit her graduate study for two years and a half. She received the award as one of the best presenters in Natural Pigments Conference for South-East Asia in three consecutive years.



**Heriyanto** received his B.Sc in chemistry from Satya Wacana Christian University, Indonesia, in 2004. In 2008 and 2009, He obtained M.Sc. as a double degree program in Biology from Satya Wacana Christian University, Indonesia and in Chemistry from Kwasei Gakuin University, Japan. Currently, he is a Ph.D student in the Faculty of Biochemistry, Biophysics and Biotechnology, Jagiellonian University, Poland.

He worked as a research assistant from 2004 to 2009 and then continues his work as a researcher at Ma Chung Research Center for Photosynthetic Pigments (MRCPP), Universitas Ma Chung, Indonesia. Since 2015, he has been invited as a lecturer in the Department of Chemistry, Universitas Ma Chung, Indonesia. He has an experience in the analysis of natural pigments for almost 14 years. His research interests include pigment analysis, analytical chemistry, spectroscopy and chromatography, as well as biochemistry of photosynthetic pigments.



**Leenawaty Limantara** finished her graduate study in Kwasei Gakuin University, Japan, majored in the physical chemistry related to photosynthetic pigments in light harvesting antenna. She has been involved in several post-doctoral research in Japan, United States, United Kingdom, and Germany.

She is an invited lecturer and principal investigator in Ma Chung Research Center for Photosynthetic Pigments, Universitas Ma Chung. She has been engaged in many studies related to chlorophyll since 1991 and received many research grant from both national and international institution. Currently, she is the rector of Universitas Pembangunan Jaya, Jakarta, Indonesia

Dr. Limantara has published her work in many international journals, chapter of book, review, and national peer reviewed journal. She is the founder as well as chairwoman of the Association of Pigment Researchers in Indonesia. She is also the first Indonesian ambassador scientist for the Alexander von Humboldt Foundation, Germany.

# **Polymer Chemistry**



# Physical Effects of Pre-hydrolysis and Alkali Treatment of Empty Fruit Bunch (EFB) Fibers

Mohammad Aliff Shakir, Mohd Firdaus Yhaya, and Mardiana Idayu Ahmad

**Abstract**—This study focused on the physical effects of pre-hydrolysis and alkali treatment of empty fruit bunch (EFB) fibers collected from one of oil palm industry in Penang Malaysia. The pre-hydrolysis times used were 20 min, 40 min, 60 min, and 80 min. While for alkali treatment, duration of 2 hours was applied by using 17%, 22%, 27% and 32% of sodium hydroxide (NaOH) treatment. From this study it was found that the amount of extractives being removed was increased with the increasing of time, while the hemicellulose content was decreased. In addition, lignin content was reduced when high concentration of alkali charge was used. Moreover, the longer the pre-hydrolysis time, the greater the loss of hemicellulose, which subsequently increased the size of capillary. Also, gradual removal of lignin during the pulping process caused reduction of fiber length and pore structures in the fibers. Thus it can be said, from this study continuous treatment (pre-hydrolysis and alkali treatment) was found to increase the performance of the fibers up to a certain limit before declining.

**Index Terms**—Pre-hydrolysis, alkali treatment, empty fruit bunch fibers, hemicellulose, lignin.

## I. INTRODUCTION

Oil palm is one of the important productions which was introduced to Southeast Asia such as Malaysia and Indonesia by European traders in the early 19<sup>th</sup> century [1]. The production of oil palm in this region has helped to change its agriculture and economy scenarios [2]. In this production, huge amount of biomass waste [3] in the form of empty fruit bunches (EFBs), oil palm trunks (OPT), oil palm fronds (OPFs), palm pressed fibers (PPFs) and palm shells are produced [4]. EFBs are available in abundance as fibrous material in which there is 230-250kg EFBs in 1000 kg of freshly fruit bunch. EFBs consist of 41.3-45% cellulose, 25.3-33.8% hemicellulose, and 27.6-32.5% lignin [3], [5]. From this, we can see that the most significant material in EFBs is cellulose, which has gained great interest amongst researchers and industries. This material can be converted into value-added products and other potential applications in chemical, food, and composite industries.

Cellulose is an abundant biopolymer which formed by the combination of multiple glucose monomer at  $\beta$ -1, 4 glycosidic bond [1]. Cellulose can be found as intertwined microfibrils in the cell wall of plants to reinforce the plant by giving mechanical strength [2]-[4]. It has 39% of amorphous

structure that may contribute to water absorption and 61% crystalline structure [5]. The drawback of using cellulose in order to isolated crystalline region usually using acid hydrolysis in order to remove amorphous region [6], [7]. Hemicellulose is a combination of many types of cyclic saccharides such as xylose, mannose, and glucose. It consists a highly branched random structure which mainly from amorphous region [3]. Hemicellulose is soluble in hot water and attached to cellulose by hydrogen bond. So, by removing hemicellulose, it may cause physical changes of fibers which led the fiber to have less dense and rigidity that will influence moisture absorption [8].

Lignin is formed by a repeating unit of phenyl-propane units from an amorphous region consisting of aromatic units such as guaiacyl, syringyl and phenylpropane [3]. The lignin behavior during any chemical treatment could not be easily accessed or degraded due to the presence of strong carbon-carbon linkages and other chemical groups such as aromatic groups [12]. Thus lignin acts as a matrix of a fiber material which connects cellulose and hemicellulose together [9], [10]. Thus, by removing the lignin, blockage will be discarded and would produce higher pore structures in fiber. This factor also will allow water molecule to transfer in short time with less resistance.

Due to the important roles of these substances, many analyses are conducted in the efforts to convert EFB fibers into value-added products. Previous research reported that, the high purity unbleached cellulose pulp could be obtained from EFB via pre-hydrolysis treatment and soda pulping [11]. Pre-hydrolysis is a water treatment process that usually applied before pulping process. The mechanism involves steam power, where the fibers is pressurized at high pressure and high temperature in digester. At this point, hemicellulose in the fibers will be hydrolyzed, lignin will be modified, increasing access to surface area, decreasing the crystallinity of the cellulose and its degree of polymerization [12], [13]. For lignin removal, the process will take place during pulping process. Pulping process involves alkali treatment where the lignin would be extracted from the fibers. There are few pulping methods to remove lignin in fibers such as mechanical pulping and chemical pulping. Mechanical pulping uses mechanical force in order to separate and break bonding between fibers until they fragment. So, the main objective of mechanical pulping is to maintain some part of lignin in order to achieve high yield production. However, mechanical pulping has low aging resistance where it has a tendency to discolor. Meanwhile chemical pulping uses alkali treatment

Manuscript received August 15, 2017; revised November 15, 2017.

Mohammad Aliff Shakir, Mohd Firdaus Yhaya, and Mardiana Idayu Ahmad are with the Universiti Sains Malaysia, Malaysia (e-mail: {alip6001, laxmia707, drmia707}@gmail.com).

such as sodium hydroxide and sodium sulphite. In this process, the fiber is cooked in digester at high temperature and high pressure. This is intended to dissolve the lignin. In this treatment, the usage of higher concentration of alkali treatment will result in more lignin to be removed. However, it might cause cellulose degradation which will shorten the fiber length. By comparing both method, chemical pulping able to give better quality in optical and mechanical properties compared to mechanical pulping [14].

Removing hemicellulose through pre-hydrolysis contributes to enlarge capillary spaces in the fiber. It helps to improve the capillary action of fiber during water absorption. Capillary action is an ability of a fluid to flow in narrow spaces without any external assistance forces. In order to achieved equilibrium balance, the capillary action able to lift up and transfer the liquid into material even against gravity [15]. The speed of absorption and the forces for lifting the liquid against gravity are depending on the diameter of capillary [16], [17]. Previous study showed that the chemical composition such as hemicellulose and lignin affected the diameter of capillary and porosity of the fiber [8]. Throughout the literature, it can be seen that the understanding of chemical composition helps to improve fibers for future application. Thus, this work was performed to study the chemical composition of EFB fibers using pre-hydrolysis and alkali treatment. Data from this study would be useful in the determination of optimum chemical compositions in the EFB fibers that will affect the swelling properties of these fibers.

## II. MATERIAL AND METHODS

### A. Empty Fruit Bunch Fiber (EFB) Preparation

In this study, EFB fibers collected from one of oil palm industry in Penang Malaysia were used. Two types of chemical treatments were used in terms of: i) time for pre-hydrolysis and; ii) alkali treatment during the pulping process. The pre-hydrolysis time used was 20 min, 40 min, 60 min and 80 min. A duration of 2 hours was applied by using 17%, 22%, 27% and 32% of sodium hydroxide (NaOH) for alkali treatment. The chemical composition of EFB fibers after the chemical treatments was determined by using a few methods. Extraction method was used to remove extractives by following TAPPI T204 om-88 procedure. In order to determine hemicellulose content in EFB fibers, methods from Wise et al. and TAPPI T 203 om-93 procedure were applied [18]. While in determining the lignin content of each pulp sample, method from TAPPI T 22 os-74 procedure was used. After pulping process, fiber analysis in terms of length after pulping process was determined using a fiber analyser (model Sherwood INST FAS-3000).

### B. Handsheet Formation

Then, handsheet of the pulp after treatment was formed using pulp stock with consistency of 0.3%. The stock was prepared by using 24 g of oven dry weight pulp and was diluted with 8 L of distilled water in disintegrator at 15,000

revolutions per minute. The formation of handsheet was started by pouring 400 mL of stock solution into a handsheet machine tank. Water was filled in the tank and aerated to disperse the pulp. Then the water was drained, and the remained pulp formed handsheet on a mesh plate. The wet handsheet was pressed using a roller and was let to be dried under room condition (20°C) for one night. The dried handsheet was then prepared to cross-linking process.

### C. Crosslinking Process

In cross-linking process, 5 g of citric acid powder and 100 mL of distilled water were used. Citric acid and distilled water were mixed to 5% consistency solution in a beaker. The solution was stirred continuously until citric acid was fully dissolved. The citric acid solution was applied to the dried handsheet using pressurised spray until fully wetted about 50 ml. Then, the dried handsheet which was applied with citric acid was let to dry in a conditioned room (20°C) for 24 hours. As drying process completed, the samples were heated for 30 minutes in an oven at 145°C and later formed cross-linked handsheet. The cross-linked handsheet was then cut into strips (1.5 cm width with length 9 cm). All strips were dipped into a glass of test tube containing distilled water (about 1 cm dipped) for capillary measurement test. Time and duration were taken as the water travelled and passed through the strips was recorded.

TABLE I: CHEMICAL COMPOSITION OF UNMODIFIED EFB AND TREATED EFB USING PRE-HYDROLYSIS TREATMENT

Sample code	Treatment Conditions	Extractives (%)	Hemicellulose (%)
A	Unmodified sample	4.00 %	23.25%
B	Pre-hydrolysis 20 min	14.40 %	14.35%
C	Pre-hydrolysis 40 min	15.20 %	9.19%
D	Pre-hydrolysis 60 min	19.20 %	4.73%
E	Pre-hydrolysis 80 min	22.00%	3.75%

TABLE II: CHEMICAL COMPOSITION OF UNMODIFIED EFB AND TREATED EFB USING ALKALI TREATMENT

	Treatment Conditions	Lignin Content (%)
A	Unmodified sample	15.14 %
B	17 % NaOH	10.42%
C	22 % NaOH	6.28 %
D	27 % NaOH	4.66%
E	32 % NaOH	1.13%

## III. RESULTS AND DISCUSSIONS

### A. Chemical Composition

The chemical composition of EFB fibers after pre-hydrolysis is shown in Table I. Sample A was unmodified fiber which was used as a control variable, while Sample B, C, D and E were treated with different conditions. From this study, it was found that the amount of extractives being removed out was increased with the increasing of time, while the hemicellulose content was decreased. This was due to the composition of hemicellulose was taken over by extractives and other components. For the longest residence time of pre-hydrolysis, the hemicellulose content was dropped to 3.75% which was 83.87% loss from the original

hemicellulose content. However, hemicellulose removal did not manage to reach 100% even after 80 min due to bonding of stable hemicellulose to the cellulose fibrils [8]. During alkali treatment, results showed that the lignin content was reduced when high concentration of alkali charge was used (Table II). The highest alkali charge which was 32% of sodium hydroxide (NaOH) removed about 92.53 % of lignin in cellulose fibrils, with remaining residue attached to the fibers. This was due to a strong carbon-carbon linkage and the presence of aromatic groups which were very resistant to chemical attack which prevented the degradation of lignin in fiber [8]. However, if higher alkali charge was used, it may trigger the carbohydrate degradation and damaging the fibers [19].

### B. Influence of Chemical Composition of Cross-lined EFB Fiber on Their Capillarity

Fig. 1 illustrates rate of water absorption of cross-linked EFB fibers after treatment. The treatment conditions for Sample B was (20 min for pre-hydrolysis, 17 % NaOH for pulping), followed by Sample C (40 min pre-hydrolysis, 22% NaOH pulping), Sample D (60 min pre-hydrolysis, 27% NaOH pulping) and Sample E (80 min pre-hydrolysis, 32% NaOH pulping). From the results in Fig. 1, it can be seen that the rate of water absorption of cross-linked EFB fibers increased with increasing pre-hydrolysis time and high alkali charge during pulping process. The increasing rate for Sample B, C and D was affected by for pre-hydrolysis time. Previous studies reported that, the rate of water absorption into fibers was affected from porosity and capillaries. As more hemicellulose was removed, the capillary spaces in fibers become bigger, and the fiber network became less dense [8].

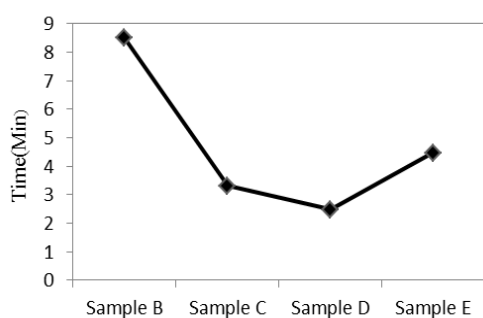


Fig. 1. Rate of water absorption of cross-linked EFB fibers after treatment.

These physical changes contributed to a better fiber arrangement. The less compact fiber network was able to enhance the water molecules to travel along its capillary cavity. However, the change in Sample E was affected by lignin content in the fiber. The lignin was the component in fiber that acted as matrix for connecting cellulose and hemicellulose [20]. It could be related to Sample B, C, and D which by removing the lignin, the blockage was also removed and producing a high porosity in fiber. This factor also would allow the water molecules to transfer along the paper strips in short time without much resistance. However, in Sample E, the progressive lignin removal was too critical which it reduced the porosity and formed a compact structure in fiber

network. Thus the passage for water molecule to travel along the fiber cavities became narrow.

Table III shows fiber length of EFB fibers after chemical treatments. Results showed that the length of fiber was reduced with increasing pre-hydrolysis time and increasing amount of alkali charge used during pulping. Based on the results, Sample E had the shortest fiber length as compared to others. This was due to the concentration of NaOH used in Sample E (32%) which was the highest. The fiber would be fibrillated more but at the same time it underwent cellulose degradation, that made the fiber shorter [19], [21]. The short fibers were able to form more fiber bonding in network that led to high density paper, while long fibers tend to entangle between them, and became more porous due to less fiber bonding. In relation to the rate of water absorption, the short fibers in Sample E formed a compact and high density paper which made it slower due to reduction of its porosity. Thus, water molecules needed longer time to travel along the fiber network of the cross-linked EFB fibers.

TABLE III: LENGTH OF EFB FIBER AFTER CHEMICAL TREATMENTS

Type of samples	Rate of water absorption (min)	Fiber Length (mm)
Sample B	20 min prehydrolysis/ 17% NaOH	0.78
Sample C	40 min prehydrolysis/ 22% NaOH	0.72
Sample D	60 min prehydrolysis/ 27% NaOH	0.70
Sample E	80 min prehydrolysis/ 32% NaOH	0.64

Fig. 2 shows the rate of speed of water absorption according to length of handsheet strips. Results showed that the speed of absorption of the paper strips did not uniform and turned to slow down from 1 cm to 9 cm length. The increasing speed water absorption was due to capillaries and porosity of paper. Large capillary spaces and high porosity of the fiber increased the rate of speed water absorption. However, due to high content of amorphous structure in EFB fiber, the dimensional stability had caused swelling in the fiber [9]. The swelling later reduced capillary spaces and closed the pore structure of the fibers. The fiber network became narrow which increased the difficulty of water molecule to pass along the handsheet strips. Thus, the rate of speed absorption reduced.

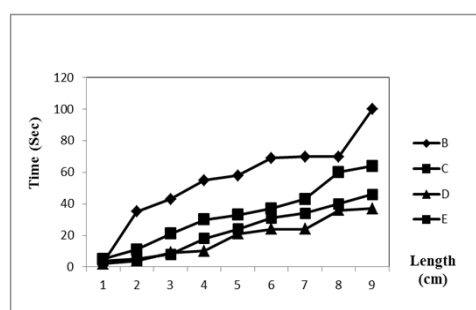


Fig. 2. Rate of speed water absorption according to length of paper strips.

### C. Effect of Hemicellulose and Lignin Removal on Moisture Sorption and Water Absorption

Table IV shows the moisture sorption and water absorption test on EFB handsheet. The result showed that with the increase of pre-hydrolysis time and high concentration of

NaOH during pulping, the percentage for water absorption and moisture sorption was increased from Sample B to Sample D. Extensive removal of hemicellulose led to modification of the fiber structures properties. The fiber became more hydrophilic and less dense due to the lignin removal. The large capillary network had allowed the water or moisture to penetrate inside the fiber network without resistance. Furthermore, the extensive lignin removal had resulted in the increase of the fiber porosity which led to increase of the amount of moisture and water absorbed. During delignification of fiber, the pore structure was produced and located between cellulose and hemicellulose, previously occupied by lignin acted as coupling agent [22]. As the alkali charge was increased, the porosity was also increased. However, the result in Sample E showed that continuous lignin removal had reduced the amount of moisture and water absorption. Based on the results, it showed that 60 min of pre-hydrolysis time and 27% NaOH were the optimum conditions of EFB fibers in this study. The removal of lignin was able to increase the pore volume at first, but extensively delignification led to collapse of the cavities, lowering the amount of the pores [23]. It might probably the small pores that turned into large one had collapsed. High amount of alkali treatment led to fiber damage which decreased the ability of fibers to retain moisture and water [24].

TABLE IV: MOISTURE SORPTION AND WATER ABSORPTION TEST ON EFB HANDSHEET

Samples Code	Water Absorption	Moisture Sorption
Sample B	441 %	9.89 %
Sample C	445 %	11.30 %
Sample D	494 %	12.97 %
Sample E	450 %	11.44 %

#### IV. CONCLUSIONS

In this study, chemical composition of EFB fibers using pre-hydrolysis and alkali treatment was carried out. From the study, it can be concluded that:

- The amount of extractives becomes increased with the increasing of pre-hydrolysis time, while the hemicelluloses content decreased.
- Lignin content reduced when high concentration of alkali charge used.
- The capillary size increased with pre-hydrolysis treatment, while the alkali treatment has increased the porosity of fiber. However, the progressive of using alkali charge affected in reducing the fiber length which made the fiber network became compact.
- The rate of speed water absorption increased by removing lignin and hemicelluloses. The progressive removal of hemicelluloses and lignin influenced the water absorption and moisture sorption properties of EFB fiber.
- Hemicellulose removal improved the capillary spaces in fibers, while lignin removal increased the porosity of the fibers. However, the high content of amorphous structure in the fiber had affected fiber swelling which reduced the rate of speed water absorption.

#### ACKNOWLEDGMENT

This study was fully supported by Sciencefund Grant, Ministry of Science Technology and Innovation (MOSTI) Malaysia with the account number of 305/PTEKIND/613330.

#### REFERENCES

- [1] S. Suganuma, *et al.*, "Hydrolysis of cellulose by amorphous carbon bearing SO<sub>3</sub>H, COOH, and OH groups," *Journal of the American Chemical Society*, vol. 130, no. 38, pp. 12787-12793, 2008.
- [2] I. Siró and D. Plackett, "Microfibrillated cellulose and new nanocomposite materials: A review," *Cellulose*, vol. 17, no. 3, pp. 459-494, 2010.
- [3] J. I. Morán, *et al.*, "Extraction of cellulose and preparation of nanocellulose from sisal fibers," *Cellulose*, vol. 15, no. 1, pp. 149-159, 2008.
- [4] A. C. O'sullivan, "Cellulose: the structure slowly unravels," *Cellulose*, vol. 4, no. 3, pp. 173-207, 1997.
- [5] I. Y. A. Fatah, *et al.*, "Exploration of a chemo-mechanical technique for the isolation of nanofibrillated cellulosic fiber from oil palm empty fruit bunch as a reinforcing agent in composites materials," *Polymers*, vol. 6, no. 10, pp. 2611-2624, 2014.
- [6] D. Bondeson, A. Mathew, and K. Oksman, "Optimization of the isolation of nanocrystals from microcrystalline cellulose by acid hydrolysis," *Cellulose*, vol. 13, no. 2, pp. 171-180, 2006.
- [7] X. M. Dong, J. F. Revol, and D. G. Gray, "Effect of microcrystallite preparation conditions on the formation of colloid crystals of cellulose," *Cellulose*, vol. 5, no. 1, pp. 19-32, 1998.
- [8] B. M. Pejic, *et al.*, "The effects of hemicelluloses and lignin removal on water uptake behavior of hemp fibers," *Bioresource Technology*, vol. 99, no. 15, pp. 7152-7159, 2008.
- [9] K. L. Spence, *et al.*, "The effect of chemical composition on microfibrillar cellulose films from wood pulps: Mechanical processing and physical properties," *Bioresource Technology*, vol. 101, no. 15, pp. 5961-5968, 2010.
- [10] L. Y. Mwaikambo and M. P. Ansell, "Chemical modification of hemp, sisal, jute, and kapok fibers by alkalization," *Journal of Applied Polymer Science*, vol. 84, no. 12, pp. 2222-2234, 2002.
- [11] C. P. Leh, *et al.*, "Optimisation of oxygen delignification in production of totally chlorine-free cellulose pulps from oil palm empty fruit bunch fibre," *Industrial Crops and Products*, vol. 28, no. 3, pp. 260-267, 2008.
- [12] S. Shamsudin, *et al.*, "Effect of steam pretreatment on oil palm empty fruit bunch for the production of sugars," *Biomass and Bioenergy*, vol. 36, pp. 280-288, 2012.
- [13] W. E. Kaar, C. V. Gutierrez, and C. M. Kinoshita, "Steam explosion of sugarcane bagasse as a pretreatment for conversion to ethanol," *Biomass and Bioenergy*, vol. 14, no. 3, pp. 277-287, 1998.
- [14] W. R. W. Daud, K. A. Wahid, and K. N. Law, "Cold soda pulping of oil palm empty fruit bunch (OPEFB)," *Bioresources*, vol. 8, no. 4, pp. 6151-6160, 2013.
- [15] K. Wong, *et al.*, "Wicking properties of linen treated with low temperature plasma," *Textile Research Journal*, vol. 71, no. 1, pp. 49-56, 2001.
- [16] J. Thomas, *et al.*, "Capillary water provision system for irrigation," *International Journal of Information Science and Computing*, vol. 2, no. 1, pp. 13-20, 2015.
- [17] Y. Tan and M. Guo, "Using surface free energy method to study the cohesion and adhesion of asphalt mastic," *Construction and Building Materials*, vol. 47, pp. 254-260, 2013.
- [18] L. E. Wise, "Chlorite holocellulose, its fractionation and bearing on summative wood analysis and on studies on the hemicelluloses," *Paper Trade*, vol. 122, pp. 35-43, 1946.
- [19] N. H. Shin and B. Strömberg, "Impact of cooking conditions on pulp yield and other parameters," in *Colóquio Internacional sobre Celulose Kraft de Ecuatorto*, 2003, pp. 59-67.
- [20] H. Chen, "Chemical composition and structure of natural lignocellulose," in *Biotechnology of lignocellulose*, Springer, pp. 25-71, 2014.
- [21] M. L. Troedec, *et al.*, "Influence of various chemical treatments on the composition and structure of hemp fibres," *Composites Part A: Applied Science and Manufacturing*, vol. 39, no. 3, pp. 514-522, 2008.
- [22] A. Scallan and A. Tigerström, "Swelling and elasticity of the cell walls of pulp fibres," *Journal of Pulp and Paper Science*, vol. 18, no. 5, pp. J188-J193, 1992.
- [23] L. Salmén and J. Berthold, "The swelling ability of pulp fibres," *Fundamentals of Papermaking*, pp. 683-701, 1997.

- [24] I. Rauvanto, *The Effect of Oxygen Delignification on Fiber Properties in Kraft Pulp Production-a Review*, Julkaisu/Report-Lappeenranta teknillinen yliopisto, Kemiantekniikan osasto, 2003.



**Mohammad Aliff Shakir** is a master student from School of Industrial Technology, Universiti Sains Malaysia. His major focus is in chemical modification of fibers, composite materials and application of polymer. He has been awarded a silver medal in Novel Research and Innovation Competition (NRIC) in 2015.



**Mohd Firdaus bin Yhaya** obtained his PhD from University of New South Wales, Australia. He is currently a senior lecturer in School of Industrial Technology, Universiti Sains Malaysia. His research interests are in angstromtechnology, coatings chemistry and technology, click chemistry, and green chemistry.



**Mardiana Idayu Ahmad** earned her PhD in sustainable energy technologies from the University of Nottingham, UK in 2011. She is a member of Institution of Engineering & Technology (IET) UK and World Society of Sustainable Energy Technologies (WSSET). Her primary research interests include renewable & sustainable energy technologies, IAQ and building ventilation, environmental management and risk assessment.